UNIVERSITY OF NAIROBI

SCHOOL OF ENGINEERING

DEPARTMENT OF ENVIRONMENTAL AND BIOSYSTEMS ENGINEERING

NUMERICAL MODELLING OF PHYSICAL PROCESSES IN DRYING AND STORAGE OF SELECTED AFRICAN LEAFY VEGETABLES.

BY

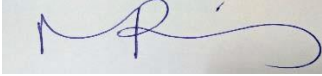### GIBSON SHIYONZO PETER MUTULI

F80/51801/2017

BSc. Ind. Chem. (Makerere University), MSc. Env & Bios. Eng. (University of Nairobi)

A thesis submitted for the partial fulfillment for the award of Ph.D. in **ENVIRONMENTAL AND BIOSYSTEMS ENGINEERING**, in the Department of **ENVIRONMENTAL AND BIOSYSTEMS ENGINEERING** of the University of Nairobi

2020

DECLARATION

This is my original work and has not been presented for an award of a degree in any other university.

SIGNATURE: DATE: 17th August, 2020

This Thesis is submitted with our approval as University supervisors:

<u>**SUPERVISORS:**</u>

Duncan O. Mbuge; PhD:

SIGNATURE…………………………. DATE: 17th August, 2020

Ayub N. Gitau; PhD:

SIGNATURE…....................................….DATE:

Declaration of originality

Name of student: Gibson Shiyonzo Peter Mutuli

School: Engineering

Department: Environmental and Biosystems Engineering

Course Name: PhD in Environmental and Biosystems Engineering

Title of Work: **NUMERICAL MODELLING OF PHYSICAL PROCESSES IN DRYING AND STORAGE OF SELECTED AFRICAN LEAFY VEGETABLES.**

1. I understand what plagiarism is and I'm aware of the university policy in this regard;

2. I declare that this research thesis is my original work and has not been submitted elsewhere for examination, an award of a degree or publication. Where other works or my own work has been used, this has properly been acknowledged and referenced in accordance with the University of Nairobi's requirements;

3. I have not sought or used the services of any professional agencies to produce this work;

4. I have not allowed, and shall not allow anyone to copy my work with the intention of passing it off as his/her work;

5. I understand that any false claim in respect of this work shall result in disciplinary action in accordance with the University of Nairobi anti-plagiarism policy.

Signature: ....

Date: :   ………………………..

THESIS

6%
SIMILARITY INDEX

5%
INTERNET SOURCES

2%
PUBLICATIONS

4%
STUDENT PAPERS

MATCH ALL SOURCES (ONLY SELECTED SOURCE PRINTED)

2%

★ arunmujumdar.com

Internet Source

Dean;
School of Engineering

Exclude quotes	On	Exclude matches	< 5 words
Exclude bibliography	On		

CHAPTER ONE : INTRODUCTION

1.1 Background:

The African Leafy Vegetables are plants in which the leafy parts, including the succulent stems, flowers, and very young fruits, are used as vegetables and are indigenous to the African communities. Their role in the food consumption patterns of African households is highly variable and depends on factors such as poverty status, degree of urbanization, distance to fresh produce markets and time of the year (Shiundu and Oniang'o, 2007). There has been a significant increase in the consumption and production of these vegetables in recent times due to their associated benefits. The most important species include Spider plant (*Cleome gynandra*), African nightshades (*Solanum villosum* and *Solanum scabrum*), pumpkin leaves (*Cucurbita moschata*), Cowpeas (*Vigna unguiculata*), vegetable amaranths (*Amaranthus blitum*), Jute mallow (*Corchorus olitorius*), Slender leaf (*Crotalaria ochroleuca* and *Crotalaria brevidens*) and African kale (*Brassica carinata*), representing seven botanic families, namely Amaranthaceae, Brassicaceae, Capparaceae, Cucurbitaceae, Fabaceae, Solanaceae and Tiliaceae (Abukutsa-Onyango). **Plate** *1-1* shows a photo of some of the common species of African leafy vegetables. These vegetables are cultivated for seeds, but their leaves are also popular a vegetable. The vegetables' consumption is limited by their seasonal availability. However, in areas where seasonality is a critical factor in limiting availability, promotion of home gardening and local preservation technologies like fermentation and sun drying have been applied to maintain the supply (Muchoki, 2007).

ABSTRACT:

In the food industry, drying is a significant unit operation that has evolved from ancient times. Researchers have sought to optimize the process by developing novel technologies that improve energy use and optimize food quality. These solutions are required in sub-Saharan Africa where it is reported that the post-harvest losses of the produce are significantly high (upto 50%), mainly due to lack of technical packages for preservation. On the other hand, there is a problem with malnutrition and nutrient deficiency. African Leafy Vegetables are indigenous to Africa and have been identified as having potential for upscaling and addressing food security and nutrient deficiency. This study sought to develop a technical package that would preserve the vegetables by drying so as to address the problem of post-harvest losses of the African leafy vegetables and hence improve on nutrition in diets of the people of sub-Saharan Africa. Specifically the study identified the pertinent parameters in the numerical modelling of convective food drying; developed and validated models for the physical processes in the convective drying process; and modelled the food water interaction of the vegetables and identify suitable storage conditions of the dried ALVs

Relevant literature was reviewed to identify the pertinent parameters relevant to the drying of leafy vegetables. The experiments were conducted to validate theoretical models developed for the physical processes in the convective drying process and to simulate the food water interaction of the vegetables and identify suitable storage conditions of the dried ALVs. Five species of the vegetables were selected for the study; *Corchorus olitorius* (Jute Mallow), *Crotalaria ochroleuca* (Slender Leaf), *Vigna unguiculata* (Cowpea), *Solanum villosum* (Nightshade) and *Amaranthus blithum* (Amaranthus).

Drying experiments were done at 30, 40 and 50ºC in a convective laboratory dryer and drying curves were fitted to existing models, moisture diffusivity and activation energy trends were also determined as well as shrinkage from the change in leaf thickness. Vitamins A, C, and E were analyzed using spectroscopy and high-pressure liquid chromatography in freshly harvested vegetables and after drying at 40ºC and storage for 60 days. Fresh and dried vegetable samples inoculated with aspergillus spores were incubated at 40ºC under 96%, 82%, 74% and 32% relative humidity for ten days for Aflatoxin B1, B2, G1 and G2 analysis. Sorption isotherms were carried

using saturated salt solutions at 30, 40 and 50ºC; between 14 and 83% relative humidity. Night drying when solar energy is not available was explored through the use of a desiccant called super absorbent polymer (SAP) for improving drying air characteristics. Theoretical models to describe shrinkage and transport phenomena were also developed and implemented on COMSOL Multiphysics 5.2. Another theoretical model to estimate energy was developed using the Clausius–Clapeyron equation and Peleg model.

Drying occurred in the falling rate period and Page model simulated the drying pattern of the vegetables with a ≈97% correlation between the empirical and predicted values with the model prediction being precise above 0.5 moisture content on w.b. Shrinkage was found to be a function of moisture loss at a range of 89 to 98% with a linear correlation. The rate of moisture loss and activation energy correlated with air temperature. The trend in the drying characteristics and moisture transport of the vegetables was unique with each vegetable. The theoretical models developed were corrected with experimental results and could be applied to various food products. Drying at 40ºC and storage for 60 days realized retention in the scale range of 50 to 75% for Vitamins A, C and E. Energy requirement could be accurately estimated from the model developed. For optimization of energy use for drying, it was found that SAP could be used to improve inlet air stream characteristics for moisture uptake through the reduction of the moisture load in the stream. It was revealed that the SAP can be reused by drying it, and thus a mechanism that would enable simultaneous adsorption and desorption would enable continuous use of the fabric. The sorption curves provided valuable information about the hygroscopic equilibrium of the vegeables. They gave a clear idea on the stability domain of the vegetables after drying. From the sorption curves, it is recommended that the product should be stored under low relative humidity because it shows an increasing food water interaction with increasing relative humidity under ambient temperature conditions.

The study showed that drying is an effective way to preserve African leafy vegetables.

Keywords: African leafy vegetables, drying, modelling, sorption, shrinkage, storage.

Table of contents

List of Figures

List of photos:

List of Tables:

List of Plate:

CHAPTER ONE : INTRODUCTION

1.1 Background:

The African Leafy Vegetables are plants in which the leafy parts, including the succulent stems, flowers, and very young fruits, are used as vegetables and are indigenous to the African communities. Their role in the food consumption patterns of African households is highly variable and depends on factors such as poverty status, degree of urbanization, distance to fresh produce markets and time of the year (Shiundu and Oniang'o, 2007). There has been a significant increase in the consumption and production of these vegetables in recent times due to their associated benefits. The most important species include Spider plant (*Cleome gynandra*), African nightshades (*Solanum villosum* and *Solanum scabrum*), pumpkin leaves (*Cucurbita moschata*), Cowpeas (*Vigna unguiculata*), vegetable amaranths (*Amaranthus blitum*), Jute mallow (*Corchorus olitorius*), Slender leaf (*Crotalaria ochroleuca* and *Crotalaria brevidens*) and African kale (*Brassica carinata*), representing seven botanic families, namely Amaranthaceae, Brassicaceae, Capparaceae, Cucurbitaceae, Fabaceae, Solanaceae and Tiliaceae (Abukutsa-Onyango). *Plate 1-1* shows a photo of some of the common species of African leafy vegetables. These vegetables are cultivated for seeds, but their leaves are also popular a vegetable. The vegetables' consumption is limited by their seasonal availability. However, in areas where seasonality is a critical factor in limiting availability, promotion of home gardening and local preservation technologies like fermentation and sun drying have been applied to maintain the supply (Muchoki, 2007).

Amaranth
spider plant

Plate 1-1. Photos of common African Leafy Vegetables (Odhiambo and Oluoch, 2008)

Food needs preservation mainly to stop spoilage, to make them available throughout a year, to maintain desired levels of nutritional properties for the longest possible time span and to make value-added products. Amongst these, spoilage is the foremost reason for employing food preservation techniques. Spoilage occurs during handling or due to mechanical, physical, chemical or microbial damage (Mujumdar and Devahastin, 2000). Common methods for preservation of fruits and vegetables are freezing, vacuum packing, canning, preserving in syrup, food irradiation, adding preservatives and dehydration or drying. Application of canning and freezing methods would yield to higher retention of the taste, appearance, and nutritive value of food; drying is an excellent way to preserve foods that can add variety to meals and provide delicious, nutritious snacks. Drying describes the process of thermally removing volatile substances to yield a solid product of required moisture content. One of the biggest advantages of dried foods is that they take much less storage space than canned or frozen foods (Chakraverty *et al.,* 2003). Though drying is one of the most cost-effective ways of preserving foods of all variety it is an energy-intensive process. The process can be achieved by the use of hypertonic solutions, microwave or hot air-

drying methods. In the development of advanced drying techniques, freeze-drying has been reported as the most effective method to dry high-value food products, however, it is associated with tremendous costs (Chou *et al.,* 2001). Fluidized bed drying which is reported to have high thermal efficiency could be used with the application of low temperatures to achieve an optimized drying process. The method has been applied for granular materials due to their fluidity property. Drying technology has been advanced through intensive research and development processes. The process involves experimentation, numerical and simulation analysis of proposed technological advancements in drying technology. Experimentation would involve data collection on the model process(es) or/and prototype equipment, on the other hand, the use of numerical, computational modelling combined with the simulation process will collect data on a geometric model. Numerical modelling has turned out to be an efficient tool for understanding the comprehensive equipment and process environment/performance. The models that could be developed in a drying environment include; heat and mass transfer and physicochemical models. In this study modelling has been applied to simulate drying of the leafy vegetables, to understand physical processes that occur during drying.

For populations in sub-Saharan Africa, African leafy vegetables (ALVs) are a vital dietary component. The region is reported to have among the world's lowest intake of micronutrients, almost less than half the World Health Organization recommendations on a daily intake of 400g (Mazzocchi *et al.,* 2008, World Health, 2005). The integration of ALVs into the World Health Organization's global fruit and vegetable initiative has a pivotal role in the success of the global initiative in the sub-continent. Addressing the existing barriers to improve the availability and consumption of these vegetables would play an important part in the success of this initiative.

1.2 Problem statement and justification:

Cases of annual episodes of malnutrition, starvation, droughts, and famine in Sub-Saharan Africa are well documented. Though food production has improved, it is reported that the post-harvest losses of the produce are still significantly high, up to half the produce mainly due to lack of technical packages for preservation among other factors (Shiundu and Oniang'o, 2007). In general, cases of food losses tend to be highest in countries where the need for food is greatest in Sub-Saharan Africa (FAO, 2011, Joardder and Masud, 2019, Hodges *et al.,* 2014). Preservation

methods in use i.e. solar drying, fermentation and hydrating are both insufficient and produce low-quality products with regard to organoleptic and nutritional qualities. Hot air drying has been identified as a simple and cost-effective method of preservation. However, the drying process is not well documented, moreover, there is a need to determine the stability and rewetting properties of the dried product.

African leafy vegetables have been identified as promising for up-scaling and addressing food security (Muthoni *et al.,* 2010). They have nutritional and medicinal value, local adaptation, market availability, are well known and widely consumed in tropical Africa. They are a rich source of nutrients including Vitamin A, vitamin C, folic acid, riboflavin and minerals such as iron and calcium and have the potential for the production of phytochemicals (Shiundu and Oniang'o, 2007). With a nutrient deficiency in sub-Saharan Africa especially during droughts, these vegetables can offer food-based approaches to solving malnutrition and nutrient deficiency which are long-term and more affordable if well addressed (FAO, 2011).

Existing knowledge suggests that these vegetables may be dried and stored for several months and such an intervention would make the vegetables available when and where they are needed most.

1.3 Objectives:

1.3.1 Overall objective:

To optimize the drying of African leafy vegetables through numerical modelling and determine the appropriate storage conditions

1.3.2 Specific objectives:

The specific objectives are to:
a) Identify the pertinent parameters in the numerical modelling of convective food drying;
b) Develop models for the physical processes in the convective drying process;
c) Validate models developed for the physical processes in the convective drying process:
d) Model the food water interaction of the vegetables and identify suitable storage conditions of the dried ALVs

1.3.3 Research questions:

a) What is the suitability of drying as a method for preservation for leafy vegetables?

b) What are the suitable conditions for storage of dried/ fresh vegetables?

c) What is the stability and safety of the dried vegetables with storage?

1.4 Scope of the study:

This study focused on investigation of the physical processes that occur drying and storage of the vegetables. It was limited to selected Sfrican green leafy vegetables: African nightshades (*Solanum villosum*), Cowpea leaves (*Vigna unguiculata*), vegetable amaranths (*Amaranthus blitum*), Jute mallow (*Corchorus olitorius*), Slender leaf (*Crotalaria ochroleuca*). Jute mallow and slenderleaf breaks down into a pasty substance when cooked while the remaining maintain their original structure.

CHAPTER TWO : LITERATURE REVIEW

2.0 Introduction:

Drying is a significant unit operation in food processing presently and its application spans from ancient times. Its advancement has realized a broad scope of application (even to foods traditionally preserved by other methods e.g. foods in liquid form like milk) and improved on the quality of the dried product in terms of nutritional and organoleptic characteristics (Motevali et al., 2011, Wilhelm et al., 2004a). Food material contains complex organic molecules (vitamins, proteins, and carbohydrates). The process conditions in drying affect directly the quality of the dried product: the nutritional and organoleptic characteristics of the food material (in terms of the nutrients, color, taste, and flavor) (Mutuli and Mbuge, 2018, Sun *et al.,* 2018). Understanding drying systems is key to their optimization.

This thesis presents literature reviewed from advanced drying methods, numerical modelling of convective drying, storage conditions and general aspects of African leafy vegetables. The review in literature was made with a view to a comprehensive understanding of the preservation of leafy vegetables through drying.

2.1 General Concepts in Food Drying:

2.1.1 Drying for Food Safety and Security:

Tropical countries have a high population density with a significant segment plagued by food security problems. A major cause of the food insecurity is postharvest losses which are significantly high due to the lack of knowledge and appropriate infrastructure facilities, inappropriate food handling, harsh climatic conditions, the small scale of operation, and limited automation of the postharvest operations. Fresh fruits and vegetables account for 20 to 40% w/w, grains and cereals 10 to 30% w/w, leading to significant economic losses. Fruits and vegetables are important sources of essential dietary nutrients such as vitamins, minerals, and fiber. Because the moisture content of fresh fruits and vegetables is greater than 80% wb, they are classified as highly perishable commodities. Keeping the product fresh is the best way to maintain its nutritional value, but most storage techniques require low temperatures, which are difficult to maintain throughout the distribution chain (Curcio et al., 2015).

Drying is a suitable alternative for postharvest management, especially in countries like Kenya where the cold chain is poorly established and handling facilities are inadequate. It should be noted that over 20% w/w of the world's perishable crops are dried to increase their shelf life (Erbay and Icier, 2010). The preservation of cereals, grains, fruits, and vegetables through drying dates back from ancient times and was based on sun and solar drying techniques. Poor quality and product contamination led to the development of alternate drying technologies. The most applicable methods of drying fruits and vegetables includes freeze, vacuum, osmotic, cabinet or tray, fluidized bed, spouted bed, ohmic, heat pump, and microwave drying and combinations thereof (Ertekin and Firat, 2017). In addition to these drying methods, advanced techniques such as particulate medium drying, conduction drying, infrared drying, and superheated steam drying are used for drying of cereals and grains.

Apart from freeze-drying, applying heat during drying through conduction, convection, and radiation are the basic techniques used to force water to vaporize, and forced air is applied to enhance the removal of vapor. The choice of drying method depends on various factors, such as the type of product, availability of a dryer, cost of dehydration, and quality of the desiccated product. Energy consumption and quality of dried products are other critical parameters in the selection of a drying process. To reduce the use of fossil fuel, electrical energy is an alternate source of energy for drying applications, especially where electricity is generated by a renewable energy source such as hydropower or wind power (Raghavan *et al.,* 2005).

Drying of fruits and vegetables has been typically by convective drying. Several studies have addressed the problems associated with conventional convective drying. Some important physical properties of the products changed, such as color, texture, and chemical changes affecting the flavor, nutrients, and shrinkage. In addition, convective drying produces poor rehydration characteristics in the dried product. The high temperature of the drying process causes loss of micro-nutrients. Lowering the process temperature has great potential for improving the quality of dried products. However, in such conditions, the cycle time and the associated cost are too high. To reduce operating costs, different pretreatments and new low-temperature and low-energy drying methods have evolved.

2.1.2 Pretreatments for Drying:

Biomaterials could be subjected to certain pretreatments before drying to minimize possible adverse changes during drying and subsequent storage. The diffusion of moisture through thick and waxy skin during the drying process is difficult. To improve the drying rate of high moisture content materials with thick layers, pretreatments prior to drying are considered.

Living tissue responds to peeling and cutting by showing increased respiration, ethylene synthesis, and phenolics metabolism. This also leads to loss of sugars and other solubles, which may affect flavor and quality. Wounded plant tissues synthesize and polymerize phenolic compounds and lignins, which in turn will affect the color, texture, and flavor of the dried food material. Pre-treatments applied to food material usually stop/retard the metabolism of wounded tissue and affect the course of drying and quality of the final product.

2.1.3 Heat and Mass Transfer in drying process:

Drying is a combined/simultaneous heat and mass transfer operation for which energy must be supplied to remove moisture from the material domain. Air is the most common medium for transferring heat to a material domain and two important processes occur mass transfer to the material surface and from the surface to the surrounding air. To achieve dried products of high quality at a reasonable cost, the process must proceed rapidly. The main factors that affect the drying rate are; size and geometry, the orientation of material towards heat transfer medium, properties of material and drying chamber. Usually, for agricultural products, the initial drying rate is constant and then could either proceed at the same rate or change to falling rate period. Several models describing the internal mechanisms of moisture transfer have been suggested by several authors, but it is important to note that no generalized model currently can sufficiently describe explain the mechanism of internal moisture transfer for all food materials (Cohen, 2011). The rate of drying during the constant rate period may be determined using either heat or mass transfer equations. In practice, the heat transfer equation gives a more reliable estimate of the drying rate than mass transfer equations (Akpinar, 2006).

To estimate the average drying time during the falling rate period, several researchers have used Fick's second law of diffusion. From studies of transport mechanisms of fruits and vegetables, it

has been found that moisture and temperature profiles and drying times could be predicted with satisfactory accuracy using Fick's diffusion law. (Akpinar, 2006, Akpinar *et al.,* 2003, Azzouz *et al.,* 2002). The air humidity has the prominence effect on the first falling rate period and the temperature dependence of the drying rate. Models that have been developed on diffusivity vary in complexity depending on the variables that were considered; models have been developed dependent solely on temperature; and temperature and moisture content, as well as shrinkage. Food geometry is also an important factor that authors have considered in developing models (Defraeye *et al.,* 2016).

2.1.4 Mathematical Models in drying:

For the optimization of the drying process in terms of quality of the product and operating cost, prediction of the rate of drying with the help of suitable models becomes necessary wherein experimental drying data are correlated with mathematical equations to have a semi-empirical approach to describe the complex phenomena involved in the drying of food materials. Drying rate equations and rate parameters obtained for such equations help in the design and control of various drying apparatus.

Drying kinetics of food materials is often described in the literature with the help of a straight-line equation (2.1) which is a simplified form of Fick's law.

$$\frac{M - M_e}{M_i - M_e} = Ce^{-KE}$$

2-1

where C is a constant, K is the dehydration constant (M, is the average moisture content (kg water/kg dry matter), M_i is the initial moisture and M_e is the equilibrium moisture. This simple approach is not always applicable due to the complexity of the transport mechanism in foods during drying.

Drying rate equations have been derived to describe the kinetic behavior of drying process and the different aspects of air drying of fruits and vegetables (Mutuli and Mbuge, 2015, Yaldiz *et al.,* 2001, Ertekin and Yaldiz, 2004, Midilli *et al.,* 2003, Akpinar *et al.,* 2003). The authors have constructed drying rate curves for agricultural products, determined the critical moisture content,

drying constant, effective diffusivity and activation energy diffusion and discussed the possible diffusion mechanism based on the concept of internal and external resistance. They found the nature of the product to be the major factor influencing its drying behavior. Study of the effect of air flow rate on kinetics of carrot drying showed that above 6000 kg/m²h, airflow rate had no influence on drying rate as evidenced by the value of D/γ^2 (where D = apparent diffusivity and γ = half the thickness of the cube) and the rate remained almost constant (Doymaz, 2004).

The development of mathematical models has yielded results that have aided drying and food engineers to optimize the design of food drying systems. The concept is still evolving witnessed by the new publications from researchers. The theoretical aspects of mathematical modelling are covered in chapter three; theoretical framework.

2.1.5 Drying Techniques:

The type of dryer and drying method is suited to a specific food material. Several methods are applied in drying of fruits and vegetables, including; sun drying, atmospheric dehydration processes, continuous processes, such as tunnel, belt trough, fluidized bed, and foam-mat drying. Spray drying is suitable for fruit juice concentrates and vacuum dehydration processes are useful for low moisture high sugar fruits like peaches, pears, and apricots. Factors on which the selection of dryer/drying method depends include the form of raw material and its properties, desired physical form and characteristics of the product, necessary operating conditions and operation costs.

The principles of these processes have been discussed and described in several books/articles. Further developments that have occurred in their applications and modifications are reviewed briefly in the sections herein.

2.1.5.1 Vacuum Drying:

The basic principle of vacuum drying involves a reduction in pressure causing the expansion of water molecules in the vapor phase and escape of vapor occluded into pores. It is suitable for heat-sensitive materials due to low-temperature applications. In the case of osmotic dehydration, when the pressure is restored, the pores can be occupied by the osmotic solution, increasing the available

mass transfer surface area. The effect of vacuum application during osmotic dehydration is explained in terms of osmotic transport parameters, mass transfer coefficient, and interfacial area. Vacuum pressure (50–100 mbar) is applied to the system for the drying time to achieve the desired result (Bazyma and Kutovoy, 2005).

2.1.5.2 Freeze-Drying:

Freeze drying of biological materials is one of the best methods of water removal and its products are of much higher quality compared to any other drying technique. Freeze-drying involves quick freezing of free moisture present in the biomaterial and subsequent sublimation of the ice fraction where water passes from the solid to the vapor phase. Due to the very low temperature, all the biochemical and microbiological activities are retarded, which results in a better quality of the final product. Recently, the market for organic products has increased and therefore, freeze-drying of fruits and vegetables is gaining ground. In recent years, freeze-drying of small fruits (strawberry) received attention from several researchers. It has been shown that low processing temperature improved the sensory quality of dried fruits. Strawberries dried at $20^{\circ}C$ retained better quality than at $60^{\circ}C$. A comparative review of drying technologies showed that freeze-drying, vacuum drying, and osmotic dehydration are considered too costly for large-scale production of dried horticultural products (Khin *et al.,* 2005, Shishehgarha *et al.,* 2002).

2.1.5.3 Supercritical CO_2 Drying:

Supercritical CO_2 drying is a relatively new technique predominantly in the research and development stage for various heat-sensitive, high-value commodities in the food and pharmaceutical sectors. The critical point of CO_2 gas is at 304.17 K and 7.38 MPa. CO_2 can be made to dissolve in the available free moisture of the biomaterial. The combination of pressure and temperature as process parameters can cause sudden expansion of CO_2, resulting in moisture escaping from the biomaterial. This has emerged as an attractive unit operation for the processing of biomaterial. When used in combination with osmotic dehydration, it is possible to vary the solvent of the medium within certain ranges as desired without changing the composition of the solvent. There is no significant improvement in water loss due to this technique but it significantly reduces solids gain (Brown *et al.,* 2008, Kudra and Mujumdar, 2009). Brown *et al.,* 2008

performed supercritical CO_2 drying of carrots. Carrots dried in the supercritical fluid environment retained their shape much better than air-dried carrots, which underwent shrinkage.

2.1.5.4 Ultrasonic Drying:

Cavitation, a phenomenon produced by the sonication, consists of the formation of bubbles in the liquid, which can collapse and generate localized pressure fluctuation. This has effects like that of vacuum and supercritical CO_2 drying. When used in combination with osmotic dehydration, acoustic streaming can affect the thickness of the boundary layer that exists between the stirred fluid and solid. This ultimately increases the mass transfer during osmotic treatment. The mass transfer rate depends on the pressure and frequency of the wave produced by sonication (Raghavan *et al.,* 2005). Accelerated effective diffusion of up to 14.8% was obtained for atmospheric freeze-drying with a fluid bed. The faster drying in ultrasonic-assisted atmospheric freeze-drying is assumed to be due to a higher mass transfer rate at the solid-gas interface, caused by a reduced boundary layer due to a higher turbulent interface. Thus, high-intensity, airborne ultra-sound used with modern drying systems have great potential to accelerate drying, reduce investment and production costs,   and improve product quality (Bantle and Eikevik, 2011, García-Pérez *et al.,* 2011). Garcia-Perez *et al.,* 2011 found that the application of ultrasound in drying processes has great potential due to the improvement in both the internal and external mass transport as described by the Weibull empirical model and the diffusion model they developed. Ultrasound application in drying involves the use of sound waves at very high frequencies (over 16 kHz) are above the threshold of the human ear and can cause hearing loss in operators if safety precautions are not taken. Another limitation of the use of ultrasound for drying of foods is that the intensity of ultrasound required to achieve significant mass transfer enhancement can lead to the formation of free radicals (Mothibe *et al.,* 2011).

2.1.5.5 Centrifugal Drying/Dewatering:

Spinning masses exert centrifugal force on the available free moisture, mechanically expelling them out of the biomaterial. This can be used in combination with other drying techniques to enhance mass transfer. For example, in one study, applying centrifugal force (64 g) during osmotic dehydration resulted in mass transfer enhancement of 15% w/w. Research studies focusing on the

optimization of various factors such as solvent, solute, plant tissue, the permeability of tissue, mass transfer rate, and solids gain are necessary to make the unit operation more successful. This method is applied in the dewetting of fresh vegetables that have been washed prior to their packaging. Centrifugal dewatering techniques are predominantly applied in waste-water treatment plants. (Chu and Lee, 2001).

2.1.5.6 Heat Pump Drying:

Conventional dryers heat the air using high-quality energy (such as electricity or fuels) and vent a stream of moist, hot air at the exhaust, leading to a significant energy loss. Conventional heat recovery systems using heat exchangers to preheat the inlet air stream recover only the sensible heat component of the exhaust air. When heat pumps are introduced in the system, they recover the latent heat of evaporation of water lost in the exhaust from the dryer as well. By placing the evaporator of a heat pump in the exhaust stream, the air leaving the dryer is cooled (thereby recovering the sensible heat component) and then dehumidified (thereby recovering the latent heat) by the refrigerant. The heat thus added to the refrigerant is then rejected at the condenser of the heat pump to the stream of air entering the dryer, thus increasing its temperature. When the air leaving the dryer is recirculated, the added benefit of dehumidification of the drying air is also realized, increasing its potential to achieve better drying.

One of the main advantages of HPD-assisted drying is the retention of quality and its successful application to drying highly valued heat-sensitive materials. A purging technique, where the air in a HPD dryer was replaced with nitrogen and carbon dioxide during drying, resulted in better final color (i.e., less browning) of dried apple, guava, and potato pieces (Hawlader *et al.,* 2006). Moreover, the porosity and rehydration characteristics of the product were superior compared to material dried under a vacuum (Hawlader *et al.,* 2006). Comparing the drying of apple cylinders in a heat pump dryer versus an electrically heated dryer, the HPD dryer was shown to use 40% less energy and result in a 25% faster-drying rate, yielding a better quality product in terms of color, texture, and rehydration ratio. High levels of rehydration ability and floatability, as well as desirable color characteristics, were obtained when green peas were dried in a fluidized bed heat pump dryer under atmospheric freeze-drying conditions (Gabas *et al.,* 2004). Comparing microwave-assisted heat pump drying to freeze-drying of guava, mango, and honeydew melon,

the microwave-assisted process increased the drying rate, lowered shrinkage, and resulted in a better appearance of the end product, at lower cost. Heat pump dryers have great potential for industrial applications, particularly for high-value crops, due to the superior quality of the resulting products, simplicity of design, and low energy use (Regalado *et al.,* 2004).

2.1.5.7 Superheated Steam Drying:

Drying with superheated steam (SS) eliminates air and the drying takes place in a medium composed entirely of steam. The additional sensible heat present in the super-heated steam is used to dry biomaterial. The water vapor evaporated from the product can be used to dry the product by recycling the same and providing additional sensible heat. Moreover, any conventional convection and conduction dryer can be easily adapted to use superheated steam. Fixed bed, fluidized bed, flash, impingement, pneumatic, and spray dryers use superheated steam technology for quality drying of produce.

Air impingement is used for baking and cooking of products such as potato chips, pizza, cookies, and flat bread and in the paper industry in the final stages to form sheets of paper. This method can prepare low-fat potato chips (Rahman and Labuza, 2007). SS-processed potato chips retained more vitamin C and had a better texture than air-dried samples. It was observed that mass transfer followed Fick's law of diffusion and heat transfer within the potato was considered to follow Fourier's law of heat conduction (Leeratanarak *et al.,* 2006). However, attention should be given to the effect of SS impingement drying on product quality, including shrinkage, crispness, and microstructure.

Trials indicated that superheated steam drying can be effectively used for numerous products like corn starch, potato starch, and other particulate materials, taking advantage of fluidized beds if particles are not too large or too fine to be fluidized. The model for SS drying in a fluidized bed was developed based on diffusivity theory and uses a number of assumptions. Among them are (1) condensation of water vapor on samples occurs below the boiling point of water, (2) all of the heat transferred to the sample surface is used for evaporation when the sample temperature is equal to the boiling point, (3) the boiling point of water changes the pressure at the local point of the sample, (4) overall heat transfer coefficient on the sample surface includes thermal radiation from the

drying medium, and (5) the drying process is complete when the temperature of the sample is higher than the boiling point of water. (Taechapairoj *et al.,* 2006, Heinrich *et al.,* 1999) developed mathematical models for granular solids under normal pressure, which considered different heat and mass transfer mechanisms in three distinct drying periods; steam flow was assumed as plug flow, and the interaction between particles and steam was ignored. (Yang et al., 2011b) developed an unsteady, axisymmetric two-dimensional mathematical model for a superheated steam fluidized bed–drying process using a Eulerian model to describe the turbulent flow of vapor and solid phases.

They concluded that the model can be used to predict the spatial distribution of various thermodynamic and hydrodynamic parameters for the given boundary conditions, operating conditions, and physical properties of vapor and particles. Food products that are sensitive to high temperatures have a high potential to be processed with SS flash drying when processing them under a vacuum. Pneumatic (flash) drying is a process in which the transporting gas changes into superheated steam. It is mainly used to dry organic compounds such as lignite, bark, peat, and pulp.

2.1.5.8 Hybrid Drying/Combination Drying:

Hybrid drying techniques are becoming common because the combined technology receives the benefits of the individual process. Several combined drying systems have been tested. There exist a vast possible number of combinations and as technology continues to improve, more will be developed. Combination drying is considered the best way to reduce energy consumption and improve quality. Optimization of energy through mathematical modeling is another important way to reduce energy consumption. Intermittent drying and electro-drying technologies are also used to reduce energy consumption. Among these different hybrid methods, microwave-assisted drying techniques have been studied extensively.

Microwave technology uses electromagnetic waves that pass through the material and cause its molecules to oscillate, generating heat. Microwave heating generates heat within the material and heats the entire volume at about the same rate. When the material couples with microwave energy, heat is generated within the product through molecular excitation. Microwave technology can be combined with conventionally heated drying units and they are amenable to easy automation. The

overall ratio of moisture loss to solids gain was higher in microwave-assisted osmotic dehydration than in conventional osmotic dehydration. Microwave-assisted drying uses electromagnetic energy in the frequency range of 300 MHz to 300 GHz; 2,450 MHz being is the most commonly used frequency. Microwaves are generated inside an oven by stepping up the alternating current from domestic power lines at a frequency of 60 Hz up to 2,450 MHz. A device called a magnetron is used to accomplish this. The use of microwave energy for drying has been demonstrated to require moderately low energy consumption. The volumetric heating and reduced processing time make microwaves an attractive source of thermal energy. Because microwaves alone cannot complete a drying process, to further improve the efficiency of the microwave process, it is recommended that techniques such as forced air or vacuum be used in combination with microwaves (Chou *et al.,* 2001)

To control the product's temperature, either power density (W/g of material) or duty cycle (time of power on-off) must be controlled. Microwaves are usually most beneficial during the falling rate drying period (Changrue *et al.,* 2004). As the material absorbs the microwave energy, a temperature gradient occurs where the center temperature is greater, forcing the moisture out. Almost all of the drying takes place in the constant rate period and the falling rate period is highly minimized by the application of microwaves (Schubert and Regier, 2005). The dielectric loss factor of a material is a measure of the ability of the material to dissipate electric energy (Wang *et al.,* 2002). Dielectric properties are specific only for a given frequency and material properties. The dielectric properties change as a function of temperature and moisture; hence, the uniformity of moisture and drying temperature governs the uniformity of the drying process.

The use of microwave energy in drying offers reduced drying times and complements conventional drying in later stages by specifically targeting the internal residual moisture. The drying of potato slices with microwaves demonstrated that good quality dried products can be achieved by varying power density and duty cycle time. In dried carrots, improved color, shrinkage, and rehydration properties were obtained. The quality of raisins dried by microwave was superior to hot air-dried samples in color, damage, darkness, crystallized sugar, stickiness, and uniformity (Song *et al.,* 2007, Wang and Xi, 2005).

The advanced drying methods have significantly revolutionized drying of food material, but even after more the drying of biomaterial for food, fiber, and fuel remains a highly complex phenomenon, posing enormous challenges to scientists and engineers in terms of energy efficiency of the process and the resulting product quality. Therefore, drying engineers have their efforts directed towards improving the drying systems that are available.

2.1.5.9 Convective drying systems:

The essence of all drying processes is the removal of volatile substances (moisture) from a mixture to yield a solid product. In general, drying is accomplished by thermal techniques, and thus involves the application of heat, most commonly by convection from a current of air. During the convective drying of solids, two processes occur simultaneously, namely: transfer of energy from the surrounding environment; and transfer of moisture from within the solid. Therefore, this unit operation may be regarded as a simultaneous heat and mass transfer process. Moreover, the rate at which drying is accomplished is governed by the relative magnitude of the two processes.

2.2 Convective Food Drying Modelling Approaches:

Drying is a significant unit process applied in food preservation and its evolution has borne technology that is applicable to a wide range and variety of food products than any other food preservation method. It is a physical process that involves thermal removal of moisture/volatile substances from a material(s) to attain a required moisture content and should yield high product quality and achieve high throughput at frugal operational costs (Motevali *et al.,* 2011). Drying is usually an energy-intensive unit operation, and thus the need to use efficient processes and equipment. Moreover, in modern times, most equipment lifecycle is evaluated from its efficiency in energy consumption (Strumillo, 2009). There is, therefore, continuous development of drying systems to achieve innovative drying technologies through intensive research and development, through experimentation, numerical and simulation analysis of proposed technological advancements in drying technology, through design and performance/trouble-shooting assessment of systems and equipment. Experimentation is the backbone of the research and development process, but it is complemented by numerical modelling and simulation to reduce costs and time inputs. For experiments, data is usually analyzed by making correlations of appropriate parameters

which results in algebraic equations i.e. linear or non-linear equations whose solution would show changes in process inputs. On the other hand, numerical simulation involves describing a system using representative elementary volume(s) under particular physical processes i.e. mass and heat transfer. The physical processes are defined by models in form of partial differential equations whose solution under defined boundary conditions (defined under the property parameters in *Table a*) would give equipment and process environment/performance (Jangam, 2011, Kumar *et al.,* 2014). The models can easily be interpreted using the scale approach *Figure 2.1* and thus categorized as macroscale and microscale models. The microscale models consider physical processes at a microscopic scale while the macroscales consider the food material as a continuum for which each point within the material is considered to be representative elementary volume and it is selected not to have variations in representative elementary volume.

Table a. Fundamental parameters when Modeling drying of porous material (Versteeg, 2007).

Parameter	Parameter property
Transport phenomena	Mass, both mass and heat, conjugated and non-conjugated
Dimension and Geometry	1Dimension, 2Dimension, 3Dimension
Scale	Macro, micro, multiscale approach
Transfer coefficients	Empirical, simulation (CFD), semi-empirical, optimization
Solution methods	Finite Discrete Method, Finite Volume Method, Finite Element Method, numerical method
Thermophysical properties	Isotropic, anisotropic, variable properties
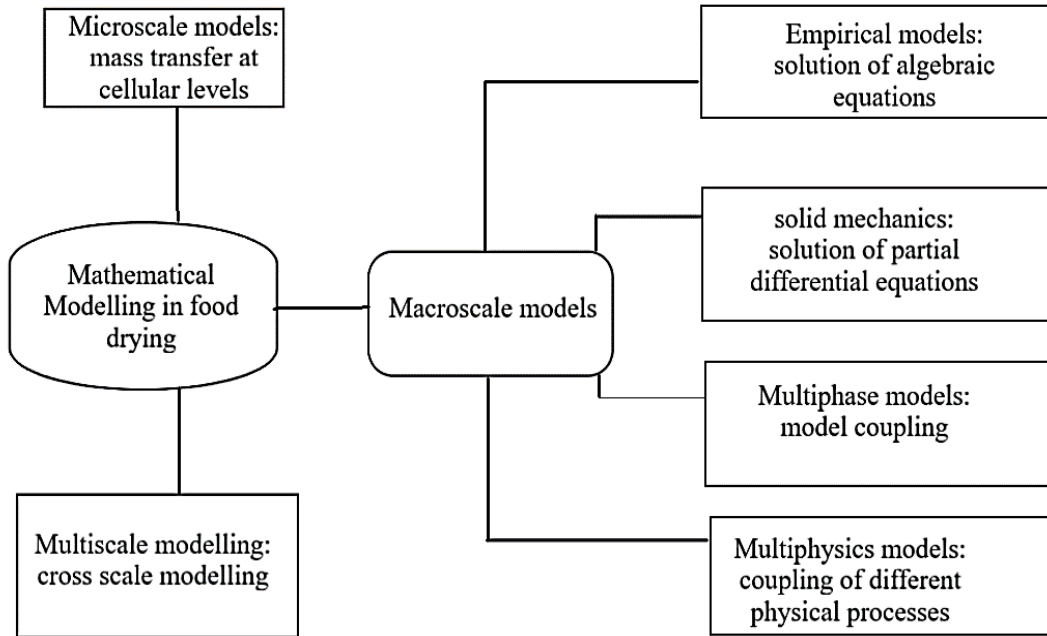
Figure 2.1. Mathematical modelling approaches (Defraeye, 2014, Castro *et al.,* 2018).

Numerical modelling in food engineering is still a developing phenomenon. Most researchers have applied to analyze the physical processes that occur in the drying process. Dried food quality is increasingly gaining significance due to the dynamic consumer preferences and the need to maintain the micronutrients in the food. Therefore, researchers are increasingly applying numerical modelling to food drying to process and equipment design and to optimize on quality of dried foods. The aim of this review is to comprehend on several alternatives in convective food drying modelling in the recent past using the scale modelling approach, and coupling of models with properties that enable modelling considerations such as shrinkage and quality deterioration modelling such as colour, texture and bioactive compounds based on studies reported in the literature in the recent past. Through their comparison and analysis, the future perspectives and challenges in drying modelling are discussed.

2.2.1 Fundamental principles in convective drying modelling:

The convective drying process is based on principles governing heat, mass and momentum transfer between solid food and surrounding air which are represented in ***Table b***.

Table b. Representative models of heat, mass, and momentum in convective drying

No. Model	Heat transport equations	Reference
1	$\frac{\delta y}{\delta x} = \nabla \cdot (\alpha \nabla T)$- The general energy PDE	(Ruiz-López and García-Alvarado, 2007)
2	$\frac{\delta T}{\delta t} = \propto (\frac{\delta^2 T}{\delta x^2} + \frac{\delta^2 T}{\delta y^2})$ -2D energy PDE	(Moraga *et al.*, 2011, Esfahani *et al.*, 2014)
3	$\frac{\delta T}{\delta t} = \propto (\frac{\delta^2 T}{\delta x^2} + \frac{\delta^2 T}{\delta y^2} + \frac{\delta^2 T}{\delta z^2})$ -3D energy PDE	(Chandramohan, 2015, Esfahani *et al.*, 2014)
	Mass transport equations	
4	$\frac{\delta x}{\delta t} = \nabla \cdot (D_{eff} \nabla X)$ - The general moisture transport PDE.	(Ruiz-López and García-Alvarado, 2007)
5	$\frac{\delta x}{\delta t} = D_{eff}(\frac{\delta^2 X}{\delta x^2} + \frac{\delta^2 X}{\delta y^2})$ - 2D moisture PDE	(Esfahani *et al.*, 2014)
6	$\frac{\delta x}{\delta t} = D_{eff}(\frac{\delta^2 X}{\delta x^2} + \frac{\delta^2 X}{\delta y^2} + \frac{\delta^2 X}{\delta y^2})$ - 3D moisture PDE	(Villa-Corrales *et al.*, 2010)
7	$\frac{\delta x}{\delta t} = \frac{1}{r}\frac{\delta}{\delta r}(rD_{eff}\frac{\delta X}{\delta r}) + \frac{\delta}{\delta r}(D_{eff}\frac{\delta X}{\delta y})$ - 2D expressed in cylindrical coordinates	(Chandramohan and Talukdar, 2010, Lemus-Mondaca *et al.*, 2013, Rodríguez *et al.*, 2014)
8	$\frac{\delta X}{\delta t} + u\frac{\delta X}{\delta x} = D_{eff}\frac{\delta^2 X}{\delta x^2}$ - 1D with shrinkage as a convective velocity	(Chandramohan, 2016, Esfahani *et al.*, 2014)
	Momentum equations	
9	$\rho \; \delta u/\delta t - \nabla("\eta + \rho" (c\_\mu k^2)/(\sigma\_k \varepsilon)) * (\nabla u + (\nabla u)^T + pu * \nabla u + \nabla p = 0 \lim_{x\to\infty}$ - momentum transport for the air in a drying tunnel represented by the standard k-ε model	(Sabarez, 2012)
10	$\rho_a C_{\rho a}\left(\frac{\delta y_\infty}{\delta t}\right) + \nabla(-\lambda_a \nabla T_\infty) + \rho_a C_{\rho a} u \nabla T_\infty = 0$ - energy balance in drying air, considering convection and conduction	(Sabarez, 2012)
	Thin-layer drying equations	
11	$MR = \exp(-kt)$; $MR = \exp(-kt^n)$; $MR = \exp[-(kt)^n]$; $MR = a\exp(-kt)$; $MR = a\exp(-kt) + c$; $MR = a\exp(k_0 t) + b\exp(-k_1 t)$; $MR = a\exp(-kt) + (1-a)\exp(kat)$; $MR = 1 + at + bt^2$; $MR = a\exp(-kt) + (1-a)\exp(-kbt)$	(Mutuli and Mbuge, 2015)

Mass transport is a fundamental mechanism in the drying process and it includes hydrodynamic flow, surface, liquid, vapor and thermal diffusion (Esfahani et al., 2014). The dominant mechanism which is a factor of the food domain moisture content and its structure governs the drying rate and would, therefore be significant in modeling. Mass and heat transfer are modelled mainly using two models: distributed (e.g. equation 2, 3, 5, 6 in **Table b**) and lumped (equation 1 and 4 in **Table b**) parameter models derived from Fourier's law (heat transfer) and Fick's second law of diffusion (mass transfer). The distributed model considers both mass and heat (external and internal) transfer which gives a good prediction of temperature and moisture gradients. On the other hand, lumped models consider uniform temperature distribution in the product that equals air temperature. But for a material of significant thickness, there could be variation in temperature in the domain therefore the assumption of isothermal conditions would skew the analysis. In that case, analysis is done thin-layer drying equations, which regards the sample domain to be of thin structure such that the temperature distribution could be assumed to be even and it is suitable for lumped parameter models (Akpinar, 2006). Thin layer modeling of a drying process can be accomplished based on an empirical/semi-empirical approach or principles of physics and mathematics (theoretical models). For the empirical/semi-empirical drying models, they are relatively simpler to compute and interpret mathematically i.e. developed from moisture content/ moisture ratio and drying time correlation (Ertekin and Firat, 2017). The empirical models are inadequate in the description of key physical principles. Henderson and Pabis, logarithmic, two-term exponential, Newton, Page and Midilli, and Kucuk models are examples of semi-theoretical thin layer drying models used to predict the drying curves (Lemus-Mondaca *et al.,* 2013). Further reading on the derivation of the semi-theoretical models can be obtained from (Erbay and Icier, 2010). The theoretical models can be expressed to consider either both the solid and air domain (conjugated) or just the solid domain only (non-conjugated) (Defraeye and Radu, 2017, Lamnatou *et al.,* 2010, Lemus-Mondaca *et al.,* 2017, Sabarez, 2012). From literature, most authors have applied reported on the application of non-conjugated models compared to conjugated models.

2.2.2 Macroscale models:

2.2.2.1 Empirical models:

These models have predominantly been applied in the description of the drying characteristics of fruits and vegetables. They are developed based on experimental analysis of the physical processes that occur during drying and they encompass the thin-layer drying models. Some of the models are listed in *Table b* under number 11.

Several authors have reported the use of thin-layer drying models to estimate the drying time, heat and mass transfer and energy consumption (Meisami-Asl *et al.,* 2009, Gupta and Alam, 2014, Tzempelikos *et al.,* 2015, Mutuli and Mbuge, 2015, Krishna Murthy and Manohar, 2012). However, the thin-layer drying models are inadequate in predicting the drying behavior of food materials, due to the varying drying methods, conditions and characteristics of the food material. Conditions that affect the drying of a porous food material include air velocity, air temperature and material thickness (Meisami-Asl *et al.,* 2010, Kumar *et al.,* 2012). Most authors have studied the effect of air velocity to drying rate of the product at flow rates of less than 1.5 m/s (Tzempelikos *et al.,* 2014, Darici and Şen, 2015, Meisami-Asl *et al.,* 2009, Perez and Schmalko, 2009, Guan *et al.,* 2013). Their findings inferred to a direct correlation of drying rate and airflow rates, but that is significant for products with high starch like rice, potatoes, and corn at those studied airflow velocities. The effect flow velocities on drying rates of fruits and only become significant at a velocity of more than 2.5 m/s, which is an important design parameter to be considered when designing dryers for use on different food crops. The geometry of the food material i.e. shape and size has been studied by several authors. In thin-layer drying, it is expected that there is a uniform distribution of air around the material and temperature in the material domain. The authors integrated the shape factor into the kinetics of the drying model (Garau *et al.,* 2006, Panyawong and Devahastin, 2007b, Abasi *et al.,* 2009, De Michelis *et al.,* 2013, Márquez and De Michelis, 2011). The authors presented linear models of shrinkage for different food material; however, the food material is known to exhibit either elastic, hyper-elastic, elastoplastic, or viscoelastic properties. Therefore, it is expected that most food shrinkage models would be largely non-linear. There are also diverse physics that occur during drying and affect the food geometry which cannot be sufficiently comprehended by empirical models. Therefore, most of the empirical shrinkage

models developed have an inexplicit representation of the exact changes that occur in the food geometry during drying.

Moisture loss from a food material can be calculated empirically as effective diffusivity e.g. considering food material as a slab as shown in equation 2.2.

$$MR = \frac{M_t - M_e}{M_o - M_e} = \frac{8}{\pi^2} \sum_{n=0}^{\infty} \frac{1}{(2n+1)^2} exp\left[-\frac{(2n+1)^2\pi^2 D_{eff} * t}{4l^2}\right] \qquad \text{2-2.}$$

Where D_{eff} is effective moisture diffusivity (m^2/s), l is half-thickness (drying from both sides) of vegetable, t is drying time (s); MR, M_t, M_o M_e are moisture ratio, moisture content at a specific time, initial moisture content, equilibrium moisture content respectively.

D_{eff} is a function of domain temperature, moisture content, and structure. In calculating D_{eff} it is assumed that the effect of internal conditions is negligible compared to external conditions. That concept may not hold for all conditions, and the resistance to the external transfer of moisture from the food domain surface may vary at different external conditions ranges of air temperature and velocity. The ranges in which some of the conditions are insignificant for different food materials have not been stated by most authors.

Empirical models are frequently used in predicting the trends of microbial infestation, color, micro-nutrients and bioactive compounds during drying. However, they cannot be coupled with thin-layer drying models. The empirical models express relationships between the quantity of nutrient, color, microbial load and environmental variables or parameters such as temperature, moisture content, relative humidity and time. Researchers who have applied empirical modelling have developed correlations between the process variables and food parameters' content (Akdaş *et al.,* 2015, An *et al.,* 2015, Curcio *et al.,* 2015, Gupta and Alam, 2014, Mutuli and Mbuge, 2018). In practice, the models have been improved significantly due to the advancement in the analytical methods and equipment that are applied in determining the microbial infestation, color, micro-nutrients, and bioactive compounds.

In summary, the thin-layer models are important in describing the drying patterns of food material, but cannot be used to elaborately describe the underlying physics of the process. There are a lot of

gaps that are left when developing the models due to the inadequacy of the models in describing the underlying physics of the process and material during drying. Recent trends in research show that more the use of thin-layer drying modelling is diminishing in preference to physics-based modelling.

2.2.2.2 Multiphase models:

The application of the Multiphase model in drying is useful for the analysis of simultaneous heat and moisture transfer. Several authors have reported the use of single-phase transport for moisture transfer i.e. the diffusion-based models. The single-phased models are simple to apply but lack the fundamental physics of food processing (Kaya *et al.,* 2008, Mabrouk *et al.,* 2012, Golestani *et al.,* 2013, Kumar *et al.,* 2016, Khan *et al.,* 2017). Multiphase models distinctly consider transport mechanisms of water as liquid and vapour separately, therefore, giving a better understanding of the process. The formulation of multiphase models considers the representative elementary volume as a sum of the volume of three phases (gas, water, and solid). The solid phase volume is comprised of bound water volume and a non-transportable solid matrix (dry mass). Therefore, the mass balance equations are formulated with those mentioned considerations. Energy balance is formulated based on the heat transfer processes occurring in and outside the food material domain (Curcio, 2010). The development of the models relies on physical properties of the material (porosity, permeability, capillary diffusivity, thermal conductivity, density) and transport data but there exists a significant lack of the mentioned attributes for food materials. Therefore, most of the multiphase models developed are made from simplistic assumptions (Halder and Datta, 2012a, Halder *et al.,* 2011, Dhall *et al.,* 2012a, Dhall *et al.,* 2012b).

Drying transforms the material domain and changes such as crust formation, shrinkage, pore evolution, and intermittent evaporation occur, which should be considered to obtain reliable models. A multiphase model developed by (Curcio *et al.,* 2008) described a simultaneous transfer of momentum, heat, and mass inside the food considering weak internal evaporation. The transport in the food material was not characterized either as capillary or molecular diffusion. In another model (Curcio, 2010), a theoretical model was presented for drying potato based on the k-ω approach. This model was an improvement in the previous one by the author and it had capability in simulating drying characteristics of food materials accounting for the effects of velocity, relative

humidity, and temperature on drying rate. It has been shown by the author that the coupling of heat and mass transfer equations to shrinkage can yield models that realistically describe the physical processes during drying. The multiphase models developed are formidable, but they cannot be applied to diverse food materials due to the assumptions made. The convection energy transfer and material shrinkage were ignored, which are significant processes that affect the physics of material and process during drying, thus the models lacked accurate presentation of the phenomena occurring during drying.

In another model that shows the effect of porosity and shrinkage, Young's modulus equation developed at room temperature was applied (Gulati and Datta, 2015). The Young's modulus equation is known to be a function of mechanical properties of the material, moisture content, and temperature but only moisture content was considered and the model was developed based on a non-hygroscopic material yet it was proposed for a hygroscopic material. The model developed by (Mercier *et al.,* 2014) also ignored the important aspect of convection. Though he argued that the convective flux of both liquid and water vapor is almost insignificant as compared to capillary flux because convective flux comes from a negligible gas pressure gradient.

The aspect of bound water has been a challenge to many researchers yet it affects food drying fundamentally. Bound water occurs as intracellular water and cell wall water (Caurie, 2011). The cell wall water has distinguishing characteristics; it cannot act as a solvent, can only be frozen below the freezing point of free water, and it exhibits negligible vapor pressure which causes a variation of the binding energy of bound water. This strongly affects the drying process, since it requires more energy to remove the bound water than free water. Bound water should be removed for the food to be characterized as dry, but that also affects material structure as it causes anisotropic shrinkage and could also result in stability problems during storage. Most authors have not considered bound water but have considered all the water as free water implying that there exists no water in the solid matrix (Datta, 2007, Halder and Datta, 2012b, Gulati *et al.,* 2015, Joardder *et al.,* 2017b).

Generally, multiphase modeling has evolved and authors have developed formidable models that can be applied to predict the physical processes. However, to obtain accurate models material

properties need to be developed and this is a gap the researchers in the food industry need to address.

2.2.2.3 Multi-physics Modelling:

Physical processes of mass, momentum and heat transfer occur in a drying process between the environment and material, inside the material and between materials interfaces (***Table c***). Multi-physics models are a result of the coupling of these physical processes. The definition of physics depends on the drying technique and the properties of the material. Numerical approximations are applied to solve the model equations (Cohen, 2011).

Coupling of heat, mass transfer and physical processes for example deformation, radiation, airflow; (bio)chemical or biological (degradation) processes would help develop models that would be important to optimize on food processing in terms of quality and safety parameters (Chen *et al.,* 2012, Akdaş *et al.,* 2015). Developing novel drying systems does require an unprecedented integrative Modeling approach.

Table c. Transport processes during a drying process

Transported variable	Heat	Liquid	Vapour	Air	Solid
Transport mechanisms	• Diffusion • Advection	•Diffusion •Convection	• Diffusion • Convection	•Diffusion •Convection	• Mechanical deformation
Volumetric source/sinks	• Phase change • Electromagnetic radiation • Chemical binding/release energy	•Phase change •Chemical binding/release of water •Gravity	• Phase change	None	• gravity
Driving forces	• Temperature • Concentration	•Capillary pressure •Gas/liquid pressure •Concentration •Temperature	• Gas pressure • Concentration • Temperature	• Gas pressure • Concentration • Temperature	•Water content •Temperature

Models with Shrinkage:

Empirical models have been applied generally applied in the study of shrinkage. Correlations are made based on volume change and moisture content as shown in equation 2.3.

$$\frac{V}{V_0} = f\left(\frac{X}{X_0}\right)$$

2-3.

where V is the volume of a material at any time t; V_0 is the volume before drying; X is the moisture content of the material at any time t and X_0 is the initial material moisture content. The correlations yield linear, nonlinear or polynomial models which can be used in combination with any drying models to predict the evolution of shrinkage with time (U.H.Joardder *et al.,* 2015, Aguilera and Lillford, 2008, De Michelis *et al.,* 2013, Golestani *et al.,* 2013). However, in many cases, an empirical drying model and a shrinkage model cannot be coupled (Katekawa and Silva, 2007). A solution of the models using model static model inputs (product characteristics and experimental conditions) would skew the results. To improve the accuracy of the model solutions, a constant update of the model inputs is required. This approach generates a better description of the drying process than the noncoupled models as the paths through which heat and mass must be transferred would be continuously adjusted according to the movement of the sample–drying medium interface during the computation (Niamnuy *et al.,* 2008a, Kittiworrawatt and Devahastin, 2009, Suvarnakuta *et al.,* 2007). This modelling approach assumes that the material undergoing drying is isotropic and homogeneous; moisture transfer is only by liquid diffusion; and no vaporization (and hence no pore formation) occurs within the drying material, which may not generate pragmatic results. The approach involves the use of the following set of transport equations 2.4 and 2.5:

$$\rho C_P = \frac{\partial T}{\partial t} = k\nabla^2 T$$

2-4.

$$\frac{\partial X}{\partial t} = D_{eff}\nabla^2 X$$

2-5.

where ρ, Cp, k and D_{eff} are the material density, specific heat, thermal conductivity, and effective moisture diffusivity.

Authors have also applied shrinkage models based on the continuum mechanics of food materials. The models include linear elastic, elastoplastic, hyper-elastic and viscoelastic (***Table d***). The linear elastic model is an elementary mechanistic model of shrinkage prediction that applies Hooke's law as a constitutive principle. Mechanical characteristics are considered as continuous and it is valid for stress that does not produce yielding. Authors have presented linear models that assume deformation occurring due to simultaneous change in heat and moisture during drying. The linear elastic model is dependent on mechanical and thermal properties of a material that are a function of temporal boundaries of temperature (Niamnuy *et al.,* 2008b, Ochoa *et al.,* 2002). The elastoplastic model describes both elastic and plastic properties, due to being stretched beyond the elastic limit. Two dimensional models in axial and radial direction have been presented by authors. It was concluded that the axial and radial shrinkage coefficients are significantly different (Yang *et al.,* 2001, Llave *et al.,* 2016). The hyper-elastic model is applied on non-elastic material. The stress-strain correlation is a function of strain energy density function and can be defined by a nonlinearly elastic, isotropic, incompressible and generally independent of strain rate. Hyper-elastic models developed have considered food material as rubber or polymer material exhibiting nonlinear stress-strain behavior. It is assumed that the change in mechanical properties due to drying causes the food to transform from a soft rubbery state to a hard glassy state (Katekawa and Silva, 2007, Kurozawa *et al.,* 2012, Dhall and Datta, 2011). A viscoelastic model describes the property of a material that exhibits elastic and viscous characteristics. Elastic materials do not dissipate energy when a load is applied, then removed. However, a viscoelastic substance looses energy when a load is applied then removed. Viscoelasticity is studied using dynamic mechanical analysis by applying small oscillatory stress and measuring the resulting strain (Sakai *et al.,* 2002).

Existing mechanistic models' have been developed based on assumptions that minimize model complexity in formulation and solution. For example, it is considered that fruits and vegetables are deformed on a small scale and therefore they have used Hooke's law for up to 10% strain levels during drying. However, it could not apply for different types of food materials because most of the fruits and vegetables undergo a large anisotropic deformation when they are subjected to

simultaneous heat and mass transfer processes during drying (Dhall and Datta, 2011, Gulati and Datta, 2015). Moreover, the viscoelastic material models in the existing literature have some limitations. For instance, to reproduce the actual material's viscoelastic behavior (with creep and relaxation phases) many parameters are needed which makes the model more complex. Moreover, the parameters are found through best fitting numerical procedures which can lead to meaningless parameters from a physical point of view (for example, negative coefficients of stiffness and viscosity in spring and dashpot). Besides this, most of the current literature has used the classical Maxwell model; however, this model cannot accurately predict the creep property of the viscoelastic fruits and vegetables (Rahman *et al.,* 2018, Joardder *et al.,* 2017a, Joardder *et al.,* 2015, Curcio *et al.,* 2016).

Table d. Continuum mechanics-based shrinkage models for food materials.

Model	Material/geometry	Reference
Elastic	Spaghetti-Infinite cylinder	(Ponsart *et al.,* 2003)
	Potato-Parallelepiped	(Chemkhi *et al.,* 2004)
Elastoplastic	Potato-Cylinder	(Curcio and Aversa, 2014)
	Semolina hydrate-Hollow cylinder	(Akiyama and Hayakawa, 2000)
Hyperelastic	Hamburger patty/Potato Slab-Cylinder/slab	(Dhall and Datta, 2011)
	Potato-Slab/cylinder	(Gulati and Datta, 2015)
Viscoelastic	Amylose starch granules & sucrose-Brick shape	(Itaya *et al.,* 1995)
	Potato-Square section	Perr´e & May (2001)
	Potato-Cylinder	Sakai *et al.,* (2002)

Material Properties in Modeling Drying Process:

Processing equipment and their respective operating systems are designed with the specificity of material(s) to be processed in perspective. Therefore, the properties of food material are a prerequisite in the precise design of either food process systems or processing equipment or both, to realize the efficient operation and control of the plants. Generally, food material (engineering)

properties are highly associated with its composition (chemical and structural organization over different spatial scales). Challenges arise when the properties are required in modeling a food process: nature of food material, precise determination of food material properties and the functional dependence of food material to processing conditions are some of the challenges that could arise. The biological materials usually have compositional variations, inhomogeneities, and anisotropic structures properties that would vary according to the environment to which the material is exposed to and usually it is difficult to control a single property in isolation.

Precise modeling of food processes requires identification of expressions for each food material, including the composition variables (e.g., moisture, ash content, lipids, carbohydrates, and protein), structural variables (e.g., porosity and tortuosity), and processing variables (e.g., temperature and pressure). Computational engineering techniques, such as the finite element, finite volume, and discrete element methods have been applied in evaluating spatial and temporal dependent properties. The methods have necessitated an elaborate analysis of the change in properties compared to experimental methods and an accurate prediction of the properties. The engineering properties include thermal (specific heat, conductivity, diffusivity); structural and geometrical (density, porosity, particle size, and shape); mechanical (textural and rheological); others (mass transfer surface tension, etc.)

In modeling a drying process, these properties are not necessary but are vital for characterization and prediction of the quality of the dried product.

Quality Modeling:

Nutritional changes in food material during a dehydration process are far-ranging depending on the characteristics and composition of the food material. Color, nutrients and other biochemical properties could be modeled to better predict the quality of the dried product (Valdramidis *et al.,* 2012, An *et al.,* 2015, Kowalski and Szadzińska, 2014). Empirical models commonly applied in predicting changes of micronutrients e.g. vitamins and bioactive compounds especially in fruits and vegetables. The models are based on correlations between the micro-nutrient and variables in the drying process as shown in equation 2.6.

$$C = f\ (T, X) \hspace{6cm} \text{2-6.}$$

Where C is the concentration of the micronutrient, T and X are variables associated with drying medium and process. e.g. temperature, material thickness, moisture content.

Correlations could result in linear, non-linear, or polynomial models and usually, fruits and vegetables have a good fit for the non-linear model (Suvarnakuta *et al.,* 2005, Khazaei *et al.,* 2008, Mutuli and Mbuge, 2018).

The use of physics-based models is still a developing phenomenon and studies have considered generic theoretical models like fuzzy logic, genetic algorithms and artificial neural network (ANN). Nutrients have been predicted using first-order reaction models, multilayer perceptron (MLP) models, and combined models; 1st order kinetics and MLP models gave a good fit for potatoes; the combined model for cabbage (An *et al.,* 2015).

Most authors have modeled food quality characteristics relative to energy and mass transfer by applying kinetic models. The models are based on the Arrhenius equation, which gives temperature and time dependence on quality parameters. Weibull model has been mainly used to predict structural deformation, microbial inactivation but also color and chemical deterioration (Xiao *et al.,* 2015, Jiang *et al.,* 2017, Jiang *et al.,* 2014, Wang *et al.,* 2017b, Tian *et al.,* 2016, Wang *et al.,* 2017a). Other models that have been used include the Williams–Landel–Ferry (WLF) equation which is derived from polymer science and the Eyring–Polanyi model from physical chemistry (Barsa, *et al.,* 2012). The WLF model applies thermal death time and glass transition temperature in the description of the kinetics of some nutrient deterioration of food under thermal treatments. Mechanistic models have made it possible to combine the physics-based models with physio/biochemical kinetic models: (Lespinard *et al.,* 2009) modeled the shrinkage and enzyme inactivation of mushrooms using COMSOL Multiphysics package under thermal treatment; (Curcio *et al.,* 2015) also developed a multiphase transport media model to predict microorganism inactivation and color change during drying. (Defraeye *et al.,* 2016) has also combined heat and mass transfer process of the intermittent drying process with a biological kinetic model for quality prediction during drying. In the development of these models, material properties for the food materials were largely estimated. There is very limited material in the available literature that deals with coupling models. Therefore, the coupled models did not highlight the representation that is needed for a high-quality product and process design. The coupled models should also consider

the kinetics of the overall quality changes in multiphase rather than focusing on the retention of specific attributes of dehydrated food products.

Authors have researched on different process parameters e.g. intermittent, continuous drying under fluidized conditions among others, on how they influence the nutrient retention and other physical processes(Thomkapanich *et al.,* 2007, Holowaty *et al.,* 2012, Mutuli and Mbuge, 2018, Tian *et al.,* 2016). A comparison of the findings of the different studies shows that conventional drying intermittent methods would result in a high retention rate of micronutrients. In practice, the intermittent method would require longer cycle times and reconfiguration of processes and equipment. The uptake of such technology for commercial-scale drying could be a challenge.

2.2.3 Microscale modelling:

Most researchers have used the macroscopic continuum approach because of the rather ease of application and solution of partial differential equations (PDEs), however, the models inadequately describe the microstructural properties of the tissue during drying. Microscale modeling is applied to describe moisture movement in the material domain and can be achieved through cross-scale modeling and multiscale modeling. Cross-scale modeling is implemented by considering a diverse range of length scales within a single computational setup. The challenge in using this modeling approach is that it yields sophisticated models that would have a high computational capability requirement associated with solving them concurrently. In the multiscale modeling sub-models based on different modeling principles, techniques and or even software are developed and computed distinctly. The accuracy of this modeling depends on the distinct sub-models and the coupling of the sub-models. In multiscale modeling, the computational cost is relatively lower in comparison with cross-scale modeling, even with a large number and high variability of the sub-models. Multiscale modeling could adopt either a series way or parallel way of coupling the sub-models. For the latter, case sub-models at different scales are solved simultaneously (Defraeye *et al.,* 2012, Ho *et al.,* 2008). The structural heterogeneity, cell level material properties and coupling of the sub-models that describe the relevant physics in each scale have hindered the use of the multiscale model (Joardder *et al.,* 2015, Perré, 2006).

Researchers have developed microscale models to study water transport inside fresh food. (Fanta *et al.,* 2014) developed a model coupled model to study water transport and mechanical deformation, nevertheless, the model was restricted to a small range of moisture variation, and it did not consider the effect of temperature on moisture transportation in micro-level, though the variation of temperature and the moisture are considerably high in the drying process. The existing microscale model did not consider both contributing physics related to temperature and moisture variation. Another model known as the mesh-free model that can be applied in simulating micro-level changes in plant-based foods at diverse moisture contents has been developed by several researchers (Liedekerke *et al.,* 2011, Karunasena *et al.,* 2014). The influence of the change of moisture content on the cell wall and the cell area was investigated. Smoothed particle hydrodynamics (SPH) and a discrete element method (DEM) were used to simulate the cellular tissue of the plant-based food material with cell mechanics incorporated to simulate the cell-wall wrinkling due to moisture loss. The approach was insightful; however, the cellular-level transport process was not addressed in the study. Additionally, there is no conclusive agreement in the literature regarding this wrinkling effect. Recent experimental investigations have shown significant cell-wall breakage instead of wrinkling due to drying of food material (Khan *et al.,* 2018).

The existing microscale drying models consider the cellular structure of the plant-based food material as circular and ignore the influence of intercellular space on the transport process during drying. However, it has been reported that the cellular structure of the food materials does not have a regular shape and the presence of intercellular spaces have an influence on the moisture transport in food materials, and the presence of intercellular space plays a great role in the moisture transport in food materials (Abera *et al.,* 2013, Aguilera and Lillford, 2008, Ho *et al.,* 2010). Therefore, it is necessary to have a proper microstructural model of plant-based food material to analyze the transport process properly.

The limitations described above need to be addressed to obtain a mechanistic understanding of the fundamental physics involved in the convective drying process. Considering the limitations and the technical challenges of the existing models, there is a critical need to develop a microscale

model based on the microstructure of plant-based food material that can handle the high temperature and moisture variation of the drying process.

2.2.4 Multiscale modelling:

The multiscale models have mostly applied for estimating molecular diffusion and explaining mass transfer mechanism and it is greatly related to microscale modelling. Presently it is a developing concept that can be applied in developing models that incorporate several microstructural elements (geometric properties of the cell, cellular water potential, mechanical properties of the cell wall, the presence of fluid in the cell as well as intercellular spaces) that can produce models on food structures profile with drying, some publications made are presented in *Table e*. Different scales of a biological material that could be considered in modelling a multi-scale process in drying are highlighted as shown in *Figure 2.2*. Multi-scale modeling has been applied to the post-harvest storage of vegetable and fruits; to evaluate water diffusion co-efficient in apple skin; in the description of the metabolic gas exchange in pear fruit in post-harvest storage, and cellular respiration modeling (Ho *et al.,* 2010, Ho *et al.,* 2008).

For Multiscale modeling, there is a challenge in developing food material properties during active drying and phase transitions which would require numerous and acutely precise experimental setups to generate the required data which is also a challenge. The models developed are quite sophisticated which would imply high computational costs associated with solving the model equations.
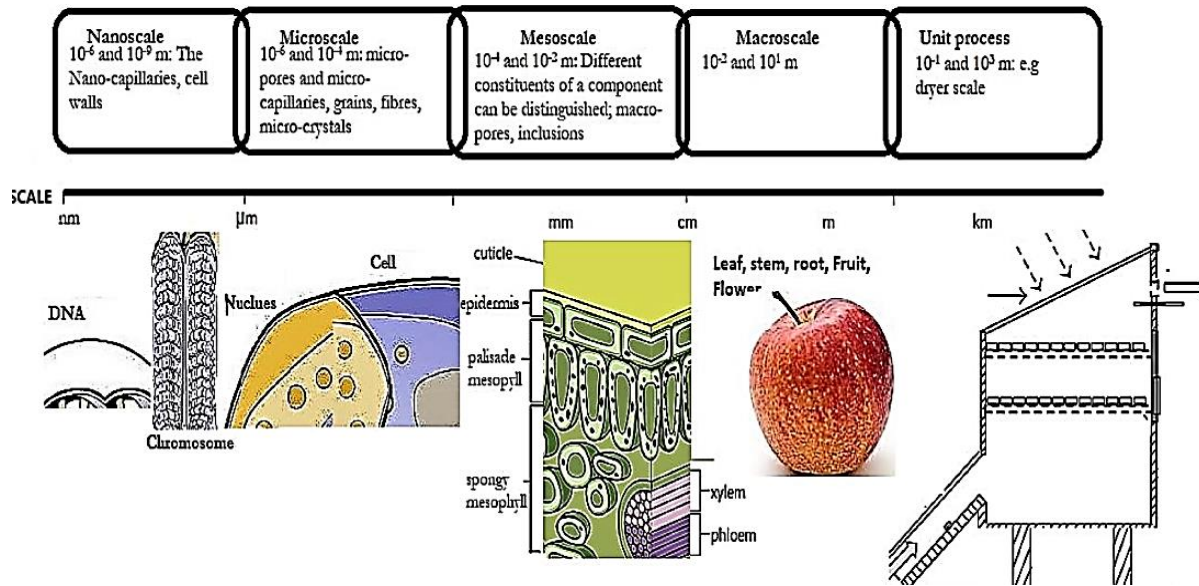
Figure 2.2. A schematic Representation of different scales in modelling (Castro *et al.,* 2018, Rahman *et al.,* 2018)

Table e. Some microscale models for convective drying.

Authors	Objective
(Van Liedekerke *et al.,* 2010)	Developing microscale transport for Apple
(Aregawi *et al.,* 2014)	Developing water transport model for apple
(Rakesh and Datta, 2011)	Multiphase porous flow for potato slab
(Defraeye *et al.,* 2013)	Microstructure characterization of apple
(Veraverbeke *et al.,* 2003)	Microscale water transport

2.2.5 Computational fluid dynamics (CFD):

Computational fluid dynamics (CFD) applies advanced numerical methods to solve the governing partial differential equations (PDEs) of heat and mass transfer and mass, momentum and energy conservation in fluid flow problems (Norton and Sun, 2006). The 3-d and temporal visual output in CFD make it a good platform for investigating airflow, temperature profile, relative humidity, residual moisture content amongst others during the drying processes. With these outputs obtained by inducing variability in boundary conditions, the product characteristics can be obtained thereby describing its drying pattern at given conditions and this can enable engineers to design new

equipment or optimize the geometry of existing ones. The accuracy of a CFD simulation depends on the user's expertise and knowledge, hence there is a high probability that its accuracy could deviate from the practical application. Nevertheless, CFD simulations still give good qualitative outputs which are a guiding tool for the design process. CFD has also been widely applied in many industries for the design process; including aerospace, shipping, automobile amongst others. With increased user expertise and refining of the CFD software, it is a robust platform which not only drying engineers, but other technical professionals could design novel technologies. The CFD software available is either on the open-source platform or used with a commercial license. They include Ansys, Openfoam, Autodesk, Simscale among others. The use of CFD in drying technology is growing and has been review by several authors (Defraeye, 2014, Jamaleddine and Ray, 2010, Kuriakose and Anandharamakrishnan, 2010, Fletcher *et al.,* 2006, Norton and Sun, 2006). A simulation flow process is presented in ***Figure 2.3***.

To use CFD the user must develop a model by accurate definition of variables, suitable mathematical equations selection, and their solution methods and appropriate boundary solutions (Jamaleddine and Ray, 2010). The equations would rely upon the fundamental laws of conservation of mass, momentum, and energy -continuity equation, Newton's second law of motion the first law of thermodynamics, as shown in ***Figure 2.2***. The equations show the functional dependence of desired flow properties to external forces (Norton and Sun, 2006).

To successfully carry out a CFD analysis, it is necessary to use engineering graphics software such as AUTOCAD, SpaceClaim, ANSYS DesignSpace, etc. to digitize the physical structure to be modelled (geometry creation). It is usually better to have a simple geometry since complex geometries require expertise in model cleanup and mesh preparation. Failing to execute the mentioned steps would often skew the results in undetectable ways. Meshing is also one of the most important factors that affect the accuracy of the simulation. The meshing quality is measured by the orthogonal quality with ranges from 0 to 1 from poor to good respectively. The aspect ratio and skewness of the cells in the mesh are also important factors considered in the process. A high-quality mesh directly correlates to the simulation accuracy.
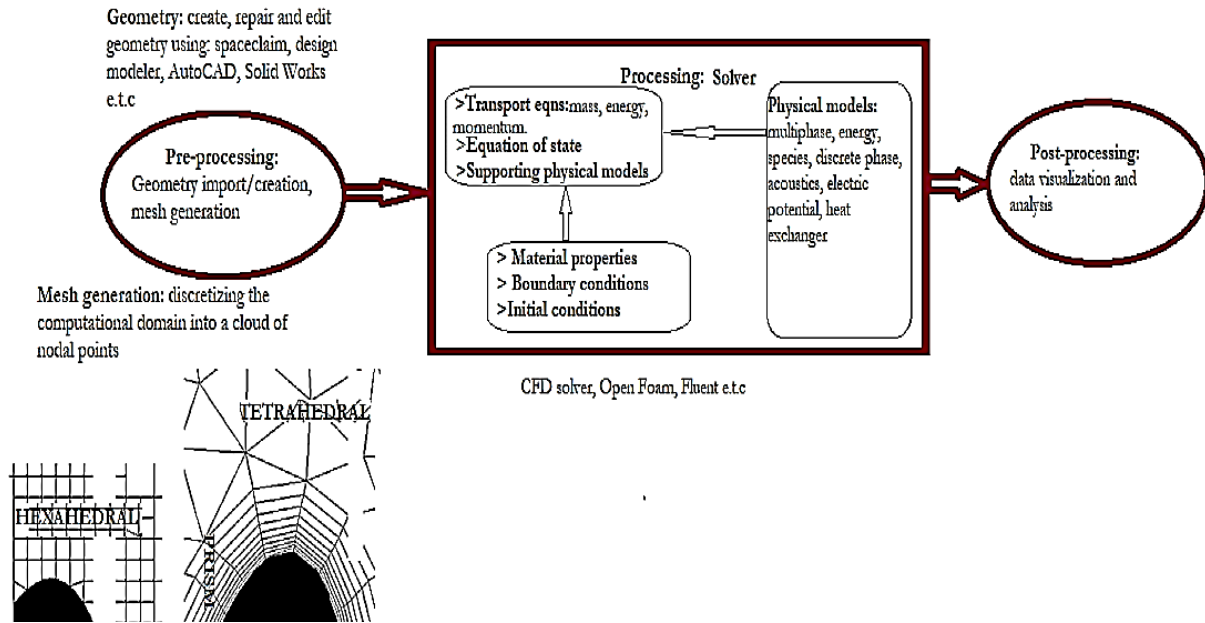
Figure 2.3. Schematic flow of a CFD simulation process (Xia and Sun, 2002, Fluent, 2013)

The choice of an appropriate technique for Modeling the fluid continuum is important for a better analysis of numerical data, solving the flow problems, and interpretation of the solution. Among the different techniques, the most important ones are the finite difference method (FDM), finite element method (FEM), and finite volume method (FVM). These approaches obtain the same solution at high grid resolutions but have a different range of applications. The FDM was identified as the simplest to implement, and useful in solving preliminary flow problems and for developing mathematical models. However, it was found to have limited application in real-time engineering problems due to the typical geometrical complexities of the systems used in the industry.

The appropriate choice of the modeling approach for the fluid continuum holds significance for precise numerical data evaluation, fluid flow problems, and results in the analysis. Finite difference (FDM), finite element (FEM), and finite volume (FVM) methods are the most significant methods of modeling. At significantly high grid resolutions, these methods return almost identical solutions with the diversity of their applications withstanding. For ease of application, most researchers have reported that the finite difference method is rather straightforward to use but has limited application in engineering problems especially where the problem in question has complex geometric configurations. The limitation arises from complexities that arise in solving the resultant

massive equations assigned to each grid node which often would result in the iteration results not converging. However, if high computational capabilities are available then the equations can be solved through advanced techniques.

FEM and FVM methods have been applied to solve more intricate geometric configurations with a good degree of accuracy (Defraeye, 2014). A comparison of FEM and FVM is that the latter has been implemented with considerably high accuracy and with limited challenges. In the application of FEM, there is an intensity of calculations involved with no physical significances and this aspect creates difficulties in the programming and understanding of the method whereas for FVM there is an ease in the comprehension of the calculations, simplicity in programming, and versatility of use(Norton and Sun, 2006).

CFD codes are widely available and are always undergoing continuous reformation to improve on their accuracy and capability to simulate complex problems. The commercial codes from ANSYS Inc., (CFX and FLUENT) are dominant with users and have a variety of educational and industrial applications (Xia and Sun, 2002). Other CFD codes that are popular with users and are reported to be accurate and powerful are PHEONICS, FLOW 3D and STAR-CD. PHOENICS codes are reported to have strong capabilities in modeling flow through porous media, conjugate heat transfer and Newtonian and non-Newtonian fluid flow (Ramachandran *et al.,* 2018). FLOW 3D is also reported to be substantively accurate especially in the modeling of free-surface flows and also it has elaborate features such as liquid-vapor and liquid-solid phase change simulations which could be useful for drying and cooling processes modeling. The STAR-CD offers ease of use when modeling any unstructured meshes. Generally, most researchers use CFD codes with capability in the modeling of flow through porous media, multiphase flows, non-Newtonian fluids and flow-dependent properties.

2.2.4 Challenges and future perspectives in convective food drying modelling:

Food material is up made of complex structure and therefore in developing models several researchers have relied on assumptions. The accuracy of the models proposed by various authors depends on the availability of important physical properties that determine heat and mass transfer. These properties include mechanical properties, thermal conductivity, permeability, and water

diffusivity. There is a lack of sufficient data on these properties, moreover, experimental determination of the real-time coefficients is complex and therefore researchers apply estimated values in modeling, which can yield significant variations and errors in final solutions (Joardder *et al.,* 2015).

Most researchers have proposed models that have excluded shrinkage, pore formation, crust formation to simplify the computation. In developing multiphase models, key aspects such as shrinkage, and bound water have been excluded (Halder *et al.,* 2011). The literature on bound water transport consideration in multiphase models is scarce. From the literature cited herein, the authors assumed that the water inside the food domain to be bulk water. The loss of bound water from the food domain is responsible for the collapse in cell structure which results in shrinkage of the material. Authors have not yet developed models that show the link between material shrinkage and different types of water transport.

In multiscale modeling, the structure and properties of food material and the phenomena occurring at the pore scale are essential for interpretations. A major challenge would be to explain the water transport phenomena in the intercellular level which would yield inaccurate statistics for designing and the validation of the model. The structural heterogeneity in the microstructure of the food materials makes it complex to generate an accurate representative elementary volume for the computation. Due to the large variations in size and shapes of cells, several statistical techniques have been proposed to build the microstructure of the food materials. Developing bidirectional relationships between sub-models due to the variations in boundary conditions would also arise. Authors have reported that the application of periodic boundary conditions would yield better results (Curcio, 2010, Dhall *et al.,* 2012a, Kumar *et al.,* 2014).

Heat application to food material will cause an increase in negative physical and biochemical characteristics. These characteristics are important parameters in food quality but literature lacks comprehensive models based on quality aspects during drying. The development of these models could result in complex models that may be difficult to validate. If the effects of factors such as pH and oxygen on nutrient degradation are factored in, it would yield to better models but maybe complex in formulation, solution, and validation

The future perspectives should be towards developing integral models that couple multiple physical processes e.g. coupled heat, mass, deformation and airflow. Models that encompass biochemical processes are important in predicting organoleptic quality and micro-nutrients loss should include the models that should be developed. The development of these models will witness the advancement of drying through the identification of complex and often conflicting interrelations in multi-objective tasks e.g. optimizing drying rate while maintaining micro-nutrient and organoleptic quality. Such inter-relations between (bio)chemical and physical processes of heat and mass transfer can unveil better pragmatism of the drying process and therefore, evaluation of drying systems can be achieved i.e. product losses, off-spec products, total throughput, process economics and energy consumption. To achieve integral modelling, user-friendly simulation software should be developed that would enable a simple implementation of the relevant physics.

In summary, accurate models of food processes, which include all the physics, still do not exist because fundamental, physics-based modelling for food processing model is still in the developing stages and this is ultimately the challenge for future researchers in the food industry.

2.2.5 Conclusion on Convective Food Drying Modelling Approaches:

Evolving modelling methods for convective dehydration of porous food material have been reviewed with the challenges and prospects being identified. In drying modeling, the future outlook is promising especially for the physics-based methods which are widely used for research purposes, though they are being limited by the availability of material properties data. Experimental methods are still the pinnacle of the research with the modelling approaches just playing a complementary part. The experimental methods are also important in the development of computational modelling approaches. The development of computational modeling approaches will be enhanced if drying engineers can be actively involved in developing software rather than computer scientists. These methods would play an increasingly important role in developing noble drying systems to achieve energy efficiency and optimum product quality.

2.3 Sorption Isotherms for Foods:

The state of water plays a crucial role in food preservation. The quality of preserved foods depends upon the moisture content, moisture migration, or moisture uptake by the food material during

storage. The extent of sorption of water by or desorption from a food product depends on the vapor pressure of water present in the food sample and that in the surroundings. The moisture content at which vapor pressure of water present in the food equals that of the surroundings is referred to as equilibrium moisture content (EMC) (Mujumdar and Devahastin, 2000). Relationship between EMC and corresponding relative humidity at constant temperature yields the so-called moisture sorption isotherm. For a given material the EMC increases with relative humidity but decreases with an increase in temperature. The phenomenon where the EMC during the adsorption and that during the desorption process is different is called ''hysteresis.'' Water activity is commonly used to characterize food quality and is defined as (equation 2.7):

$$a_w = \frac{P}{P_O} = \frac{ERH}{100}$$
2-7.

where P is the vapor pressure of water in the food material at any given temperature (Pa), P_0 is the vapor pressure of pure water at that temperature (Pa), aw is the water activity (dimensionless), and ERH is the equilibrium relative humidity (%).

Five types of isotherms were described by (Brunauer *et al.,* 1938) ***Figure 2.4***. Type 1 is the well-known Langmuir isotherm, obtained assuming monomolecular adsorption of gas by the porous solids in a finite volume of voids. Type 2 is the sigmoid isotherm obtained for soluble products, which exhibits asymptotic trend as water activity approaches 1. Type 3, known as the Flory-Higgins isotherm, accounts for a solvent or plasticizer such as glycerol above the glass transition temperature. Type 4 isotherm describes adsorption by a swellable hydrophilic solid until a maximum of hydration sites are reached. Type 5 is the BET multilayer adsorption isotherm, observed for adsorption of water vapor on charcoal; it is related to types 2 and 3 isotherms. The two isotherms most commonly found in food products are types 2 and 4.

Water adsorption by foods is a process wherein water molecules progressively and reversibly combine with the food solids via chemisorption, physical adsorption, and multilayer condensation (Van den Berg and Bruin, 1978). An isotherm can typically be divided into three regions; the water in region 1 that represents strongly bound water with the enthalpy of vaporization considerably higher than that of pure water. The bound water includes structural water (H-bonded water) and

monolayer water, which is sorbed by hydrophilic and polar groups of the food components (polysaccharides, proteins, etc.). Bound water is unfreezable and is not available for chemical reactions or as a plasticizer. In region 2, water molecules bind less firmly than in the first zone. The vaporization enthalpy is slightly higher than that for pure water. This class of constituent water can be looked upon as the continuous transition of the bound to the free water. Properties of water in region 3 are close to those of the free water that is held in voids, capillaries, crevices, and loosely binds to the food materials (Iglesias and Chirife, 1976b).

Measurement and modeling of sorption isotherms of food materials has attracted numerous researchers because of their value in industrial practice. Comprehensive reviews on sorption behavior of foods have been published (Rahman and Labuza, 2007, Labuza and Altunakar, 2007, Al-Muhtaseb *et al.,* 2004, Bell and Labuza, 2000).
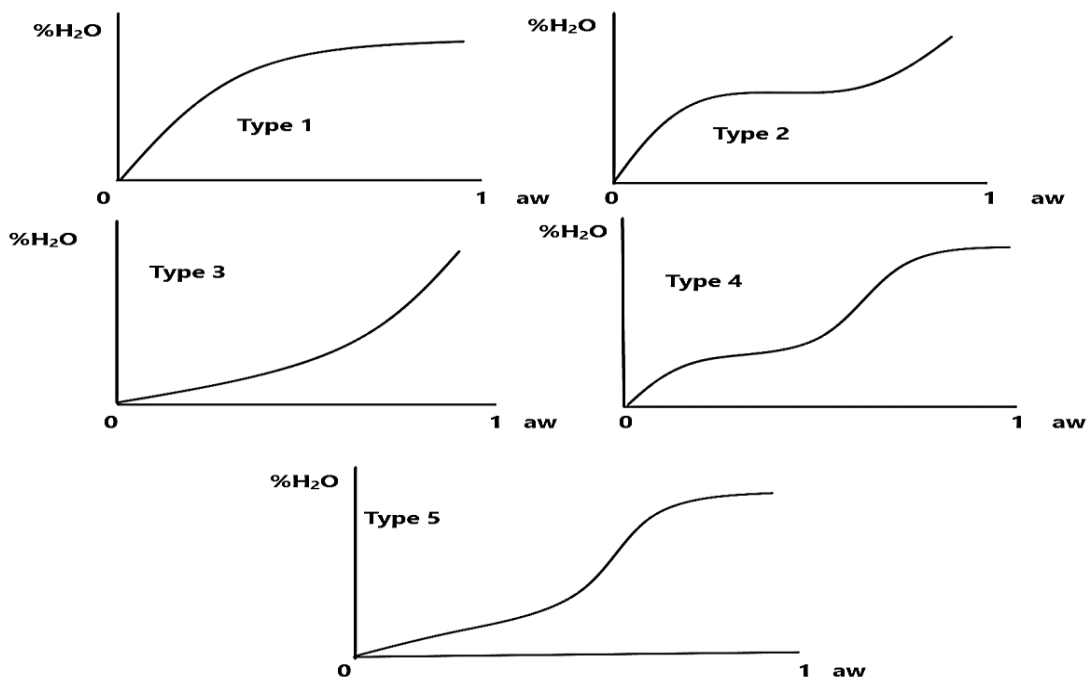
Figure 2.4. Types of isotherms
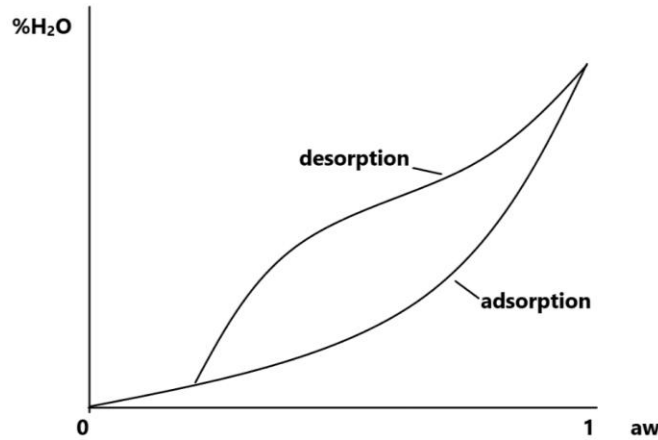
Figure 2.5. A typical sorption isotherm showing the phenomenon of hysteresis

Several scientific papers have been published covering a very wide range of products. A review of the main theories of the sorption phenomenon in foods and different mathematical models commonly used to describe sorption behavior is presented herein.

2.3.1 Thermodynamics of Sorption:

When water is removed from a food product, heat is absorbed because water has to be removed against a water activity gradient or against increasing osmotic pressure. The isosteric heat of sorption, also called differential enthalpy, is an indicator of the state of water held by the solid material. Net isosteric heat of sorption (ΔHS) is the difference of total heat of sorption (ΔHd) in the food and the heat of vaporization of water ($\Delta Hvap$) associated with the sorption process and can be computed from experimental data using Clausius-Clapeyron equation (2.8):

$$\left[\frac{d(In\ aw)}{d(\frac{1}{T})} \right]_M = \frac{-\Delta Hs}{R} \qquad \text{2-8.}$$

where the isosteric heat of sorption is associated with sorbed molecules at a particular moisture content (M). Integrating Eq. (2.9) using the associated boundary conditions:

$$\int_{aw1}^{aw2} d(In\ aw) = -\frac{-\Delta Hs}{R} \int_{T1}^{T2} d(\frac{1}{T}) \qquad \text{2-9.}$$

$$In\left(\frac{aw2}{aw1}\right) = \frac{\Delta Hs}{R}\left[\frac{1}{T_1} - \frac{1}{T_2}\right] \qquad \text{2-10.}$$

where aw1 and aw2 represent water activities at temperatures T1 and T2, respectively, and R is the universal gas law constant (8.314 kJmol^{-1}K).

Several assumptions are made implicitly in applying the Clausius-Clapeyron equation. First, the heat of vaporization of pure water (ΔH_{vap}) and the excess heat of sorption ΔH_S are assumed not to change with temperature. Secondly, the equation applies only when the moisture content of the system remains constant to time (Tsami *et al.*, 1990b, Tsami *et al.*, 1990a) From the isotherms determined at least at 10^{0}C apart, aw at any other temperature should be predictable from Eq. (2.8) if the assumptions are correct. Plotting the experimental sorption isotherm in the form ln(aw) vs. 1/T for specific moisture content, ΔHs is determined from the slope (-ΔHs/R). An empirical relationship between the net isosteric heat of sorption (ΔHs) and the moisture content (M, dry basis) is expressed as

$$\Delta Hs = \Delta Ho\ exp\left(-{}^M/_{Mc}\right) \qquad \text{2-11.}$$

where ΔHo is the net isosteric heat of sorption when moisture content (M)=0. The constant MC is characteristic moisture content (kg water per kg dry matter) of food material at which the net isosteric heat of sorption (ΔHs) has been reduced by 63%. Due to the exponential decay, the net isosteric heat of sorption becomes very small at high moisture content; e.g., at M=3 Mc, ΔHs is less than 5% of ΔHo.

The net heat of sorption of water Q (kJ per kg dry matter) from dryness (M=0) to moisture content M is expressed as:

$$Q = \int_0^M \Delta Hs dM \qquad \text{2-12.}$$

Substituting ΔHs from Eq. (2.10) into Eq. (2.11) and integrating yields:

$$Q = \Delta HoMc\left(1 - exp\left[-\frac{M}{Mc}\right]\right)$$

2-13.

For very high moisture content $(M \rightarrow \infty)$, Eq. (2.13) gives the total net isosteric heat in terms of heat of sorption of water (Q_T).

$$Q_T = \Delta H_O M_C$$

2-14

The net heat of sorption of water for a change of moisture content from M1 to M2 (Q12) is expressed as:

$$Q = \Delta H_O M_C\left[exp\left(-\frac{M1}{Mc}\right) - exp\left(-\frac{M2}{Mc}\right)\right]$$

2-15.

Equation (2.15) can be used to estimate the energy required for drying a food material from moisture content M1 to M2. In drying, M1 > M2, and the net heat of desorption (Q) is negative, because an extra amount of energy is required, in addition to the heat of vaporization of water (ΔHvap), to remove the adsorbed water from the food product. The relationship between the isosteric heat (ΔHd) and differential entropy (ΔSd) of sorption is expressed as (McMinn and Magee, 2003):

$$(-In\ aw)_m = \frac{\Delta Hd}{RT} - \frac{\Delta Sd}{R}$$

2-16

Applying Eq. (2.16) at different moisture contents, the dependence of ΔHd and ΔSd on moisture may be determined. The compensation theory proposes a linear relationship between ΔHd and ΔSd (Aguilera and Lillford, 2008, McMinn and Magee, 2003):

$$\Delta H_d = T_\beta \Delta S_d + \alpha$$

2-17

The isokinetic temperature (T_β) and constant α are computed using linear regression of Eq. (2.17). A parameter may be neglected due to its negligible contribution to the enthalpy change. The compensation theory may be further used to evaluate the effect of temperature on the sorption behavior by applying Eq. (2.17) (Aguilera and Lillford, 2008):

$$-In(aw) = \Delta Hd/R \left(\frac{1}{T} - \frac{1}{T\beta}\right)$$ 2-18

2.3.2 Measurement of Sorption Isotherms:

Many methods are available for the determination of water sorption isotherm. These methods may be classified into three categories: (1) gravimetric, (2) manometric, and (3) hygrometric. The gravimetric method involves the measurement of mass changes that can be measured both continuously and discontinuously in dynamic and static systems. Manometric methods involve sensitive manometers to measure the vapor pressure of water in equilibrium with a food material of given moisture content. Hygrometric methods measure the equilibrium relative humidity of air in contact with a food material at given moisture content. Dew point hygrometers detect the condensation of cooling water vapor. Electronic hygrometers measure the change of conductance or capacitance of hygrosensors (Troller, 1977).

The most common technique, for which a recommended procedure has been defined in the European project COST 90, uses thermostatted jars filled at the bottom with supersaturated salt solutions to maintain the desired air relative humidity ((Baucour and Daudin, 2000a)). However, this method encounters some problems at high humidity ranges due to (a) excessive equilibration times and (b) its inability to produce and control high relative humidities. Baucour and Daudin developed a rapid but accurate method to measure moisture sorption isotherms of solid foods in the water activity range 0.9–1. This method avoids the drawbacks of the saturated salt solution method by blowing calibrated air along thin slices of material at a high velocity to impose an intensive water vapor exchange between air and samples.

2.3.3 Mathematical Models of Isotherms:

Numerous attempts have been made to describe the sorption isotherms mathematically. While some models have been derived theoretically based on thermodynamic concepts, others are an extended or modified form of these models. Some of the widely used mathematical models are presented in the following paragraphs.

2.3.3.1 Langmuir Equation:

Based on monomolecular layers with identical, independent sorption sites, Langmuir proposed the following physical adsorption model:

$$aw\left(\frac{1}{M} - \frac{1}{Mo}\right) = \frac{1}{CMo} \qquad \text{2-19}$$

where M_0 is monolayer sorbate constant and C is a constant. The relation described by Eq. (2.14) yields the type I isotherm.

2.3.3.2 Brunauer-Emmett-Teller (Bet) Equation:

The BET isotherm equation is one of the most widely used models and gives a good fit for a variety of foods over the region $0.05 < aw < 0.45$. It provides an estimate of the monolayer value of moisture adsorbed on the surface (Chirife and Iglesias, 1978). The BET equation is expressed as:

$$\frac{M}{M_0} = \frac{Caw}{(1 - aw)[1 + (C - 1)aw]} \qquad \text{2-20}$$

$$\frac{aw}{(1 - aw)M} = \frac{1}{MoC} + \frac{C - 1}{MoC}aw \qquad \text{2-21}$$

where M is the equilibrium moisture content (kg water/kg dry matter), M_0 is the monolayer moisture content on the internal surface (kg water/kg dry matter), and C is a dimensionless parameter related to the heat of sorption of monolayer region.

The theory behind the development of the BET equation has been questioned due to the assumptions that (a) the rate of condensation on the first layer is equal to the rate of evaporation from the second layer, (b) binding energy of all of the adsorbate on the first layer is same, and (c) binding energy of the other layers is equal to that of pure adsorbate. The assumptions of uniform adsorbent surface and absence of lateral interactions between adsorbed molecules are incorrect in view of the heterogeneous food surface interactions.

2.3.3.3 Modified Oswin Equation:

The Oswin equation is a mathematical series expansion for a sigmoid-shaped curve and is represented as:

$$M = K \left(\frac{aw}{1-aw}\right)^{N}$$

2-22

Here, K and N are constants. The parameter K was found to be a linear function of temperature. The Oswin equation may be modified as

$$M = (A + BT)(\frac{aw}{1-aw})^{N}$$

2-23

$$Or \qquad aw = \left[(\frac{M}{A+BT})^{-C} + 1\right]^{-1}$$

2-24

with C = 1/N

2.3.3.4 Modified Halsey Equation:

Halsey developed an equation to describe the condensation of multilayers, assuming that the potential energy of a molecule varies inversely as the Cth power of its distance from the surface (Halsey, 1948). The equation is

$$aw = exp\left(-\frac{AM^{-C}}{RT}\right)$$

2-25

Because the use of the term RT does not eliminate the temperature dependence of constants A and C, Iglesias and Chirife simplified it to the form (Iglesias and Chirife, 1976b):

$$aw = exp(-A'M^{-C})$$

2-26

where A' is a new constant.

They analyzed parameter *A* of the Halsey equation and found that it could be related to temperature by an empirical exponential function. A new modified Halsey equation was therefore proposed:

$$aw = exp\left[\frac{-exp\,(A + BT)}{M^C}\right] \qquad\qquad 2\text{-}27$$

where A, B, and C are constants.

They reported that the Halsey equation described 220 experimental sorption isotherms of 69 different foods in the range of $0.1 < \text{aw} < 0.8$.

2.3.3.5 Modified Henderson Equation:

Henderson presented an equation of the form (Henderson, 1952):

$$aw = 1 - exp(-ATM^C) \qquad\qquad 2\text{-}28$$

(Thompson *et al.,* 1968) modified the Henderson equation by adding another constant to the temperature term. The modified Henderson equation becomes:

$$aw = 1 - exp[-A(T + B)M^C] \qquad\qquad 2\text{-}29$$

where A, B, and C are constants.

Henderson's equation has been applied to many foods, but compared to the Halsey equation, its applicability has been rather limited.

2.3.3.6 Chung-Pfost Equation:

Chung and Pfost developed a model based on the assumption that the change in free energy for sorption is related to the moisture content (Chung and Pfost, 1967)

$$aw = exp\left[-\frac{A}{RT}exp(-BM)\right] \qquad\qquad 2\text{-}30$$

Later, in order to obtain a better fit, Pfost et al. 1976 added a new parameter to the temperature term and combined the R parameter in constant term. The modified Chung-Pfost equation is expressed as:

$$aw = exp\left[\frac{-A}{T + C}exp(-BM)\right] \qquad\qquad 2\text{-}31$$

2.3.3.7 GAB Equation:

van den Berg refined the Langmuir and BET theories and proposed a new equation with three parameters having physical meanings (Van den Berg, 1984):

$$\frac{M}{Mo} = \frac{CKaw}{(1 - Kaw)(1 - Kaw + CKaw)}$$ 2-32

$$\frac{M}{Mo} = \frac{(C - 1)Kaw}{(1 - Kaw + CKaw)} + \frac{Kaw}{(1 - Kaw)}$$ 2-33

where C is a dimensionless GAB parameter related to the heat of sorption of monolayer region and K is a dimensionless GAB parameter related to the heat of sorption of the multilayer region.

Equation 2.33 is divided into two additive terms, the first one describes the classical mono-molecular layer expression in Langmuir's adsorption isotherms and the second term describes the multilayer adsorption corresponding to Raoult's law. Parameters K and C can be expressed by Arrhenius type equations (Van den Berg, 1984):

$$C = C' \exp(\frac{-\Delta Hc}{RT})$$ 2-34

$$K = K' \exp\left(\frac{-\Delta Hk}{RT}\right)$$ 2-35

where $\Delta H_C = \Delta H_M - \Delta H_q$; $\Delta H_K = \Delta H_l - \Delta H_q$ $(kJ\ mol^{-1})$

ΔH_l is the heat of condensation of pure water (kJ mol^{-1}); ΔHm is the total heat of sorption of monolayer (kJ mol^{-1}); ΔH_q is the total heat of sorption of multilayer covering the monolayer (kJ mol^{-1}); and C_0, K_0 are the constants of entropic character.

The GAB model underestimates the water content values at high water activities (aw > 0.93). The discrepancy under-lines two facts: (a) this type of model is unsuitable for high humidity range, and (b) the saturated salt solution method does not afford sufficient information to get a complete

sorption curve. The GAB model was refined for higher water activities by (Timmermann, 1989, Viollaz and Rovedo, 1999). They modified the GAB model by inserting a new parameter to add a third sorption stage without changing the values of the usual parameters defined in the GAB model.

Analysis of GAB isotherm

Equation 2.33 can be rewritten in one-parameter form:

$$W = \frac{1}{1-X} - \frac{1}{1-(1-C)X} \qquad\qquad 2\text{-}36$$

where W=M/M0 and X=Kaw are new coordinates. Equation 2.33 can be described for five conditions: (1) for X=0, (2) for W=1 for the so-called mono-molecular layer, (3) for X=K (i.e., for aw=1), (4) at the point of inflection W-X, and (5) potential singular points. The characteristic properties of the isotherm at these points give the limits on the parameters K and C.

1. For X=0; Eq. 2.36 gives the value W=0 identically. The shape of the sigmoid sorption isotherm may be obtained by differentiating Eq. 2.36 corresponding to the condition:

$$\frac{dw}{daw} = K\frac{dw}{dx} \geq 0$$

$$\frac{dw}{dx} = \frac{1}{(1-X)^2} - \frac{1-C}{[1-(1-C)X]^2} \qquad\qquad 2\text{-}37$$

   Substituting X=0 into Eq. 2.37, we obtain dw/dX=C, so the mentioned condition leads to the final form KC ≥0. It infers that both parameters K and C have to be of the same sign.

2. The existence of a mono-molecular layer for w=1 lead to the quadratic equation $X_m^2(1-C) - 2Xm + 1 = 0$ where Xm is the value of variable X in the mono-molecular state. The equation has the following solution for $0 < X < 1$:

$$Xm = \frac{1}{1+\sqrt{C}} \quad for\ C \geq 0 \qquad\qquad 2\text{-}38$$

In combination with condition (1) it means that both C and K have to be non-negative.

3. Substituting X=K into Eq. 2.38 and rearranging, the following equation is obtained:

$$w = \frac{KC}{(1-K)[1-K(1-C)]} \quad for \ X = k \qquad \text{2-39}$$

that must be greater than 0. This equation shows that both parameters K and C must be greater than zero. Moreover, the following condition $(1-K)[1-K(1-C)] > 0$ must be fulfilled. This inequality has two solutions:

$$\frac{a}{0} < K, C > \frac{K-1}{K}; i.e. \ C > 0 \qquad \text{2-40}$$

$$\frac{b}{K} > 1, 0 < C < \frac{K-1}{K} \qquad \text{2-41}$$

4. Points of inflection: the point of inflection of the sorption isotherm is given by the zero point of the second derivative of w-X plot. The following equation is obtained for the X coordinate (Xi) of such a point:

$$X_i^3 + \frac{3Xi}{C-1} + \frac{C-2}{(C-1)^2} = 0 \qquad \text{2-42}$$

which has a positive solution

$$Xi = \frac{Z-1}{Z^2} \ for \ C \geq 2 \qquad \text{2-43}$$

where $Z = \sqrt[3]{(C-1)}$. The relative moisture content corresponding to the point of inflection Wr is given by inserting Xi from Eq. (2.40) into Eq. (2.33)

$$Wr = \frac{Z^2 - 1}{A} \qquad \text{2-44}$$

$$where \qquad A = Z^2 - Z + 1$$

5. Singular points: No singular points can appear in Eq. (2.33) for $0 < X < 1$. This condition is fulfilled for all $K \leq 1$ but it is not fulfilled for $K > 1$.

2.3.3.8 Peleg Model:

(Peleg, 1988) developed a two-parameter model to describe the sorption curves

$$M(t) = Mi + \frac{t}{(K1 + K2t)} \qquad \text{2-45}$$

where M(t)=moisture content after time t (% dry basis), Mi=initial moisture content (% dry basis) and k1, k2 are constants. According to this model, equilibrium moisture content ME when t→∞ is given by

$$ME = Mi + \frac{1}{k_2} \qquad \text{2-46}$$

Similarly, the instantaneous sorption rate dM(t)/dt is given by:

$$\frac{dM(t)}{dt} = \frac{K1}{(K1 + K2)^2} \qquad \text{2-47}$$

and the initial rate (at t=0) by 1=K1. Equation (2.44) can be easily transformed to a linear relationship:

$$\frac{t}{[M(t) - Mi]} = k1 + k2t \qquad \text{2-48}$$

Peleg, 1993 also developed a four-parameter model:

$$M = K_1 a_w^{n1} + K_2 a_w^{n2} \qquad \text{2-49}$$

where k1, k2, n1, and n2 are constants (n1 < 1) and n2 > 1). The model expressed by Eq. 2.43 has no monolayer incorporated in it. However, plots of $\frac{aw}{[M(1-aw)]}$ vs aw are used to determine the monolayer value with the BET model are still expected to be practically linear over a water activity range of up to about 0.4. This is because at this range of aw Eq. 2.43 can be approximated by

$$M \cong k1 a_w^{n1} \quad (n < 1) \qquad \text{2-50}$$

And

$$\frac{aw}{[M(1-aw)]} = \frac{aw}{[k1a_w^{n1}(1-aw)]}$$

<div align="right">2-51</div>

The plot of $a_w/[a_w^{n1}(1-a_w)] \, vs. \, aw \, (k_1 = 1)$ is linear in this water activity range and for a range of n1 values. The intercept is positive when n1 is greater than 0.3.

$$\frac{aw}{[M(1-aw)]} = \frac{\frac{aw}{k1}}{\left[a_w^{n1}\left(1+\left(\frac{k1}{k2}\right)a_w^{n1-n2}\right)(1-aw)\right]}$$

<div align="right">2-52</div>

the added term $\left(1+\left(\frac{k1}{k2}\right)a_w^{n1-n2}\right)$ in the denominator tends to lower the magnitude of $M(1-aw)$ as the magnitude of aw increases.

2.3.4 Research Results for Sorption Isotherms of Food Materials:

Modeling of the sorption behavior of a variety of food materials has been carried out by many researchers. A list of recent research done after 2000 on different types of food materials is presented in *Table f*. This list is not exhaustive; comprehensive information of sorption isotherms for different food materials has been published.

Table f. Works on sorption isotherms of food materials

Food	Temperature (ºC)	a_w	Best fitted model	Reference
berries	4, 13, 27	0.11, 0.87	GAB	(Khalloufi *et al.*, 2000)
Mushroom	4, 13, 27	0.12, 0.75	GAB	(Khalloufi *et al.*, 2000)
Cocoa beans	25, 30, 35	0.08, 0.94	BET (aw< 0.5)	(Sandoval and Barreiro, 2002)
Starch, potato	30, 60	0.11, 0.83	GAB, Halsey	(McMinn and Magee, 2003)
Pumpkin seed flour	10, 25, 40	0.11, 0.85	GAB	(Menkov and Durakova, 2005)
Cured beef and pork	10, 20, 25, 35, 49	0.10, 0.94	Peleg, GAB	(Delgado and Sun, 2002b)
Chicken meat	4, 30	0.25, 0.94	Ferro-fontan, GAB	(Delgado and Sun, 2002a)
Hazelnuts	25	0.11, 0.90	GAB	(Güzey *et al.*, 2001)
Rough rice	0, 5, 10, 15, 20, 25, 30, 35	0.259, 0.935	Modified Chung-Pfost, modified Henderson	(San Martin *et al.,* 2001)
Yoghurt powder	35	0.4, 0.99	Modified Chung-Pfost	(Stencl, 2004)
Gelatin gel	20	0.75, 0.98	Ferro-fontan	(Baucour and Daudin, 2000b)
Crystalline lactose powder	12, 20, 30, 40	0.11, 0.98	Timmermann-GAB, GAB	(Bronlund and Paterson, 2004)

2.3.5 Statistical Testing of Sorption Models:

Statistical analysis of an isotherm may be quantified through five standards: the coefficient of determination (R^2), the residual sum of squares (RSS), the standard error of the estimate (SE), the mean relative deviation (MRD), and the plot of residuals. The coefficient of determination is a statistical measure of how closely two variables are related. The coefficient of determination is a dimensionless index that ranges from 0 to 1 and reflects the extent of the linear relationship between two data sets.

The residual sum of squares (RSS) is defined as

$$RSS = \sum_{i-1}^{n} (M - Mcal)^2 \qquad\qquad 2\text{-}53$$

where M is the measured value, M_{Cal} is the value estimated through the fitting equation and n is the number of data points. The standard error of estimate (SE) is the conditional standard deviation of the dependent variable and has the form.

$$SE = \sqrt{\sum_{i-1}^{n} \frac{(M - Mcal)^2}{df}} = \sqrt{\frac{RSS}{df}} \qquad\qquad 2\text{-}54$$

Here, df represents the degrees of freedom of the fitting equation. If a large data set is available, Eq. 2.54 is simplified to:

$$SE = \sqrt{\frac{RSS}{n}} \qquad\qquad 2\text{-}55$$

The mean relative deviation (MRD) is an absolute value because it gives the mean divergence of the estimated data from the measured data.

$$MRD = \frac{1}{n} \sum_{i-1}^{n} \frac{|M - Mcal|}{M} \qquad\qquad 2\text{-}56$$

Plotting of the residuals $(M - M_{Cal})$ against the independent variable is also used as a measure of the distribution of errors. If the model is correct, then the residuals should be only random independent errors with a zero mean, constant variance and arranged in a normal. distribution. If the residual plots indicate a clear pattern, the model should not be accepted.

In general, low values of the correlation coefficient, high values of RSS, SE, and MRD, and clear patterns in the residual plots mean that the model is not able to explain the variation in the

experimental data. It is also evident that a single statistical parameter cannot be used to select the best model and the model must always be assessed based on multiple statistical criteria.

2.3.6 Conclusion on Sorption Isotherms for Foods:

The sorption isotherm is a common approach to describe a great diversity of retention/release phenomena. It is macroscopic and empirical; thus, it is important to verify if a thermodynamic equilibrium is attained within the reaction- (or residence-) time, both for the retention and for the release stage of the compound. The measurement method also greatly affects the results and should be chosen carefully. Researchers should develop a method that allows investigation of the sorption process microscopically or using spectroscopic methods. They would provide an efficient way to verify the assumptions made when analyzing the mechanisms involved.

The application of the thermodynamic properties of the sorption mechanisms is gradually being applied to model storage structures for food material. It has enabled an accurate design of performance characteristics of the structures. The thermodynamic properties could also be applied in modelling drying systems based on the energy requirements. There is need for researchers to incorporate this aspect when developing drying systems.

2.4 African leafy vegetables' consumption:

Quite a large number of African indigenous leafy vegetables have long been known and reported to have health-protecting properties and uses (Okeno and Chebet, 2003). Reporting on the Moringa plant (Moringa oleifera) in 1937, the British botanist Dalziel observed that the roots, leaves and twigs, as well as the bark of the tree, are used in traditional medicine. Several of these indigenous leafy vegetables continue to be used for prophylactic and therapeutic purposes by rural communities (Shiundu and Oniang'o, 2007). This indigenous knowledge of the health-promoting and protecting attributes of ALVs is linked to their nutritional and non-nutrient bioactive properties. ALVs have long been and continue to be reported to significantly contribute to the dietary vitamin and mineral intake of local populations (Sena *et al.,* 1998).

More recent reports have shown that ALVs also contain non-nutrient bioactive phytochemicals that have been linked to protection against cardiovascular and other degenerative diseases,

although (Orech *et al.,* 2005) observed that some of these phytochemicals found in some ALVs consumed may pose toxicity problems when consumed in large quantities or over a long period. Despite this body of evidence confirming the nutritional contribution of ALVs to local diets, and their health maintenance and protective properties, there has been very little concerted effort towards exploiting this biodiverse nutritional and health resource to address the complex food, nutrition and health problems.

Published information on the production of indigenous and traditional leafy vegetables tends to be anecdotal. There is very little published information or data on either the areas cultivated or the production levels of specific ALVs (Okeno and Chebet, 2003). A feature article quoting reports from the International Institute for Tropical Agriculture (IITA) indicated that the total 1998 production of leafy vegetables in Cameroon was estimated to be 93,600 tonnes of which 21,549 tonnes was of "bitter leaf", *Vernonia amygdalina*. Such valuable production data are often dispersed and difficult to compare, given the gaps in coverage and different methodologies used. Even the FAO database on vegetable production fails to capture the indigenous and traditional vegetables that are commonly used on the subcontinent. Of the 15 vegetables documented in the FAO database, only tomatoes and mushrooms have some relevance to the diets of the majority of populations on the subcontinent (Joint *et al.,* 2004). This is a serious shortcoming because information from this database is used to inform and guide policy initiatives globally and, on the subcontinent, specifically (Gockowski and Ndoumbe, 2004). Reports on the diversity of traditional leafy vegetables by Bioversity International show that there are more than 20 leafy vegetable species specific to Africa that are used in daily diets and are of nutritional importance. (Ahmed and Mohammed, 1995, Okeno and Chebet, 2003) however, reported that in contrast to cash crops, little attention has been paid to the production of indigenous leafy vegetables and so there is a dearth of data on their production levels. The availability of reliable information on the production of ALVs is crucial for any planned attempts to integrate them into the global fruit and vegetables initiative for improved health.

The Kobe framework recommends that fruit and vegetable promotion interventions should consider the whole process from production to consumption. This recommendation draws attention to the gap in knowledge and information on the production and consumption of ALVs. There is,

therefore, a dire need to close this knowledge and information gap as increasing global attention is turned towards mobilizing local biodiversity for food security and health. Information on the per capita consumption of ALVs is just as scarce as data on their production levels. It is generally believed that the introduction of exotic vegetable varieties contributed to the decline in the production and consumption of indigenous vegetables. However, literature reports of a steady decline in dietary intake of these vegetables with the emergence of simplified diets are based on the assumption of declining use as a result of declining availability (Gockowski and Ndoumbe, 2004).

Contrary to this view, (Maziya-Dixon *et al.,* 2004) reported that in Nigeria, leafy vegetables are relatively available and affordable particularly during the rainy seasons but were found to be among the least consumed foods. (Ruel *et al.,* 2005) also reported that fruit and vegetable consumption of these vegetables is low although in this study the reported common vegetables "included onions, carrots, tomatoes and cabbage", vegetables which are not representative of ALVs. In Uganda, an average consumption of 160 g/person/day during the rainy season was reported while another study amongst urban dwellers quoted in the same report estimated per capita consumption of 12 g/day. (Oguntona, 1998) reported a mean intake of 65 g/day in western Nigeria while in a more recent study in south eastern Nigeria, Hart *et al.,* 2005, reported adult per capita consumption of 59-130 g/day during the months of May-July, the peak season of vegetable production in the study area. There have been other attempts at estimating consumption patterns using household expenditures on ALVs, or general survey of usage, but these estimates indicate only trends in leafy vegetable consumption. (Gockowski *et al.,* 2003), reported that in Cameroon, ALVs remain important dietary components although household expenditure on ALVs declines as total expenditure grew suggesting that consumption decreases with increasing income. These reports provide at best only a glimpse into the consumption patterns of ALVs on the subcontinent but the information provided is very limited and so should be interpreted with caution and should not be considered as baseline information for the respective countries or regions. Nevertheless, they highlight the immense information gap on ALV consumption. There is clearly a need for more regionally targeted studies on the per capita consumption of ALVs as data from such studies provide valuable baseline information which is vital both in the development of the ongoing

WHO/FAO vegetable consumption promotion strategies as well as in evaluation of the effectiveness of current and future interventions.

Despite the abundance of African indigenous and traditional leafy vegetables, they remain under-exploited and under-utilized due to various constraints. The resolution of these production and consumption bottlenecks are crucial prerequisites for the integration of ALVs into WHO's global initiative for fruit and vegetable consumption promotion. These constraints relate to production, processing, distribution and marketing, as well as nutrition information on several regionally specific cultivars. However, one of the first items in the priority list of activities needs to be the identification of regionally common species that could constitute the starting material for planned and concerted multi-sectorial research and development activities.

There is a need to develop and promote locally appropriate processing techniques to minimize post-harvest losses and ensure regular supplies of ALVs from the production areas to consumers in peri-urban and urban centres. The easy perishability of ALVs poses major challenges with their distribution and marketing. Drying has been an African way of processing leafy vegetables to make them available during periods of shortages. Drying is one solution to the problem of perishability but it does not satisfy the needs of a large population of consumers, particularly urban dwellers who prefer freshly harvested vegetables. Furthermore, not enough is known on how drying and reconstitution when cooked affect the nutritional quality of the vegetables. There are also other food safety issues such as toxicity and microbial contamination that require research attention as strategies are put in place for the promotion of increased consumption of these leafy vegetables.

A significant number of these ALVs are not consumed particularly by the younger generation of Africans because of their unfamiliar tastes or ignorance of how to prepare them. Perhaps a crucial component of the leafy vegetable promotion strategy should be their re-introduction into the daily food habits of the peri-urban and urban populations in particular through recipes developed to show traditional and modernized ways of preparing these under-utilized food ingredients. The recipes should encourage the use of the ALVs in preparing foods other than accompanying sauces in order to ensure that the vegetables are used at least twice daily, thus increasing the opportunities for their consumption.

Community women's groups, women's cooperative groups and other women's social groups would be valuable assets in recipe development projects aimed at show-casing ALVs. Bioversity International, in collaboration with the Kenyan Centre for Indigenous Knowledge/National Museums of Kenya, has taken the lead and is in the process of publishing a compilation of regional leafy vegetable recipes in a cookbook titled "African Leafy Vegetable Cookbook" featuring recipes from several sub-Saharan African countries. Regionally appropriate measuring tools and standards need to be established to ensure specificity in portion sizes, information that will be required for promotion activities. The WHO recommendation is for a minimum daily intake of 400 g of fruits and vegetables. It is not clear from the report what proportion of this total daily intake should go to vegetables. However according to the Kobe framework document and an FAO report the recommended total daily intake is equivalent to 5 servings of 80 g each of fruits and vegetables. The FAO report goes on to suggest that "a helping of cooked vegetable or raw leafy greens similar to the size of your fist may also be considered one serving". What constitutes a serving of leafy vegetables in the African context? There are obvious cultural differences in the way vegetables are prepared and consumed.

2.5 Aflatoxin progression in leafy vegetables:

Vegetables are an important component of diets and are common around the world. Their consumption is varied with low Figures noted particularly in low-income countries, and this is associated with low affordability and availability (Miller *et al.,* 2016). Several regions in the world have vegetables that are indigenous to their local population, notably Africa which is endowed with an array of leafy vegetables suited for tropical, sub-tropical and temperate climates, which could be grown throughout the year (Hart *et al.,* 2005). The most common varieties include Jute mallow (*Corchorus Olitorius*), Slender leaf (*Crotolaria Ochroleuca*), Cowpea leaves (*Vigna Unguiculata*), Giant nightshade (*Solanum Villosum*), and Amaranthus (*Amaranthus Blitum*). The African Green leafy vegetables are valuable sources of phytochemicals like beta carotene, lutein and nutrients like vitamins and minerals like calcium, phosphorus, sodium, potassium. 100 g of the African Green leafy vegetables can provide between 60 and 140 mg of ascorbic acid, 100 mg of folic acid, 4 to 7 mg iron and 200 to 400 mg of calcium, others are known to be rich in lysine, an essential amino acid that could be lacking in other diets (based on cereal and fibres), while

others are medicinal (anticarcinogenic and anti-arteriosclerotic). Green leafy vegetables also contain polyphenols that have beneficial physiological effects on humans as antioxidants (Tumwet *et al.,* 2014).

In sub-Saharan Africa when these vegetables are harvested they usually spend a considerable amount of time in the food supply chain before being consumed (Mwai *et al.,* 2007). This exposes the vegetables to not only biological degradation but also contamination that could result in the production of mycotoxins that would be harmful to the consumer. One of the most prevalent mycotoxins in agricultural produce is aflatoxin. Aflatoxins are a group of mycotoxins produced mainly by *Aspergillus flavus*, *Aspergillus parasiticus* and *Aspergillus nomius* . It is estimated that applying the US and the EU regulatory limits for example to corn, it would cause losses of 40 to 124 million USD respectively, only in the three largest corn exporting countries i.e USA, Brazil and Argentina. In low-income countries, limited food resources and lack of awareness prevents many smallholders from discarding damaged and infected food products. A climate that promotes fungal growth and suboptimal storage procedures contributes to the extensive aflatoxin contamination in these countries (Lindahl and Grace, 2013).

The *Aspergillus sp* are ubiquitous fungal species and being saprophytic they can grow under ambient conditions on a wide variety of substrates: decaying plant and animal debris. Aflatoxins are the carcinogenic contaminants of food and feeds that are frequently responsible for health and economic concerns in many countries. There are different types of aflatoxins including AFB1, AFB2, AFG1, AFG2, AFM1, and AFM2. The European Union specifies the most conservative levels of 2ng/g and 4ng/g for AFB1 and total aflatoxin respectively, In Kenya, the acceptable level of AFB1 is 10 ng/g for total aflatoxin. This level is normally specified for Aflatoxin contamination of type B1 (AFB1) and total aflatoxin contamination (Milićević *et al.,* 2010). Aflatoxin B1 is the most potent toxic metabolite, that shows hepatotoxic, teratogenic and mutagenic properties, causing damage to mammals as toxic hepatitis, hemorrhage, oedema, immunosuppression and hepatic carcinoma. It has been classified as a Class 1 human carcinogen by the (International Agency for Research on, 2002). Natural occurrence aflatoxin in the vegetables due to uptake under field conditions during growth has been studied (Hariprasad *et al.,* 2013). Aflatoxin contamination

has also largely dwelt on cereals: maize, groundnuts, soybean (Fakruddin *et al.,* 2015, Odhiambo *et al.,* 2013, Mbuge *et al.,* 2016).

2.5.1 Conclusion Aflatoxin progression in leafy vegetables:

Previous studies on aflatoxin contamination have been biased on cereals and animal products like milk and honey. Indigenous vegetables are also a significant component in the diets of the African population but little emphasis has been put in studying the contamination that could occur in the vegetables especially in the post-harvest supply chain. Just as noted earlier, aflatoxin contamination in foods has potential adverse health and economic effects.

2.6 Food Chemical Changes Influenced by Processing:

Temperature, moisture content and water activity are important physical factors in influencing the chemistry and biochemistry properties of food product during drying and storage. Water is not only an important medium for heat transfer and heat storage but also takes part in various biochemical reactions in food. A water molecule provides protons (H+), hydroxide ions (OH-), hydrogen atoms (H), oxygen atoms (O) and radicals (H•, •OH). Hence, water may act as a solvent, reactant or dispersing agent in the food matrix (Mutuli and Mbuge, 2018). As such, the water present in dehydrated foods is very important as it affects several deterioration reactions in food such as non-enzymatic browning, lipid oxidation, vitamin degradation, enzyme activity, microbial activity and pigment stability. Moreover, dissolved species in food matrix are concentrated as water is removed during drying. As a rule, the reaction rate increases with temperature and reactant concentration. Therefore, with the simultaneous concentration of dissolved solutes and elevated temperature during drying, reaction between species can be accelerated and thus increases the destruction rate of nutritional value (Labuza and Altunakar, 2007).

Reaction rate as a function of temperature and moisture content can be used to predict the extent of the deterioration of important nutritive factors during processing. Generally, first order reaction is assumed for most food deteriorations unless the rate is too slow and zero order reaction must be (Labuza and Altunakar, 2007).

2.6.1 Browning Reactions:

Colour is one of the important quality attributes for dried food product. Although the optical property is often an assessment of the physical appearance of the product, the colour development is in fact the results of various chemical and biochemical reactions. Browning reaction, in either positive or negative way, is an important phenomenon occurring in food during processing and storage. The major reactions leading to browning can be grouped into enzymatic phenol oxidation and non-enzymatic browning. Enzymatic browning is often catalyzed by the enzymes polyphenol oxidase (PPO), where the phenolics constituents are oxidized to quinones in the enzymatic reaction and then further polymerized to melanoidins (brown pigment) that has high molecular weight. On the other hand, non-enzymatic reactions are referring to Maillard reaction (reaction between carbonyl and amino compounds), caramelization, ascorbic acid browning, lipid browning and pigment destruction. The deterioration rates of the non-enzymatic browning are closely related to temperature and water activity. In most cases, the discolouration rates increase with water activity and processing temperature.

Generally, the rates of degradation follow the zero or first order kinetics while the dependence of degradation rate constant on temperature can be described by Arrhenius-type equation. However, the browning rate decelerates at high water activity values because of dilution effect on reactants concentration. The same phenomenon occurs at low water activity because solute mobility is limited below the monolayer. Browning reaction is at maximum when water activity value is in the range of 0.5 to 0.8 in dried and partial dried foods. In addition, it has been reported that activation energy of the browning deterioration can be a function of moisture or water activity. The kinetics of colour changes in food materials during drying can be modelled by using zero order or first order degradation model.

2.6.2 Vitamins and micro nutrients deterioration:

Drying which involves simultaneous heat and moisture transfers can cause deterioration for both water soluble and fat-soluble vitamins. Water soluble vitamin C (ascorbic acid) is the most labile component among all the vitamins contained in foods. Ascorbic acid is soluble in water, making it to be easily leached from cut or bruised surfaces of food and takes part in chemical degradation

such as non-enzymatic browning. It is rapidly destroyed by heat when in certain pH range and by oxidation. Compilation of ascorbic acid decay rate as a function of water activity for various food systems done by Labuza and Tannenbaum (1972) shows that ascorbic acid destruction rate increases with water activity and temperature. The loss of ascorbic acid significantly increases at higher water content in general but the destruction rates of the organic acid, somehow, do not fall at the same values for different foods at similar water activity value. The authors suggested that it could be due to various interactions with other components or diffusion limitation in each unique food system. The reaction rates of vitamin A, B1 and B2 increase with increasing water activity levels (0.24-0.65) as well, however, the B vitamins are more stable than vitamins A and C at various water activity values. Fat soluble vitamin such as β-carotene (pro-vitamin A) exhibits the highest stability at intermediate water activity. Notable loss of fat-soluble vitamins in drying is probably due to interaction of peroxides of free radicals with the vitamins where the peroxides and radicals are produced in the oxidation of lipids. Hence, retention of vitamin A and tocopherol can be increased through minimizing lipid oxidation. The milder the heating process, the greater the retention of the fat-soluble vitamins. Furthermore, destruction rate of carotenoids can be reduced when increasing the moisture content, similar trend occurs to lipid oxidation. However, increasing the moisture level increases the destruction rate for other vitamins (Mutuli and Mbuge, 2018).

2.6.3 Storage Stability:

This is concerned with the organoleptic, physical, and chemical changes that take place in the dried fruit and vegetables during storage and the rates at which these changes occur. Darkening and loss of flavour are the major types of deteriorations of dried fruits and vegetables in storage.

Sulphur dioxide content, storage temperature, and light, packaging material, moisture content, antimicrobial treatment and trace elements are the major factors affecting food storage stability. Only free sulphite is effective in retarding the formation of pigment materials. During storage, the loss of Sulphur dioxide determines the practical shelf life of the dried product with respect to spoilage through non-enzymatic browning. Storage of products at semi-tropical or summer temperatures requires residual sulphites to prevent darkening and flavour bittering, and to make the dried fruit less favorable medium for growth of micro-organisms. Sulphur dioxide helps to maintain a light, natural colour during storage. Darkening rates during storage is inversely

proportional to Sulphur dioxide content. Therefore, any condition accelerating Sulphur dioxide loss, in turn, accelerates the darkening of the product. One way to retard sulphite loss, thereby darkening, is the addition of oxygen scavenger pouch to the sealed packed sulphured dried fruit.

Storage temperature is of vital importance in relation to maintenance of quality. Storage of dried fruits and vegetables should be at relatively low temperatures to maximize storage life. There is an important effect of temperature on loss of Sulphur dioxide from the dried product during storage. A 20oF increase in temperature increases the rate of Sulphur dioxide loss approximately 3 times. Moreover, at higher temperatures, the rate of change in flavour also increases.

Light, during storage, is detrimental for quality. It causes a reduction in carotene content, increases the rate and amount of Sulphur dioxide loss, and thereby increases the rate of darkening. In addition, it also affects riboflavin content. Packaging material used and the package environment is another major factor in terms of storage stability. The type of package used varies with expected storage conditions. Packaging may be done under vacuum, nitrogen or atmospherically. Dried foods have moisture content below 20 % and a water activity 0.7 or below. They are hard and firm, resistant to microbial deterioration. There are critical water activities for some products below which browning is minimized. Storage stability increases with decreasing moisture content

Dried fruits and vegetables must be protected from rodents and insects during storage. Fumigation is often used to prevent insect infestation during storage and before packaging. In addition to fumigation, antimycotic agents (fungistats) are used to stabilize most prunes and figs against mould growth at 30-35 % moisture. Sorbic acid and sorbate salts are used as dips or sprays to prevent melding; Sulphur dioxide or sulphite salts are used to preserve fruits during drying from colour changes and browning, and to ward off insects. Potassium sorbate dip is the most effective one. The effectiveness depends on pH of the product. Some salts and metals are detrimental to nutritive value, flavour and storage quality. Raw materials may be exposed to these trace elements during washing or pre-treatment. Calcium has a firming effect on texture; iron and copper combine with tannins to cause blackening and may accelerate degradation of ascorbic acid. Sodium, magnesium and calcium sulphates impart bitter flavour. Certain salts of zinc, cadmium and chromium have toxic effects

2.7 Summary of Literature Review:

Literature relevant to this study has been reviewed. The summary of the gaps as concluded in the respective sections is presented in *Table g*

Table g. Summary of gaps identified in the literature review

No.	Subject	Gap identified
1	Convective Food Drying Modelling Approaches	• Development of user-friendly software for computational modeling approaches • Development of integral models that couple multiple physical processes • Development of sufficient food materials data for the development of accurate physics-based models
2	Sorption Isotherms for Foods	• application of the thermodynamic properties of the sorption mechanisms to model drying systems • development of microscopic or spectroscopic methods method that allows investigation of the sorption process
3	African leafy vegetables' consumption	• promote locally appropriate processing techniques to minimize post-harvest losses and ensure regular supplies of ALVs • promotion of their consumption through the development of recipes
4	Aflatoxin progression in the leafy vegetables'	• studies on aflatoxin progression in vegetables and fruits

:

CHAPTER THREE : THEORETICAL FRAMEWORK

3.0 Mathematical modeling of drying:

Several thin layer drying models obtained from literature were applied to obtain drying curves; moisture ratio was calculated using equation 3.1 and plotted as a function of time (Ertekin and Yaldiz, 2004)

$$MR = \frac{M_t - M_e}{M_o - M_e}$$ 3-1

where MR, M_t, M_o M_e are moisture ratio, moisture content at a specific time, initial moisture content, equilibrium moisture content respectively.

Table h. Thin-layer drying models considered in this study (Source: (Wang *et al.,* 2007, Akpinar *et al.,* 2003, Midilli *et al.,* 2002)

No:	Model Name	Model
1	Lewis	$MR = \exp(-kt)$
2	Page	$MR = \exp(-kt^n)$
3	Modified Page	$MR = \exp[-(kt)^n)$
4	Henderson and Pabis	$MR = a\exp(-kt)$
5	Logarithmic	$MR = a\exp(-kt) + c$
6	Two Term	$MR = a\exp(k_o t) + b\exp(-k_1 t)$
7	Two Term Exponential	$MR = a\exp(-kt) + (1-a)\exp(kat)$
8	Wang and Singh	$MR = 1 + at + bt^2$
9	Approximation of diffusion	$MR = a\exp(-kt) + (1-a)\exp(-kbt)$
10	Verma, L.R., Bucklin, R.A., Endan, J.B., and Wratten, F.T.	$MR = a\exp(-kt) + (1-a)\exp(-gt)$

11	Modified Henderson and Pabis	$MR = a\,exp(-kt) + b\,exp(-gt) + c\,exp(-ht)$
12	Simplified Fick's Diffusion	$MR = a\,exp[-c(t/l^2)$
13	Modified Page II	$MR = exp\,[-k(t/l^2)^n$
14	Midilli and Kucuk	$MR = a\,exp(-kt^n) + bt$

MR- moisture ratio; t- time; l- half-thickness of material; a, b, c, k, k_0, k_1, g, h, n are constants obtained from experimental analysis.

Selected models were fitted to experimental data and the respective model coefficients determined for each drying condition. This was achieved by applying the Levenberge-Marquardt algorithm on PTC Mathcad software (Version prime 5.0.0.0). To assess the goodness of the models, coefficient of determination (R^2), sum of squared error (SSE) and mean squared error (MSE) (equations 3.2, 3.3 and 3.4) were used. The best models returned a high R^2 and low MSE and SSE values.

$$R^2 = \frac{\sum_{i=1}^{N}(MRi - MR_{pre\,i}) * (MRi - MR_{exp\,i})}{\sqrt{([\sum_{i=1}^{N}(MRi - MR_{pre\,i})^2] * [\,(MRi - MR_{exp\,i})^2])}} \qquad 3\text{-}2$$

$$SEE = \sqrt{\frac{\sum_{i=1}^{e}(MR_{prev\,i} - MR_{exp\,i})^2}{e - P}} \qquad 3\text{-}3$$

$$MSE = \left[\frac{1}{N}\sum_{i=1}^{N}(MR_{prev\,i} - MR_{exp\,i})^2\right] \qquad 3\text{-}4$$

3.1 Effective Moisture Diffusivity and Activation Energy:

Using Fick's law, diffusivity was derived making the following assumptions: the vegetable is a slab since the diameter exceeds the sample thickness; uniform moisture distribution in the sample; symmetric diffusional mass transfer from the center; constant diffusion with insignificant

shrinkage; insignificant surface moisture movement resistance and instantaneous attainment of moisture content equilibrium with the surrounding (Vasić *et al.,* 2012, Hassini *et al.,* 2007).

The average leaf thickness from ten measurements of Cowpea leaves, Jute mallow, Slender leaf, Nightshade, and Amaranthus are 0.203, 0.201, 0.19826, 0.2319 and 0.20176mm. There was no significance of variance of the thickness of the leaf measurements at $\alpha = 0.05$; Fcal>Fcrit (31.951>2.579). Therefore, the leaf thickness measurements could be averaged without significant variation in dimensions. From equation 3.5 the effective moisture diffusivity could be determined.

$$MR = \frac{M_t - M_e}{M_o - M_e} = \frac{8}{\pi^2} \sum_{n=0}^{\infty} \frac{1}{(2n+1)^2} exp\left[-\frac{(2n+1)^2 \pi^2 D_{eff} * t}{4l^2}\right] \qquad \text{3-5}$$

D_{eff} -effective moisture diffusivity (m^2/s); l - half thickness (drying from both sides) of vegetable leaves (l = 0.10 mm); M_e -equilibrium moisture content; t - drying time (s). For long drying times; n = 1, then

$$MR = \frac{M_t - M_e}{M_o - M_e} = \frac{8}{\pi^2} exp\left[-\frac{\pi^2 D_{eff} * t}{4l^2}\right]; \qquad \text{3-6}$$

$$In(MR) = In\left(\frac{8}{\pi^2}\right) - \left[\frac{\pi^2 D_{eff} * t}{4l^2}\right] \qquad \text{3-7}$$

The effective diffusivity of water as a function of temperature was determined from Arrhenius equation 3.8;

$$D_{eff} = D_o exp\left(-\frac{E_a}{RT}\right) \qquad \text{3-8}$$

Where D_o (m^2/s); E_a - activation energy (kJ mol^{-1}); T-temperature of hot air (°C); R universal gas constant (8.314 J mol^{-1} K^{-1}). E_a can be determined, from the slope of the line (E_a/R) in a plot of Ln (D_{eff}) vs 1/T.

3.2 Shrinkage:

Shrinkage usually denotes sample volume change after/during drying to the initial volume (Desmorieux *et al.,* 2010). The vegetable initial volume (before drying) was determined from the following equation:

$$v = l \ x \ w \ x \ d \qquad \qquad 3\text{-}9$$

Where L-length; w-width; d-thickness

The shrinkage coefficient was defined as the relation between thickness and the initial thickness because the area of the material remains constant during drying.

$$Sc = \frac{di}{d_o} \qquad \qquad 3\text{-}10$$

Sc- shrinkage coefficient; d_i- continual thickness; d_o- initial thickness

3.3 Theoretical and specific energy determination:

The energy consumption calculated from equation 3.11 and compared to the estimate from the thermodynamic properties of desorption of the vegetables' analogy.

$$Et = \frac{A\upsilon\rho aCa\Delta TDt}{Wo} \qquad \qquad 3\text{-}11$$

Where:

- Et is the total energy in each drying phase (kW h),
- A is the cross-sectional area of the leaf,
- ρa is the air density (kg m^{-3}),
- ΔT is the temperature differences (°C),
- Dt   total time for drying each sample (h) and
- Ca is the specific heat of air (kJ kg^{-1} °C^{-1}).
- Wo is the primary mass of sample.

The minimum energy above the latent heat of vaporization required to remove water from a food material is referred to as the net heat of desorption. The Clausius–Clapeyron equation (equation 3.12), in combination with sorption isotherm data, can be used to calculate heats of desorption for diverse foodstuffs. Sorption isotherms of foodstuffs demonstrate hysteresis an indication of irreversibility, which can pose doubts on the reliability of the Clausius–Clapeyron equation for determining net heat of desorption. However, Iglesias and Chirife (1976), after analyzing works performed by other researchers who compared the Clausius–Clapeyron approach to calorimetric heats, concluded that the heats of irreversible processes are small enough to be neglected when calculating energy requirements for drying foodstuffs. A plot of $-In\,(a_w)$ vs 1/T would give a slope of Δh_d as shown in **Figure 5.9**.

$$-In\,(a_w) = \frac{\Delta h_d}{RT} - \frac{\Delta S_d}{R} \qquad\qquad 3\text{-}12$$

3.4 Theoretical model of heat, mass and momentum transfer accounting for shrinkage:

A convective drying process involves heat and moisture transport which occur simultaneously and are a function of moisture concentration in food material, temperature and air field properties. *Figure 3.1***Error! Reference source not found.** illustrates the conceptualization of the phenomena that occurs in a food drying process.
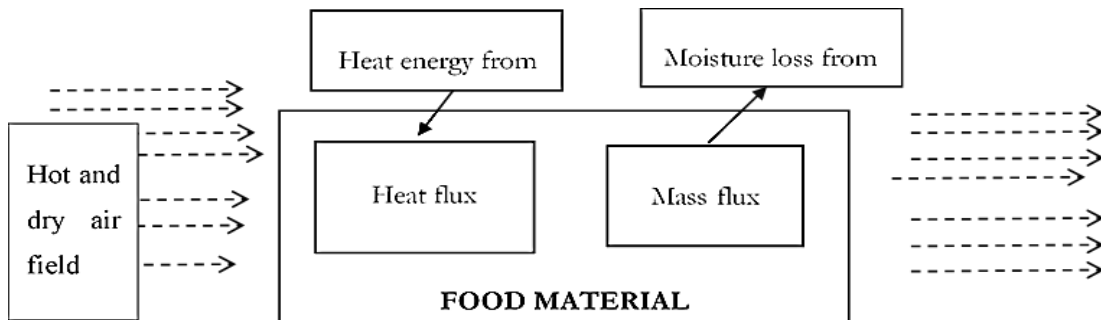
Figure 3.1. Problem formulation diagram

The food domain is considered to be of high moisture content in contact with circulating hot and dry air, moisture and heat transfers were modelled by transient mass and energy balances with the resultant net heat transfer into the food domain and mass transfer from the domain. The model was based on the following assumptions herein.

Negligible heat and mass transfer resistance through perforated food tray (Viollaz and Rovedo, 2002); the food geometry was axisymmetric. In transport of liquid water, capillary pressure prevailed over gas pressure; vapor pressure was a function of both temperature and moisture content; the food sample was assumed to be a porous continuum material; evaporation occurred over the entire food domain and also at food outer surfaces; moisture removal from the surface took place by vapor transport, diffusing into the boundary layer developing in the drying air. Vapor was convected away by the drying air, whose velocity field is expected to affect strongly the interfacial rates of heat and mass transfer; a bidimensional rectangular domain 2 by 1.5 cm with a thickness ranging from 0.2 cm was considered. Shrinkage was assumed to be limiting moisture movement. The convective influences on heat and mass transfer are from air circulation; the velocity field was evaluated by solving the non-isothermal momentum transport equations for turbulent flow, coupled with the continuity equation. It was set that evaporation would only occur at the air–food interface where the appropriate boundary conditions are specified. The boundary conditions substantially express the continuity of temperatures and heat and mass fluxes; thermodynamic equilibrium is assumed to prevail between the water concentration in air and the moisture content at the food– air interface. Physical and transport properties of air were obtained from dimensionless correlations and empirical determination.

Table i: Dimensional groups applied in calculating properties of air

Group	Definition
Nusselt number	$Nu = \dfrac{hL}{K_f} = S_t RePr = 0.0296 Re^{\frac{4}{5}} Pr^{\frac{1}{3}}$ $0.6 \leq \mathrm{Pr} \leq 60$
Sherwood number	$Sh = \dfrac{hL}{D_{AB}} = StReSc = 0.0296 Re^{\frac{4}{5}} Sc^{\frac{1}{3}}$ $0.6 \leq \mathrm{Sc} \leq 3000$
Reynolds number	$Re = \dfrac{\rho u l}{\mu}$
Prandtl number	$\mathrm{Pr} = \dfrac{C_p \mu}{K}$
Schmidt number	$Sc = \upsilon / D_{AB}$

Moisture transport in the food material is time dependent and therefore forms the unsteady-state mass transfer equation derived from Fick's law as shown in equation 3.13. Accordingly heat transfer in the food material changes with time and from Fourier's law, the energy balance leads to the unsteady-state heat transfer equation as shown in equation 3.14 (Viollaz and Rovedo, 2002, Welty *et al.*, 2001, Bird, 1960).

$$\frac{\partial C}{\partial t} + \underline{\nabla}.\left(-D_{eff}\underline{\nabla}C\right) = 0 \qquad\qquad 3\text{-}13$$

where C is the water concentration in food and D_{eff} is the effective diffusion coefficient of water in the food.

$$\rho_s C_{ps}\frac{\partial T}{\partial t} - \underline{\nabla}.\left(K_{eff}\underline{\nabla}T\right) = 0 \qquad\qquad 3\text{-}14$$

where T is temperature; ρ_s is the density of the food sample; Cps its specific heat and K_{eff} is the effective thermal conductivity.

The subscript *eff* denotes to food transport properties evaluated as effective, i.e. accounting for a possible combination of different transport mechanisms. In the porous domain, the diffusion coefficient for water vapor into air was adjusted using the Bruggeman method (equation 3-15) by assuming small evaporation rates. The energy balance does not contain any evaporation term since it is assumed that evaporation only occurs at the food surface which is exposed to the drying air. The non-isothermal flow of air within the drying chamber has been modeled by turbulent flow and the unsteady-state momentum balance coupled to the continuity equation (eqn 3.16 to 3.21) (Verboven *et al.*, 1997, Verboven *et al.*, 2001).

$$D_e = \varepsilon_p^{3/2}D_L \qquad\qquad 3\text{-}15$$

$$\rho_a\frac{\partial U_a}{\partial t} + \rho_a\underline{U_a}.\underline{\nabla U_a} = \underline{\nabla}\left[-p\underline{I} + \tau_a\right] + \frac{\nabla\varphi_a}{\varphi_a}\tau_a + \rho_a g + \frac{F_{ma}}{\varphi_a} + F_a, \quad \varphi_a = 1 - \varphi_b \qquad 3\text{-}16$$

$$\rho_b\frac{\partial U_b}{\partial t} + \rho_b\underline{U_b}.\underline{\nabla U_b} = \underline{\nabla}\left[-p\underline{I} + \tau_b\right] + \frac{\nabla\varphi_b}{\varphi_b}\tau_b + \rho_b g + \frac{F_{mb}}{\varphi_b} + F_b, \quad \varphi_b = phid \qquad 3\text{-}17$$

$$\nabla \cdot (\varphi_b u_b + \varphi_a u_a) = 0 \qquad \text{3-18}$$

$$\frac{\partial \varphi_b}{\partial t} + \nabla \cdot (\varphi_b u_b) = 0 \qquad \text{3-19}$$

$$\tau_a = \mu_a (\nabla u_a + (u_a)^T + \frac{2}{3}(\nabla \cdot u_a)I \qquad \text{3-20}$$

$$\tau_b = \mu_b (\nabla u_b + (u_b)^T + \frac{2}{3}(\nabla \cdot u_b)I \qquad \text{3-21}$$

where ρ_a is the air density; $\underline{u}$ is the velocity vector;

The energy balance in the drying air, accounting for both convective and conductive contributions, leads to equation 3.22. The water mass balance in the drying air, accounting for both convective and diffusive contributions, leads to equation 3.23 (Bird, 1960, Welty *et al.,* 2001)

$$\rho_a C_{pa} \frac{\partial T_2}{\partial t} - \underline{\nabla} \cdot (K_a \underline{\nabla} T_2) + \rho_a C_{pa} \underline{U} \cdot \underline{\nabla} T_2 = 0 \qquad \text{3-22}$$

where T_2 is the air temperature; C_{pa} is its specific heat; and K_a is the thermal conductivity.

$$\frac{\partial C_2}{\partial t} + \underline{\nabla} \cdot (-D_a \underline{\nabla} C_2) + \underline{U} \cdot \underline{\nabla} C_2 = 0 \qquad \text{3-23}$$

where C_2 is water concentration in the air and D_a is the diffusion coefficient of water in air.

The physical and transport properties of both air and food are expressed in terms of the local values of temperature and moisture content which represent a system of unsteady, non-linear partial differential equations they can only be solved by means of numerical methods.

Table j Initial conditions used in the theoretical model.

Variable	Value
Air temperature	298 K
Water concentration in air	0 mol/m3
Velocity in axial direction (uz0)	0 m/s
Velocity in radial direction (ur0)	0 m/s
Pressure in the drying chamber	1 atm
Food Temperature	298 K
Water concentration in food	3544.4 mol/m^3

A set of initial conditions, typically prevailing in an industrial drying process (**Table j**), are necessary to perform the numerical simulations. As far as the air is concerned, it was assumed that: the water concentration, was ≈ 0 mol/m^3 (corresponding to a relative humidity, Ur0, of <20%); the temperature value 298 K; and the pressure in the drying chamber was 1 atm. It was also assumed that the air was stationary (i.e. u = 0). The initial values of the food temperature and its moisture content were set equal to 298 K and 3544.4 mol/m^3, respectively. The boundary conditions are reported, for the sake of brevity, in **Figure 3.2.** The set boundaries for the modeling, where each different boundary is identified by an integer ranging from 1 to 9. At the food-air interface (boundaries 7, 8, 9), where no accumulation occurs, the continuity of both heat and water fluxes is imposed. In particular, the heat transported by convection and conduction from air to food is partly used to raise the sample temperature by conduction and partly to allow water evaporation described by considering the latent heat of vaporization. Similarly, a balance also applies between the diffusive flux of liquid water coming from the core of the sample, and the flux of vapor leaving the food surface and transported into the drying air. Moreover, the thermodynamic equilibrium at the air–food interface can be expressed as equation 3.24 (Smith *et al.,* 2001).

$$\gamma_w x_w f_w^0 = \widehat{\phi}w Y_w P \qquad\qquad 3\text{-}24$$

where γ_w, the activity coefficient of water and f_w^0, the fugacity of water, refer to the liquid phase, $\widehat{\phi}w$, the fugacity coefficient of water, refers instead to the vapor phase; Xw and Yw are the mole fractions of water in food and in air, respectively; and p is the pressure within the drying chamber. At low pressures, the vapor phase usually approximates to ideal gas behavior and can be simplified as:

$$\gamma_W X_W P_W^{sat} = y_w p \qquad\qquad\qquad 3\text{-}25$$

3.4.1 Shrinkage modelling:

Plant tissue undergoing dehydration is subjected to stresses. These stresses are developed in the material by transient fields of moisture and temperature. Thermal and moisture gradient stresses are developed simultaneously and cause shrinkage and deformation of the body undergoing drying. Thermal stresses are important only in the beginning of drying, while stresses generated by the moisture gradients occur almost during the entire drying process. Hence, shrinkage and deformation are caused mainly by stresses developed by moisture gradients. In developing this model, the assumptions made in model formulation were:

- Shrinkage was a function of moisture content

- Uniform conditions in the drying chamber

Food shrinkage was modelled defining the local total strains {dε} as a function of changes in mechanical strains {dε$_s$} (constrained deformation due to food mechanical properties) and in shrinkage strains {dε0} (the sum of a free deformation due to moisture loss). To express the free drying shrinkage strains *{dε0}*, it was assumed that the free deformation due to moisture loss was proportional to the water content variation, through a constant (the hydrous compressibility factor). The constant was estimated from the experimental data showing drying shrinkage vs. weight loss.

$$\{d\varepsilon\} = \{d\varepsilon_s\} + \{d\varepsilon_0\} \qquad\qquad\qquad 3\text{-}26$$

$$\{d\varepsilon_0\} = K_{ds}.dC_w \qquad\qquad\qquad 3\text{-}27$$

dCw is the variation in the moisture content and the hydrous compressibility factor is *Kds*
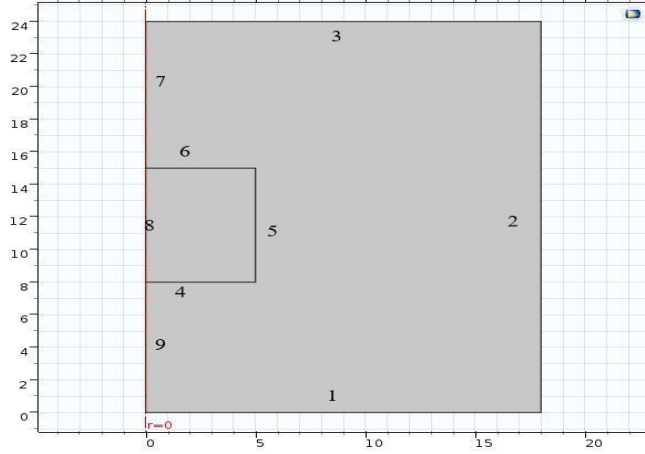
Figure 3.2. The set boundaries for the modeling

Table k: Boundary conditions applied to model

Boundary	Type of boundary condition
1	$U_r = 0$; $C = C_{air}$; $T = T_{air}$
2	$C = C_{air}$; $T = T_{air}$
	$$\left[(\eta_a + \eta_t)\left(\underline{\nabla u} + (\nabla u)^T - \left(\frac{2}{3}\right)(\underline{\nabla}.\underline{u})\underline{I}\right)\right]\underline{n} = \left\|\frac{\rho_a C_\mu^{0.25} k^{0.5}}{\left(\frac{In(\delta_w^+)}{K_C} + C^+\right)}\right\|$$ (logarithmic wall function)
3	$P = P_{atm}$
	$\underline{n}(-D_a \nabla C_2) = 0$ (convection prevailing over diffusion)
	$\underline{n}(-K_a \nabla T_2) = 0$ (convection prevailing over conduction)
7, 8, 9	Axial symmetry for (except for momentum boundary 8)
4, 5, 6	$$\left[(\eta_a + \eta_t)\left(\underline{\nabla u} + (\nabla u)^T - \left(\frac{2}{3}\right)(\underline{\nabla}.\underline{u})\underline{I}\right)\right]\underline{n} = \left\|\frac{\rho_a C_\mu^{0.25} k^{0.5}}{\left(\frac{In(\delta_w^+)}{K_C} + C^+\right)}\right\|$$ (logarithmic wall function)
	$C_2 = \gamma_w P_{vs}\frac{T}{RT}$ (equilibrium relationship)
	$\underline{n}(-D_w\underline{\nabla}C_w) = \underline{n}[(-D_a\underline{\nabla}C_2) + \underline{U}C_2]$ (mass flux continuity)
	$\underline{n}.(K_a\underline{\nabla}T_2 + \rho_a C_{pa}\underline{u}T_2) = \underline{n}.(-K_{eff}\underline{\nabla}T) - \lambda\underline{n}.(-D_{eff}\nabla C)$ (Heat flux continuity)
	$\{d\varepsilon_0\} = K_{ds}.dC_w$ (shrinkage)

The above system of unsteady, non-linear PDEs was solved by Finite Elements Method using Comsol Multiphysics 5.2. Both food and air domains were discretized into a total number of 2571

of triangular finite elements as shown in *Figure 3.3*. It was also found that the solution was independent of the grid size even with further refinements. Lagrange finite elements of order two were chosen for the components, U_a and U_b, of air velocity vector U. A Lagrange finite element of order one was used for variable p, i.e. the pressure distribution within the drying chamber. The time-dependent problem was solved by an implicit time-stepping scheme, leading to a non-linear system of equations for each time step. Newton's method was used to solve each non-linear system of equations, whereas a direct linear system solver was adopted to solve the resulting systems of linear equations. The relative and absolute tolerances were set to 0.001 and 0.0001, respectively.
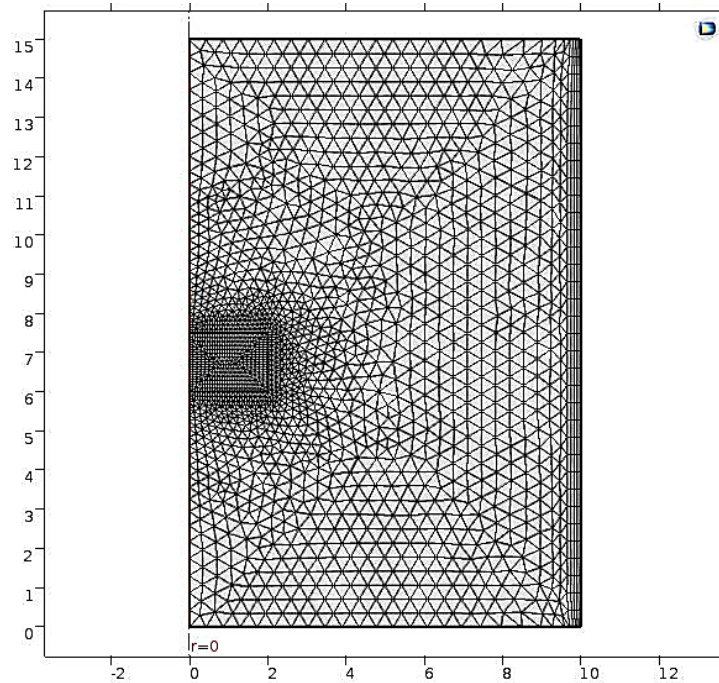
Figure 3.3. The mesh diagram

3.5 Isotherm Models:

There are several models in the literature for moisture sorption isotherms of food products. The models selected in **Table l** are the most common equations for describing sorption isotherms of food products used by researchers. The experimental data of equilibrium moisture content (Xe) as a function of water activity (aw) were fitted using the selected models.

Table l: isotherm models used for fitting sorption data

Model	Equation	Source
BET	$$emc = \frac{ABa_w}{(1 - a_w)\big(1 + a_w(B - 1)\big)}$$	(Brunauer *et al.,* 1938, Timmermann *et al.,* 2001)
Modified Halsey	$$emc = \left(\frac{In\ a_w}{-exp(A + BT)}\right)^{\frac{1}{C}}$$	(Iglesias and Chirife, 1976b)
Modified Oswin	$$emc = (A + BT) * \left(\frac{a_w}{1 - a_w}\right)^{C}$$	(Iglesias and Chirife, 1976b)
GAB	$$emc = \frac{ABca_w}{(1 - Ba_w)(1 - Ba_w + Bca_w)}$$	(Al-Muhtaseb *et al.,* 2002, Van den Berg, 1984)
Peleg	$$M = Aa_w{}^{C} + Ba_w{}^{D}$$	(Peleg, 1993)

Where M is the equilibrium moisture content d.b.; RH the equilibrium relative humidity; and a, b, c, d the models' parameters.

CHAPTER FOUR : MATERIALS AND METHODS

4.0 Introduction:

This chapter highlights how the study objectives were achieved, through the experimentation process from the sampling point to data management and statistical analyses. The experiments were carried out in different locations: the vegetable samples were grown at the University of Nairobi upper Kabete campus. The drying and sorption experiments were also conducted at the same location at the department of environmental and biosystems engineering labs. Aflatoxin experiments were done at the International Centre of Insect Physiology and Ecology (ICIPE). Nutrient analysis was done at Jomo Kenyatta University of Agriculture and Technology department of food science.

4.1 Sampling:

The samples of ALVS that were used for this study were fibrous and non-fibrous vegetables: African nightshade (*Solanum villosum*), Cowpeas (*Vigna unguiculata*), vegetable amaranths (*Amaranthus blitum*), Jute mallow (*Corchorus olitorius*), Slender leaf (*Crotalaria brevidens*). The vegetables were grown using certified seeds purchased from Kenya Seed Company Simlaw seeds, under controlled conditions of a greenhouse and appropriate agronomic practices applied. The greenhouse was constructed of polythene covering with side meshes that would allow the circulation of air when required. The temperature in the greenhouse was in the range of 27 to 32 degrees with humidity levels was between 50 to 80%. No chemical fertilizer was applied when growing the vegetables. The leaves were ready for harvesting after 3 weeks for cowpea, 4 weeks for slender leaf and Amaranthus and 6 weeks for jute mallow and nightshade under the growth conditions. Sampling of the vegetables involved harvesting by trimming the leaves for proximate experimentation. Sample preparation involved sorting and removing soiled, bruised and incomplete leaves. In the sampling process, leaves were harvested from different batches of plants to obtain an accurate representation of the characteristics found in the entire population.

4.2 Methodological approach:

➤ **Development and validation of models for the physical processes in the convective drying process**

4.2.1 Introduction:

Under this objective the drying characteristic of the vegetables were determined. The experiments were set up to study the moisture content, drying pattern, drying kinetics, the transport phenomena, nutritive value degradation and shrinkage of the leaf. The equipment that were used include a convective laboratory dryer, a HPLC, drying tray, a calibrated scale, column chromatography and UV Spectrophotometer, a micrometer screw gauge, stop watch and a desiccator.

4.2.2 Moisture content determination and drying experiment:

In experiment, samples of each vegetable type with three replications for each sample were studied and a control sample was included. The experiments were performed in accordance to all the operation requirements.

Moisture content was determined using the thermo gravimetric technique. Thermo gravimetric moisture analysis defines moisture as the loss of mass observed when the sample is heated and is based in theory, on the vaporization of water during the drying process. The sample weight was determined prior to heating and again after reaching a steady-state mass after drying. The drier was switched on an hour prior to the start of the experiment to ensure uniform distribution of heat in the chamber. The weighed vegetable samples were dried in a conventional forced-air oven at 50°C for 12 hours, followed by an additional 3 hours at 105°C, until sample weight became constant, as per the method described by (Canet, 1988) Prior to taking the weight the sample tray will be cooled in a desiccator.

The drying experiment was done for single leaves of measured dimensions. Three temperatures (30, 40, and 50°C) were applied in a calibrated Vötschtechnik® climate chamber (0-125°C ± 0.1°C temperature and 0.5 m/s air speed). The vegetables were weighed onto a 20 by 20 by 1 cm (length by width by height) perforated (1/4 " by 1/4 " aperture size) tray using a

Sartorius® scale with sensitivity 150 ± 0.001g. The vegetable leaves were spread as distinctly single leaves on the tray without overlaying each other. The drying profile was monitored by continuous weight measurements at intervals of time to the bone-dry mass ((± 0.001 change).

4.2.3 Shrinkage determination:

The study of moisture transfer and shrinkage the leaf size was of determined size and shape. Three temperatures (30, 40, and 50ºC) were used using a calibrated Vötschtechnik® climate chamber (0-125°C ± 0.1°C temperature and 0.5 m/s air speed). The vegetables were weighed onto a 20 by 20 by 1 cm (length by width by height) perforated (1/4 " by 1/ 4 " aperture size) tray using a Sartorius® scale with sensitivity 150 ± 0.001g. Selected leaves were cut into equal areas using a sharp razorblade with the aid of a paper surface of known dimensions and a Quantus micrometer screw gauge (±0.01mm, China) used to measure the leaf thickness. The thickness was determined continuously after intervals of 30 minutes to equilibrium leaf weight.

Plate 4-1. Shrinkage experimental samples

4.2.4 Nutrient content determination:

The five mentioned vegetable species (fresh and dried) were prepared for analysis of fat-soluble vitamins A (β-carotene) and E, and water-soluble vitamin C. The fresh vegetable samples were harvested for proximate analysis while the other samples were dried in a convective lab drier at 40oC for 24 hours and stored for sixty days in a dry place, at room temperature and protected from sunlight before the analyses.

Beta carotene content was analyzed using column chromatography and UV Spectrophotometer; by applying acetone and petroleum ether extraction method (Rodriguez-Amaya & Kimura, 2004). Approximately 2 grams of sample was weighed, chopped finely and placed in a mortar with about 10 mL of acetone to obtain an extract. The. The acetone extraction was progressive until the residue no longer gave color. The combined acetone extract was transferred into the 100 mL volumetric flask and 25 mL of it evaporated to dryness using a rotary evaporator. The residue was dissolved with 10 mL petroleum ether and the solution introduced into a chromatographic column, eluted with petroleum ether and beta carotene was collected in a flask. Petroleum ether was added to the beta carotene elute to make a volume of 25 mL and the absorbance was read at 440 nm in a UV-Vis spectrophotometer (Shimadzu model UV–1601 PC, Kyoto, Japan). A calibration curve was made from various concentrations of beta carotene standards.

HPLC method was applied to determine the ascorbic acid content in the samples (Vikram, Ramesh, & Prapulla, 2005). 2 g of weighed sample was extracted with 0.8% metaphosphoric acid, and made up to 20 mL of juice. The juice was centrifuged at 10,000 rpm, filtered (0.45 µ filter) and diluted with 10 mL of 0.8% metaphosphoric acid. 20 µL of the sample was injected into the HPLC machine (Shimadzu UV-VIS detector in a Shimadzu HPLC 20A Tokyo, Japan). The mobile phase was 0.8% metaphosphoric acid (Sigma Aldrich, Spain), at 1.2 mL/min flow rate and a wavelength of 266.0 nm. A calibration curve was made from various concentrations of ascorbic acid standards.

HPLC method was applied to determine the vitamin E in the samples (Stöggl, Huck, Scherz, Popp, & Bonn, 2001). 2 g of the weighed sample was extracted with 20ml of hexane, sonicated

for 30 minutes and then transferred to 50ml flask and made to the volume. The solution was filtered using cotton wool, centrifuged at 5000rpm for 10 minutes then filtered again using 0.45µm syringe filters. Analysis of the samples was by a HPLC (Shimadzu UV-VIS detector in a Shimadzu HPLC 20A Tokyo, Japan). The mobile phase was 98:2 Hexane (Sigma Aldrich Germany) to isopropanol (Sigma Aldrich Germany at 1.2 mL/min flow rate and wavelength of 292.0 nm. A calibration curve was made from various concentrations of vitamin E standards.

4.2.5 Experimental determination of SAP regeneration:

The experiment was set up using an air duct insulated to minimize heat losses as well as external heat effects. The airflow was from a fan with a variable resistor for airspeed control and air heaters were used to vary air temperature from $20^{\circ}C$ to above $50^{\circ}C$. On the system, compartments were enclosed for inserting equipment for measuring various air parameters of importance such as temperature, humidity, and velocity.

The SAP that was used has the brand name Luquafleece® supplied by BASF in Germany. In this product, sodium polyacrylate is embedded in the fabric and is white. It is in a roll of 40m long, 1m wide, and 0.003m thick sheets of fabric. For all the experiments, SAP was moist to 100% moisture content and placed perpendicular to the direction of the airflow, covering the entire duct area of dimensions 200mm $\times$ 200 mm. Only one layer of SAP was used.

To determine the effect of temperature on moisture desorption rate from SAP, the air velocity, the air temperature was varied from $20°C$ through $100°C$ in steps of $20°C$. Inlet and outlet RH were measured and recorded until the inlet and outlet RH remained constant, meaning that the SAP had attained an equilibrium moisture content. For each temperature level, the final mass and moisture content of the SAP were determined.

The effect of velocity was determined by maintaining air temperature at an average value of $50°C$. The air velocity will be varied from 0.1m/s to 5m/s in steps of 0.1m/s. The final SAP moisture content was determined for each air velocity. Set up illustrates the experimental setup.

Plate 4-2. Experimental set up photo for super adsorbent polymer characteristics.
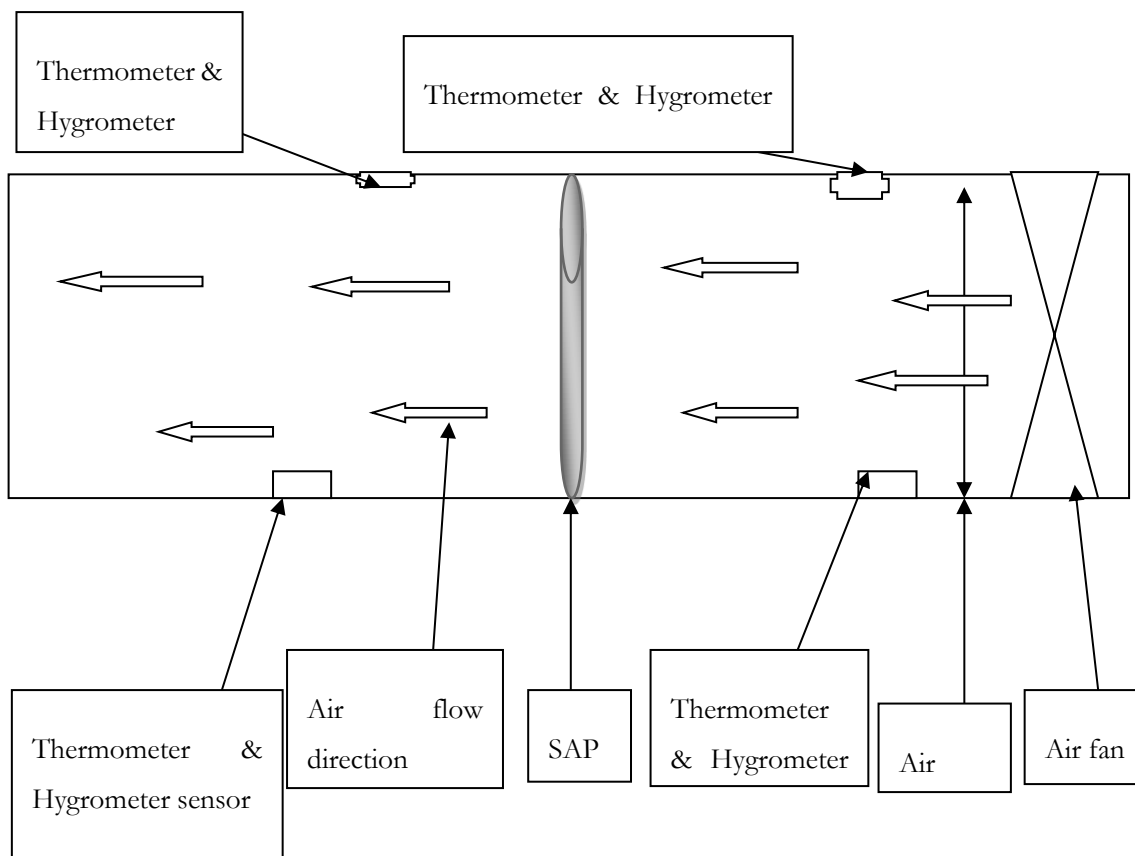
Figure 4.1. Experimental set up drawing for super adsorbent polymer characteristics.

➢ **Modeling the food water interaction of the vegetables and identification of suitable storage conditions for dried vegetables (objective 3)**

4.3 Aflatoxin analysis.

4.3.1 Aspergillus culture:

Aspergillus fungus was cultured and inoculum prepared through the following process. Czapek Dox Agar was used as media for the growth of the fungi. 49g of the media was weighed and dissolved in 1L of sterile water. The media was then sterilized in an autoclave at 120°C and 0.2MPa for 20 minutes alongside all other equipment used in the isolation process. Sampled maize presenting rotten indications was milled to fine flour and inoculum was prepared by a serial dilution process in 10ml universal bottles; 9ml sterile water and 1g of the ground flour added to the first bottle and sonicated to obtain a homogeneous solution; 1ml of the resultant solution was pipetted into the second 10mL universal bottle and 9ml of sterile water added to obtain serial dilution number one. The resulting solutions for serial dilution four to nine were plated on the media. The plates were incubated at room temperature and monitored for seven days for fungal growth. The resulting cultures were identified based on cultural and morphological characteristics using taxonomic keys. Target mold was sub-cultured to obtain pure single-spore cultures: the fungus was plated on potato dextrose agar at 25°C for five days after which the conidia were harvested by flooding a single culture with distilled water and scraping the surface mycelia with a sterile scraper. The resulting suspension was filtered through a cheesecloth to obtain the pure spore suspension (Muthomi *et al.,* 2012, Klich, 2002). The spores in the inoculum were then determined using a haemocytometer.
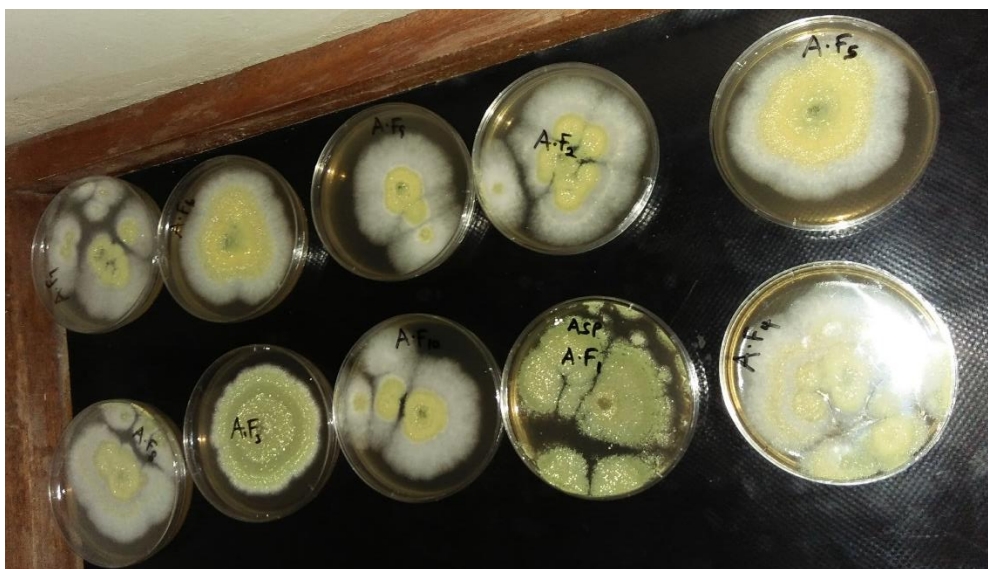
Plate 4-3. Aspergillus sub-cultured spores

4.3.2 Vegetable Samples:

The leaves of five mentioned vegetable species were prepared for analysis in this experiment and 0.1M acetic acid (Sigma-Aldrich, Germany) was used as a sterilization media; before drying at 40°C to equilibrium moisture content dried vegetables and before inoculation for fresh vegetables. Each vegetable sample was inoculated with 100 μL of inoculum and incubated at 40°C using saturated salts (magnesium chloride, potassium chloride, sodium chloride and potassium sulphate with a measured relative humidity of 32%, 74%, 84%, and 96% respectively) for seven days after which the samples were dried in a forced convection oven at a 40°C for 72 hours. The experiment included control samples both dried and fresh from each variety which were prepared and incubated in the same way but were not inoculated with the aspergillus spores. All samples were analyzed in triplicate, with each replicate collected from different batches of plants.

The aspergillus fungi growth was noted in several vegetable samples, with varying intensity of growth due to the varying conditions of incubation and the composition of the substrate to support the growth of the fungi. The samples were ground using a pestle and motor and weighed into 100 mL falcon tubes then extracted using 40 mL 84:16 acetonitrile: water. 40 μL of internal standard griseofulvin 1mg/ml was added and the solution sonicated for 30 minutes and left to settle for another 30 minutes. 6ml of the supernatant pipetted from the solution was filtered through

multistep 228 Aflapat® columns. 4ml of the filtrate was concentrated to dryness at room temperature and reconstituted using 400µl of methanol: water (80:20). The sample was then centrifuged for 3 minutes at 10000rpm for LCMS analysis.

Plate 4-4. Vegetables in an incubation box, fresh vegetables before and after incubation

Aflatoxin samples were analyzed using an Agilent 1260 Infinity HPLC system (Agilent Technologies, Palo Alto, CA) coupled to an Agilent 6120 mass detector MS with a quadrupole analyzer (Single Quad, Agilent Technologies, Palo Alto, CA). The LC was equipped with a reversed-phase, Zorbax SB C18 column, 2.1 x 50 mm, 1.8 µm (Phenomenex, Torrance, CA). The method of analysis was adopted from Kokkonen et al. (2005), briefly, mobile phase water (A) and Methanol (B) [each with 0.1% formic acid; LC-MS grade ultra-pure H2O and methanol (Sigma, St. Louis, MO)] was ran using a gradient program with initially 60:40 (A:B), to 20:80 at 12 min then to 0:100 at 20 min and maintained at this solvent proportion for 5 minutes, 60:40 from 25 min to 30 min which was the run time. The flow rate was 0.7 ml min-1. Injection volume was 5µl and data was acquired in a full-scan positive-ion mode using a 100 to 800 m/z scan range. The dwell time for each ion was 50ms. Other parameters of the mass spectrometer were as follows: capillary

voltage, 3.0 kV; cone voltage, 70 V; extract voltage, 5 V; RF voltage, 0.5 V; source temperature, 110ºC; nitrogen gas temperature for desolvation, 380ºC; and nitrogen gas flow for desolvation, 400 L/h. Authentic AFB1, AFB2, AFG1, and AFG2 standards obtained from Sigma-Aldrich (California, USA) were used to produce reference chromatograms for the four types of aflatoxins as well as the standard calibration curves from which the aflatoxin content of the test samples was determined by interpolation. An internal standard, griseofulvin was used to calculate the response factor. The internal standard is desirable when sample losses occur during sample preparation steps before analysis thus used to correct errors as a known quantity of internal standard is added to the unknown before any manipulations, the ratio of the standard analyte remains constant as the same fraction of each is lost in any operation.

Serial dilutions of the standards (0.01-100 ng/µL) analyzed by LC-MS to generate a linear calibration curve (peak area vs. concentration) with the following equation; [AFB1: y = 2e6x +24098 (R^2 = 0.994), AFG1: y=2e6x + 31605 (R^2 =0.998), AFG2: y = 2e6x +35194 (R^2 = 0.999), Griseofulvin: y = 2e6x -127662 (R^2 = 0.999)] which was used for external quantification.

4.4 Sorption- desorption experiment:

The sorption isotherms were determined at 30, 40, and 50ºC according to the method used by (Moraes *et al.,* 2008). The temperature ranges from 30 to 50ºC were chosen because they corresponded to the conditions in which the vegetables are normally stored. The static gravimetric method was used to determine the equilibrium moisture content. The isotherms experiments were carried out in five sealable glass jars. Inside each glass jar, there were saturated salt solutions to correspond to different relative humidity. The saturated salt solutions were given time to equilibrate (two to three weeks) before being used in the experiment. A single leaf was used for each experiment which was done in three replicates. The equilibrium condition was achieved when the difference between three successive measurements was 0.001 g. In this experiment, a fresh leaf dried at 40ºC for 24 hrs. for the adsorption experiment. The salts used in this experiment were: Lithium iodide, Magnesium chloride, Sodium bromide, Sodium chloride, Potassium chloride.

Plate 4-5. Harvested leaves and humidity jar used for the sorption experiment

CHAPTER FIVE : RESULTS AND DISCUSSIONS

This chapter outlines the findings and interprations of datasets obtained during study through statistical and numerical comparisons.

5.0 Pertinent parameters in the numerical modelling of convective food drying:

From literature review, the parameters in *Table m* were found to influence numerical modelling in convective food drying.

Table m: Pertinent parameters in numerical modelling of convective food drying

No.	Parameter	Author
1	Heat transfer	(Zhao and Chen, 2011, Yang et al., 2011a, Verboven et al., 2001, Moraga et al., 2012)
2	Moisture transfer	(Yao et al., 2020, Xiao et al., 2015, Wilhelm et al., 2004a, Wang et al., 2007, Moraga et al., 2012)
3	Scale analysis (Micro and Macro models)	(Van Liedekerke et al., 2010, Strumillo, 2009, Malekjani and Jafari, 2018, Lemus-Mondaca et al., 2013)
4	Physical processes (shrinkage, porosity etc)	(Yang et al., 2001, Xiong et al., 2016, Wang et al., 2017b, Wang et al., 2017a, Valdramidis et al., 2012, U.H.Joardder et al., 2015, Sakai et al., 2002, Niamnuy et al., 2008b)
5	Material properties	(Wilhelm et al., 2004b, Wang et al., 2002, Wang et al., 2017a, Wang et al., 2017b)
6	Numerical solution methods	(Xia and Sun, 2002, Wang et al., 2007, Villa-Corrales et al., 2010, Versteeg, 2007, Sabarez, 2012, Ramachandran et al., 2018)

5.1 Mathematical modelling of drying:

The drying pattern of the vegetables was described by the use of mathematical model equations. This was based on the rate of moisture loss with time at temperatures 30 40 and 50°C which were used in this study. Models developed by other researchers (*Table h*) for agricultural products were used in fitting the drying data.

5.1.1 Drying curves:

The drying curves represent the rate of moisture loss. The drying of agricultural products usually adopts a constant and a falling rate period. For a constant rate, there is an equilibrium between

water loss to the drying air from the material surface and water supplied to the surface; the converse applies to the falling rate period. The drying profile of the vegetables was obtained from a plot of moisture ratio against time as shown in ***Figure 5.1***. Generally, there is an exponential decrease in moisture ratio with time, progressively to the equilibrium moisture content. The drying pattern is almost linear but is described as exponential because the moisture content of the vegetables does not become zero when vegetables attain equilibrium moisture content with the drying air. Constant rate period of drying was infinitesimally small to be noted. The vegetables tend to adopt unique drying profiles; factors such as drying air characteristics, the geometry of the material and its orientation to the drying air, and the material characteristics take effect.

Appendix 1
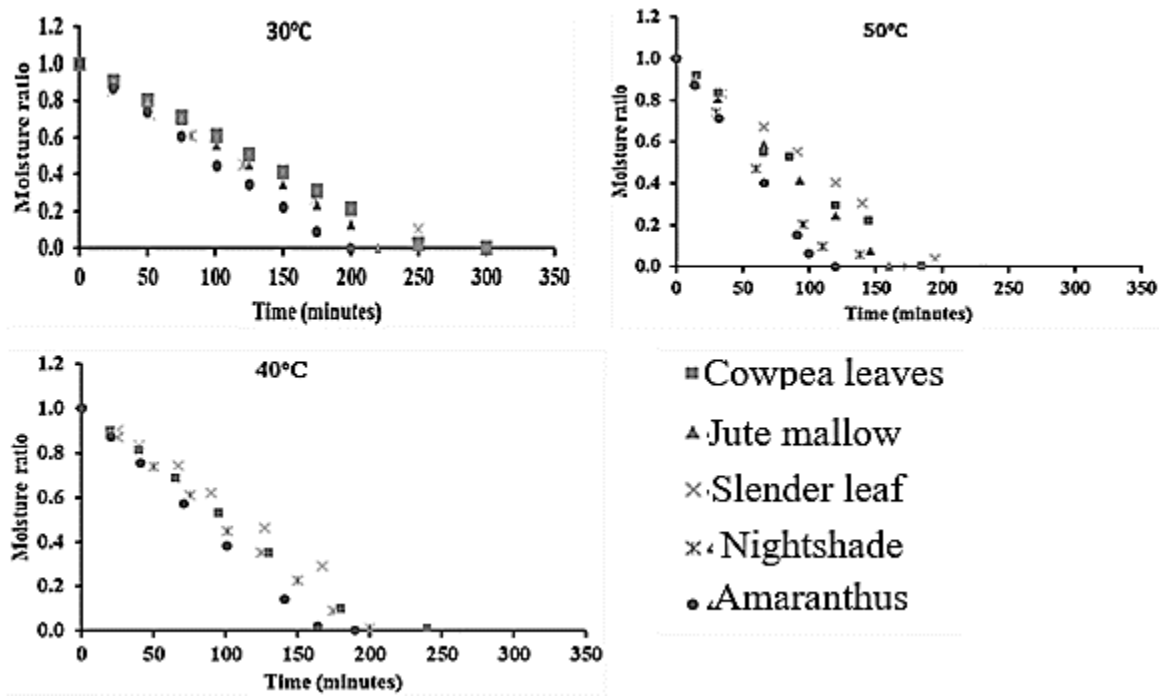
Figure 5.1. Vegetable drying profile

The drying profiles of the vegetables indicate that the moisture evaporation rate increases with an increase in air temperature and subsequent material's thermal gradient (Motevali *et al.,* 2011). Several authors have obtained comparable profiles for other agricultural products (Horuz and Maskan, 2015, Moon *et al.,* 2015, Doymaz and İsmail, 2012, Motevali *et al.,* 2011, Buchaillot *et al.,* 2009, Alibas, 2006). In this study, the relative humidity in the drying chamber was a function

of temperature and the average values were 39.4, 42.3, 47.6% at 50, 40 and 30°C respectively. There was no constant rate drying noted in all the profiles, hence the drying pattern of the vegetables was a typical falling rate period and it shows that diffusion was the main physical mechanism during the drying process.

The water in a plant cell could either be free or bound water occurs as intracellular water and cell wall water (Caurie, 2011). The cell wall water has distinguishing characteristics; it cannot act as a solvent, can only be frozen below the freezing point of free water, and it exhibits negligible vapor pressure which causes a variation of the binding energy of bound water. This strongly affects the drying process, since it requires more energy to remove the bound water than free water. Bound water should be removed for the food to be defined as dry but that also affects material structure as it causes anisotropic shrinkage, volume reduction or deformation (Datta, 2007, Halder and Datta, 2012b, Gulati *et al.,* 2015, Joardder *et al.,* 2017b). The observed decreasing drying rate almost towards the end of the drying process would be attributed to the difficulty in removing bound water.

The exponential model that describes the drying profile of the vegetables with curve fitting parameters shown in **Table n**. An observation in the drying parameters in **Table n** is that the drying rate is a direct function of the decay constant and therefore it is postulated that the decay constant represents the property of the material and the thermal energy available for moisture removal.

From **Figure 5.2**, the interaction between air temperature, time and moisture ratio is observed. A correlation analysis shows a strong negative correlation between time and moisture ratio for all the vegetables (≈-0.9). However, the correlation between temperature and moisture ratio is weak (between 0.05 and -0.08). Therefore, it is concluded that the duration of drying effectively affects the magnitude of moisture loss compared to temperature. This observation is important since water affects most reactions in the plant material during drying including nutrient degradation, color and other organoleptic properties like texture. Therefore, the limiting factor to dried food quality would be the time exposure to the drying air; therefore, optimum drying time that considers the process economics (energy and throughput) and dried food quality are vital for the production of high-quality dried food material.

Table n. Summary of Drying Curve Parameters at Different Temperatures for The Vegetables

Vegetable	Temperature (ºC)	Time coefficient	R^2 (coefficient of determination)
Cowpea Leaves	50	0.021	0.752
	40	0.014	0.786
	30	0.014	0.693
Jute mallow	50	0.024	0.789
	40	0.015	0.746
	30	0.014	0.766
Slender leaf	50	0.024	0.727
	40	0.015	0.726
	30	0.014	0.723
Nightshade	50	0.027	0.734
	40	0.014	0.689
	30	0.018	0.788
Amaranthus	50	0.035	0.770
	40	0.024	0.738
	30	0.018	0.697

Model: $MR = e^{-\acute{\omega}t}$ where ώ is time coefficient
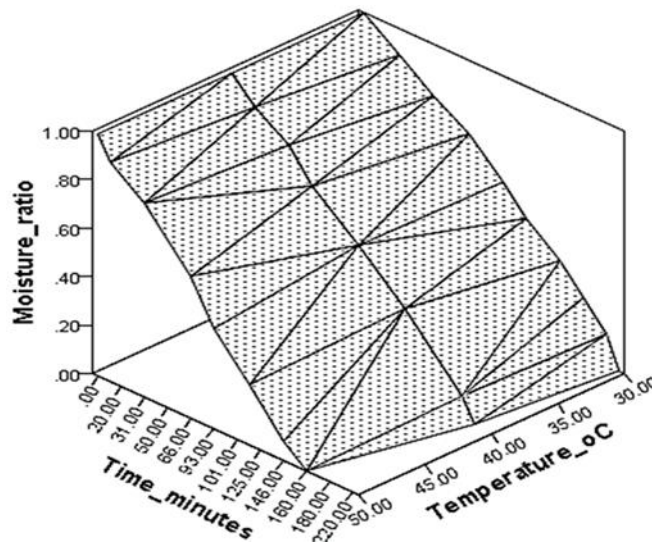
Figure 5.2. Interaction between temperature, time and moisture ratio

5.1.2 Mathematical Modelling of Drying:

Selection of the most appropriate model that describes the drying profile of the vegetables was based on statistical analysis; that returns the highest coefficient of determination (R^2), lowest the sum of squared error (SSE) and lowest mean squared error (MSE) (equations 3.2, 3.3 and 3.4) after fitting of the 14 thin-layer drying models in ***Table h***. Among the fourteen thin-layer drying models, four of them represented the drying kinetics of the leafy vegetables with high R^2 values and low SEE and MSE values. Among the four models, Page model was the most appropriate model based on its simplicity and it consistently returned the required attributes. The model could simulate the drying pattern of the vegetables with a ≈97% correlation between the empirical and predicted values. Statistical analyses on the significance of variance at α=0.05 on the values returned from each of the four models at different temperatures and the vegetable variety showed no significant difference. Therefore, the statistical parameters SEE, SME and R^2 were averaged as presented in ***Table o*** with no considerable variations of the initial data. ***Table p*** shows Page model parameters.

Table o. Drying Models' Statistical Parameters

	Page Model	**Lewis**	**Henderson and Pabis**	**Modified Page**
SEE	0.0311	0.0421	0.0649	0.0439
MSE	0.0482	0.0552	0.0797	0.0543
R^2	0.984	0.979	0.952	0.979
R^2 -coefficient of determination; SSE-the sum of squared error; MSE-mean squared error				

Table p. Page Model Statistical Parameters

Vegetable	Temperature (^{o}C)	Parameters obtained (n, k)	R^2	MSE
Cowpea leaves	30	n=1.443, k=6.772 x 10^{-4}	0.9870	0.0409
	40	n=1.3676, k=1.3419 x 10^{-3}	0.9911	0.0374
	50	n=1.2878, k=2.092 x 10^{-3}	0.9879	0.0425
Jute mallow	30	n=1.3453, k=1.2541 x 10^{-3}	0.9773	0.0534
	40	n=1.3676, k=1.3419 x 10^{-3}	0.9849	0.0488
	50	n= 1.3791, k=1.9144 x 10^{-3}	0.9809	0.0569
Amaranthus	30	n=1.6523, k=4.715 x 10^{-4}	0.9807	0.0518
	40	n=1.891, k=2.5043 x 10^{-4}	0.9679	0.0757
	50	n=1.4976, k=2.6975 x 10^{-4}	0.9718	0.0747
Slender leaf	30	n=1.4545, k=6.4169 x 10^{-4}	0.9930	0.0300
	40	n=1.2613, k=1.7195 x 10^{-3}	0.9880	0.0400
	50	n=1.2638, 2.1478 x 10^{-3}	0.9850	0.0490
Nightshade	30	n=1.1744, k=3.0516 x 10^{-3}	0.9814	0.0517
	40	n=1.4523, k=1.0312 x 10^{-3}	0.9874	0.0417
	50	n=1.5829, k=1.3637 x 10^{-3}	0.9951	0.0302

R^2 -coefficient of determination; SSE-the sum of squared error; MSE-mean squared error

The parameters k and n are dimensionless constants of the model equation. The parameter k is a function of initial moisture content, air temperature and velocity as reported by (Azzouz *et al.,* 2002), in a study of drying grapes. The n constant is a factor of the food material characteristics. They showed that the fruits which had a thicker skin had higher values of n while those with thinner skins had lower values of n. The trend was similar for a different food material but the values got were a little higher (Senadeera *et al.,* 2000). In this experiment, each vegetable variety had unique values of n but comparable to the findings by other researchers. The unique values pointed to the differences in structural differences of each vegetable variety.
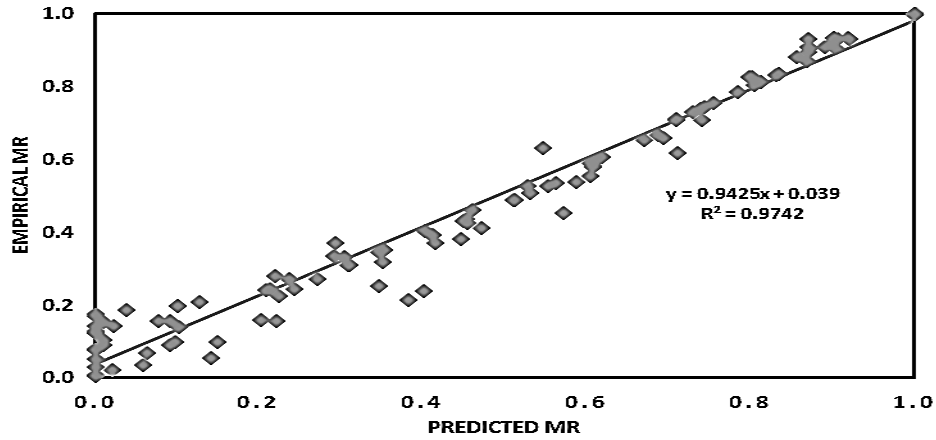
Figure 5.3. Page model fitting for all the experimental data

From the scatter plot in *Figure 5.3*, the model prediction is more precise when the vegetables have a high moisture content (almost >0.5 w.b; which corresponds to an equal value of moisture ratio).

At low moisture content, the deviation from the line of best fit is more pronounced. This phenomenon can be explained from difficulty in the removal of intercellular water and shrinkage of the product which reduces moisture loss per unit area. Although material crusting contributes to the reduction in moisture movement, in this experiment it was not observed. Therefore, to improve the accuracy of the model specifically at low moisture contents, a correction factor obtained from factors affecting moisture transport; is less than one but greater than zero could be introduced into the model to form a modified page model (equation 5.1).

$$MR = \omega + exp[-kt^n] \qquad\qquad 5\text{-}1$$

ω represents the correction factor.

To estimate the function ώ, residuals from the Page model and empirical data were plotted against drying time. Essentially, the residuals are moisture ratio values which when plotted against time would generate a model on the trend of the residuals as shown in *Figure 5.4*
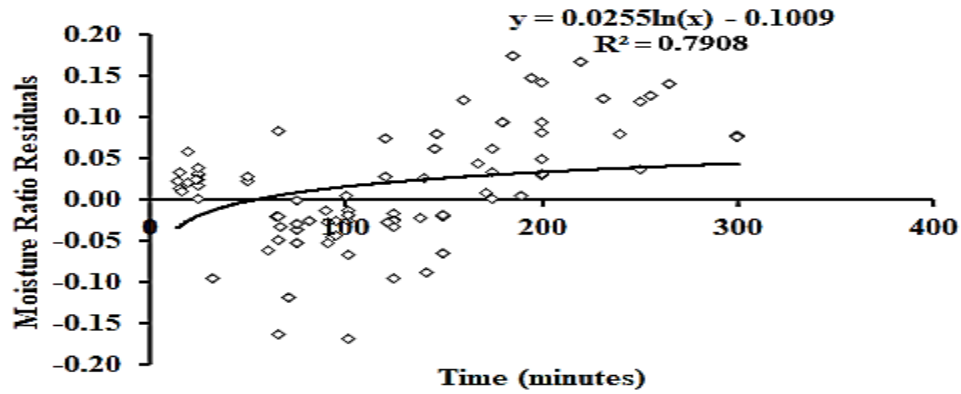
Figure 5.4. A plot of moisture ratio residuals against time

The logarithmic model represents $\acute{\omega}$ and was obtained for up to 300 minutes; therefore, the model is suitable for the time range. The proposed modified model would be as in equation 5-2. Where $\acute{\omega}$ = 0.0255 $\log_e$ t − 0.1009 and depends solely on the drying time. The figures generated from the $\acute{\omega}$ are presented in **Table q**. **Figure 5.5** shows the plot of all experimental data using the model in equation 5-2.

$$MR = 0.0255 \ log_e \ t - 0.1009 + exp[-kt^n] \qquad\qquad 5\text{-}2$$

Table q. Residual moisture ratio at different times ($\acute{\omega}$)

Time	Residual Moisture ratio
20	-0.025
40	-0.007
60	0.004
80	0.011
100	0.017
120	0.021
140	0.025
160	0.029
180	0.032
200	0.034
220	0.037
240	0.039
260	0.041
280	0.043
300	0.045
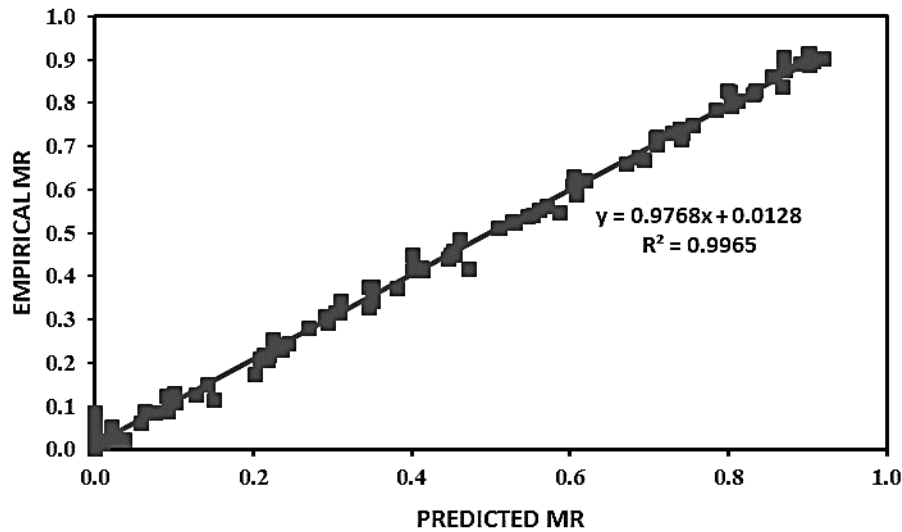
Figure 5.5. Modified Page model fitting for all the experimental data

5.2 Physico-Chemical Parameters Profile with Drying of the Leafy Vegetables.

Drying transforms the food material domain and changes such as crust formation, shrinkage, pore evolution, and intermittent evaporation occur. These changes affect consumer preference for food products, the suitability for consumption and stability during storage.

In this section, results from the investigation of physical transformation as well as micro-nutrients profiles are presented. Nutrient analysis was done for fresh, dried and stored vegetables, the color change was noted visually and shrinkage determined for different drying conditions. The trends that were reflected are presented and discussed in the subsequent sections.

5.2.1 Nutrient content analysis:

The vitamin content of the five ALV species was analyzed after drying for 24 hours at 40 ºC and storage for two months at room temperature and protected from sunlight. The relative nutrient retention in dried and stored leaves compared to the vitamin content in fresh leaves is shown in *Figure 5.6*. For all species, 50 – 75% of the Vitamin A (β-carotene), C and E levels were retained. Vitamin C was the most labile nutrient, followed by vitamin E and β-carotene; this can be explained by the difference in their water solubility, which is the highest for Vitamin C and the lowest for β-carotene. Chemical reactions affecting the nutritional quality of food are influenced

by the drying/storage temperature, moisture, presence of oxygen, and light. During drying, the concentration of the dissolved species in the food matrix increases as water is lost. The simultaneous concentration of dissolved solutes and elevated temperature results in an accelerated reaction between species, thereby increasing the rate of nutrient degradation (Mutuli and Mbuge, 2018). Nightshade and Slender leaf showed the highest β-carotene content (~10 mg/ 100 g) after drying and storage which shows that these species are excellent candidates to improve vitamin A levels, particularly in children, during the dry season. Previous studies (Jangam, 2011) revealed similar trends: enzymatic reactions caused by the increase in temperature cause a deterioration in nutrient levels. The nutrient retention level in the vegetable varied because of the initial nutrient content. The drying of all ALV species is a viable means of preservation as there is a significant nutrient level even after drying and storage for two months.
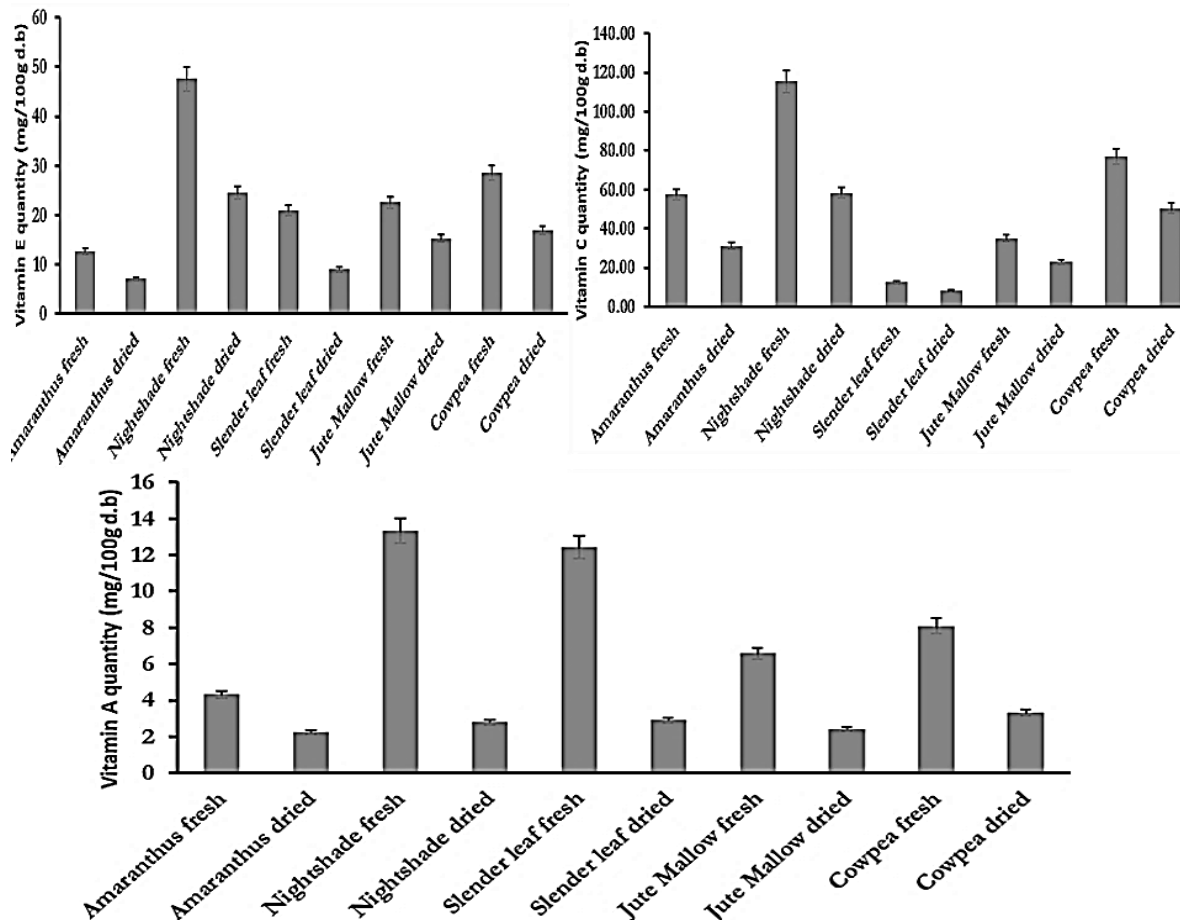
Figure 5.6. Nutrient content for fresh and dried vegetables

- 101 -

Table r Percentage nutrient retention in the dried vegetables

Sample	% Vitamin C	%Vitamin E	Vitamin A (B-Carotene)
Amaranthus	54.26	55.67	52.23
Nightshade	50.59	51.60	21.06
Slender leaf	66.40	42.77	23.44
Jute Mallow	65.31	67.63	36.58
Cowpea leaves	65.54	58.95	40.95

5.2.2. Colour:

The Colour of food material usually changes during drying due to the catalysis of chemical reactions in the food matrix. The drying air characteristics i.e. relative humidity and temperature influence these changes that result in colour degradation. In this study, color change not determined analytically but was determined visually. It was observed to change variably due to different drying conditions and the distinct physical properties of each vegetable leaf.

A leaf is a complex biological organ made of different specialized tissues comprised of cells; the larger part of a leaf structure is the mesophyll which comprises of the tissues that build up most of the interior of the leaf i.e. thinner-walled parenchymal cells or collenchymal cells with chloroplasts. The chloroplasts give the green colour to the leaf and are mainly involved in the photosynthesis process. Therefore, most of the chloroplast's breakdown during the drying process; the enzyme chlorophyllase decomposes by cleavage of phytol ring which causes the loss of the green colour (Perera, 2005, Prachayawarakorn *et al.,* 2008). That phenomenon is observed by loss of colour which was more pronounced at high temperatures or prolonged periods of drying as shown in **Figure 5.8**. Colour development is a function of chemical and biochemical reactions during drying or storage. In non-enzymatic reactions, the water activity and processing temperatures are a direct function of colour change in a material. This aspect of colour has been reported by several authors (Maskan *et al.,* 2002, McMinn and Magee, 2003, Goula *et al.,* 2006, Rapusas and Driscoll, 1995, Topuz *et al.,* 2011). Some of the authors determined the kinetics of colour change in a product and reported that colour can be modelled using modelled by using zero-order or first-order degradation model.

5.2.3 Shrinkage:

To estimate leaf shrinkage, the experiments were conducted at temperatures 30, 40 and 50°C as stated in the methodology section. From the experiment, a more elaborate analysis could be only realized at 30°C otherwise the leaf became brittle at a moisture ratio of below 0.5. Therefore between 0.5 and 0, no leaf thickness reading could be obtained. An analysis of the significance of variance in the shrinkage's coefficient at almost equal moisture ratios but at different temperatures at α=0.05 showed that the variance was not significant. Therefore, the shrinkage analysis was done with a higher certainty that shrinkage highly depends on the moisture content of the vegetable between temperatures 30 and 50°C.

The shrinkage coefficient was determined using equation 3.10. These results were plotted against moisture ratio (which corresponds to moisture content) as shown in *Figure 5.7*. **Figure 5.8** shows photos of the vegetable leaves fresh and dried at 30°C, shrinkage can be observed in the dried vegetables.
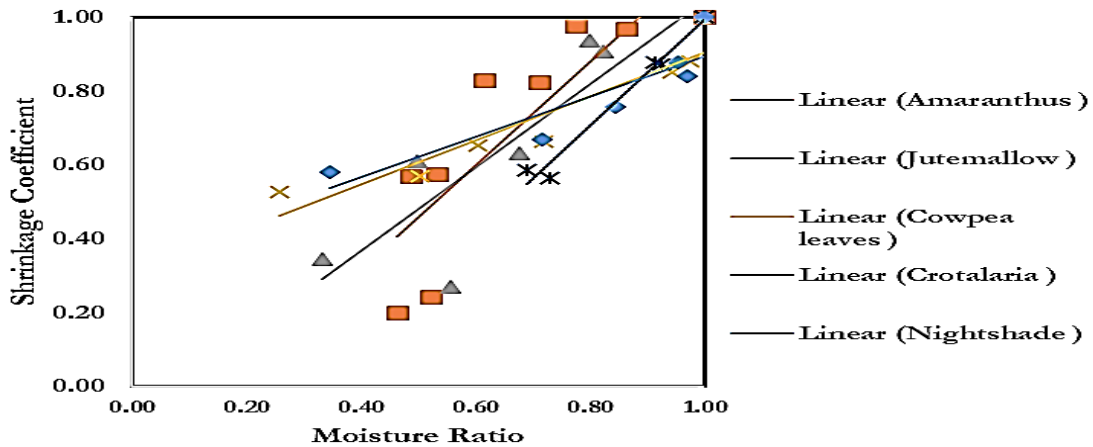
Figure 5.7. Shrinkage coefficient at 30 degrees for the selected vegetables

Figure 5.8. Photos of fresh and dried vegetables at 40ºC

The relationship between the shrinkage coefficient and moisture ratio was fitted into a linear model that is distinct for each of the vegetable variety. Each of the vegetables' variety has distinct structural material properties and composition which would affect the structural strength of the leaf and rate of moisture movement differently. There is a collapse of the cellular arrangement when space filled with water is occupied by air due to moisture loss and the exterior skin structure collapses; moisture affects the cell strength due to the turgor pressure it exerts on the cell walls (Panyawong and Devahastin, 2007a). The models in *Figure 5.7* reveal cowpea leaves and nightshade vegetables have a lower gradient (slope) than the others. Cowpea leaves and nightshade exhibit relative resilience to structural change in comparison to non-fibrous vegetables. Also, from *Figure 5.7*, Amaranthus tended to have characteristics like those of non-fibrous vegetables. At the moisture content of below ≈0.3 w.b. the vegetables began exhibiting brittleness. The linear model developed from the relation between shrinkage coefficient and moisture ratio could be used to predict shrinkage at different moisture contents and specifically between 30 and 50ºC which were the experimental conditions under this study. The average values of the relative humidity recorded at the drying temperatures were 39.1%, 41.7%, 46.4% at 50, 40 and 30ºC respectively. The models are in *Table s*.

Table s: Vegetables' linear shrinkage models

Vegetable	Shrinkage Model	R^2 value
Amaranthus	$y = 1.179x + 0.0087$	0.8814
Cowpea leaves	$y = 0.5962x + 0.309$	0.888
Nightshade	$y = 0.4526x + 0.3991$	0.8945
Crotalaria	$y = 1.4347x - 0.4412$	0.9769
Jute mallow	$y = 1.0053x + 0.0471$	0.9183
y-shrinkage coefficient; x-moisture ratio		

5.2.4 Effective Moisture Diffusivity:

Effective diffusivity describes the rate of moisture movement, no matter which mechanism is involved. In determining the effective moisture diffusivity, the natural logarithm of moisture ratio (In (MR)) was plotted against time (t) and showed a negative gradient, linear relationship (**Figure 5.9**). (Park *et al.,* 2002) reported effective moisture diffusivity values varying from 5.129 x 10^{-13} to 2.945 x 10^{-12} m^2 s^{-1} at temperatures of 30, 40 and 50°C with an air velocity of 1 m s^{-1} for 1 to 2 grams of mint leaves; (Akpinar, 2006) reported 7.04 x 10^{-12} m^2 s^{-1} for sun drying of mint leaves.

The trend observed in the leafy vegetables is that there is an increase in the diffusivity with an increase in temperature with no unique trend noted between the fibrous and non-fibrous vegetables, though there is a distinct difference in the diffusivity for each vegetable which could be attributed to differences in structural differences at the microscale level.
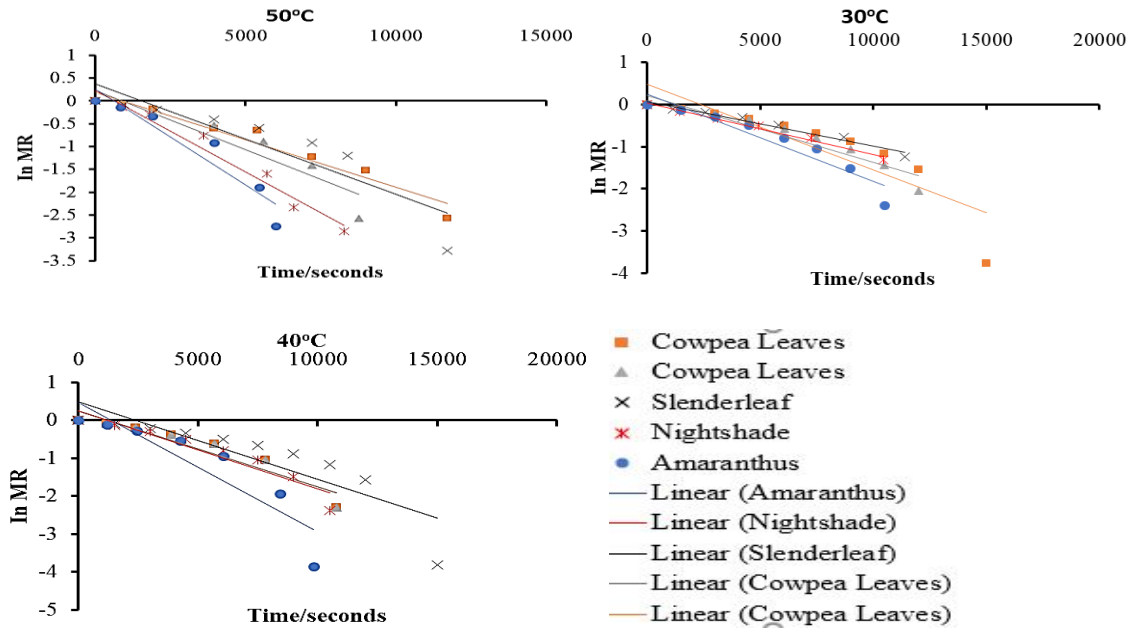
Figure 5.9. The Ln (MR) vs Time in Seconds for fibrous vegetables

Table t: Curve fitting parameter for curves presented in Fig 5.16

Vegetable	Temperature	Calculated D_{eff} (M^2/S)	slope	R^2 value	Intercept
Amaranthus	50	8.104E-09	-0.0002	0.8993	0.2659
	40	8.104E-09	-0.0002	0.8241	0.4589
	30	8.104E-09	-0.0002	0.9028	0.2528
Night shade	50	1.621E-08	-0.0004	0.9667	0.2339
	40	8.104E-09	-0.0002	0.9006	0.2512
	30	4.052E-09	-0.0001	0.969	0.0443
Slender leaf	50	8.104E-09	-0.0002	0.9741	0.3687
	40	8.104E-09	-0.0002	0.9695	0.4886
	30	4.052E-09	-0.0001	0.9709	0.066
Jute mallow	50	1.216E-08	-0.0003	0.9635	0.2328
	40	8.104E-09	-0.0002	0.9045	0.1815
	30	8.104E-09	-0.0002	0.9203	0.2127
Cowpea leaves	50	8.104E-09	-0.0002	0.9499	0.1903
	40	8.104E-09	-0.0002	0.9721	0.2359
	30	8.104E-09	-0.0002	0.9521	0.4812

From *Table t*, it can be noted that the moisture diffusivity of the leafy vegetables increased with the increase in drying air temperature. Moisture diffusivity (D_{eff}) varied from 4.052×10^{-9} to 1.216×10^{-8} m^2/s for temperature range from 30 to 50°C. These values are within the general range 10^{-9} to 10^{-11} m^2/s for drying of food materials (Maskan *et al.*, 2002). From equation 3.8 the plot in *Figure 5.9* was obtained to determine the Activation energy as presented in *Table u*.
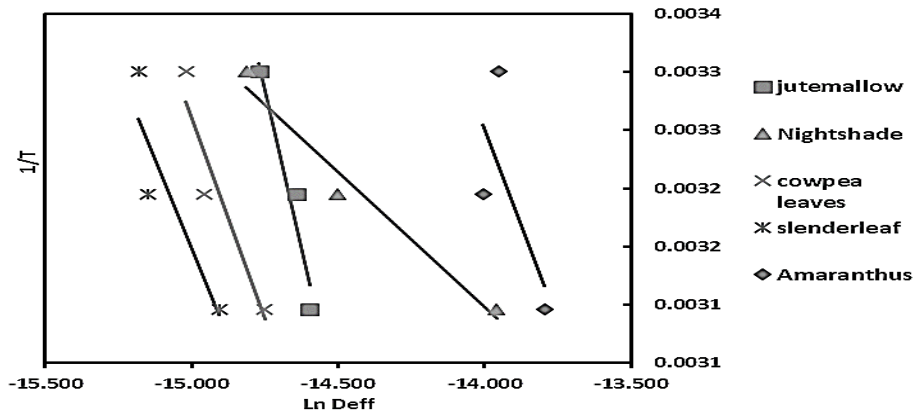
Figure 5.10. Activation energy plot

Table u: Activation energy plot parameters

Vegetable	slope	intercept	Activation Energy (kJ mol^{-1})
Amaranthus	-0.0007	-0.006	5.69394E-06
Night shade	-0.0002	-0.0002	1.62684E-06
Slender leaf	-0.0006	-0.086	4.88052E-06
Jute Mallow	-0.0011	-0.129	8.94762E-06
Cowpea leaves	-0.0007	-0.0071	5.69394E-06

5.3 Transport phenomena accounting for shrinkage:

The study of transport phenomena was based on examination of the time evolution temperature, and moisture concentration in the food slab. The model was developed and tested for three temperatures i.e. 30, 40 and 50°C. Data was exported from COMSOL Multiphysics and used to plot the graphs on excel.
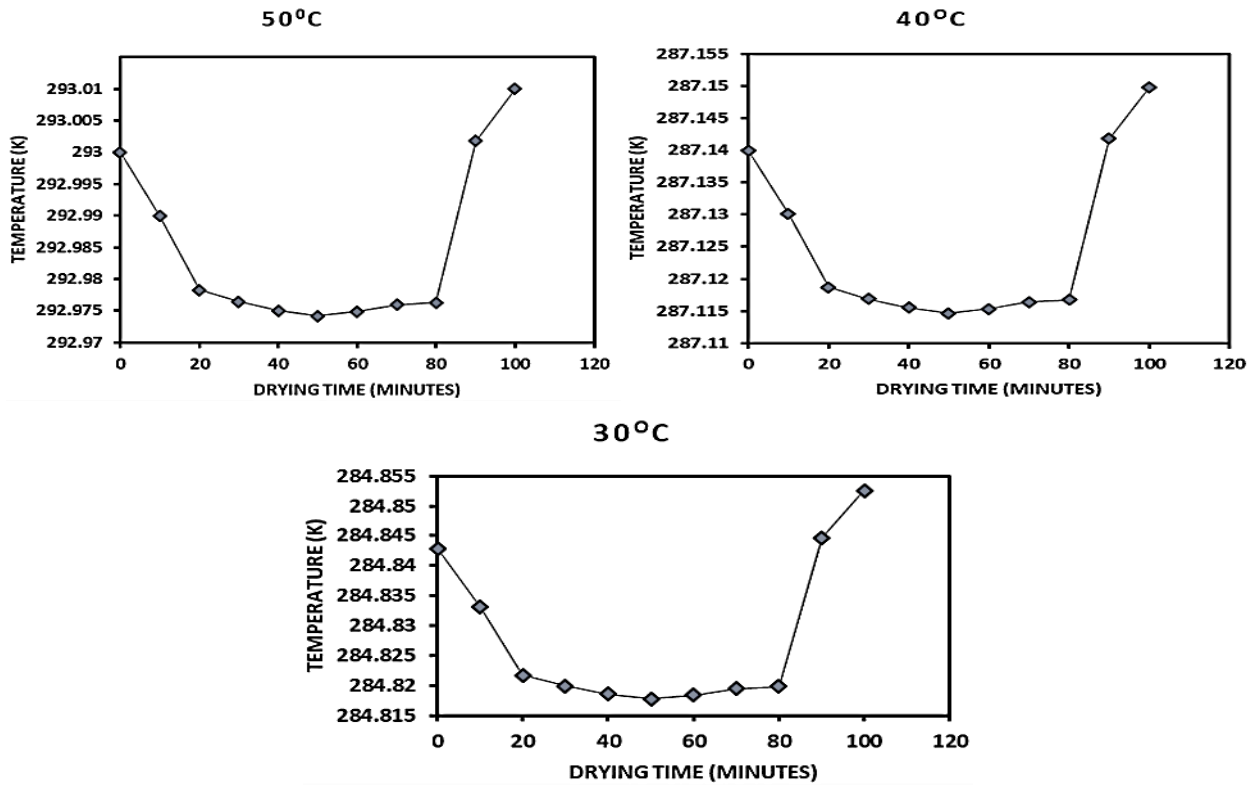
Figure 5.11. Temperature profile in the food slab
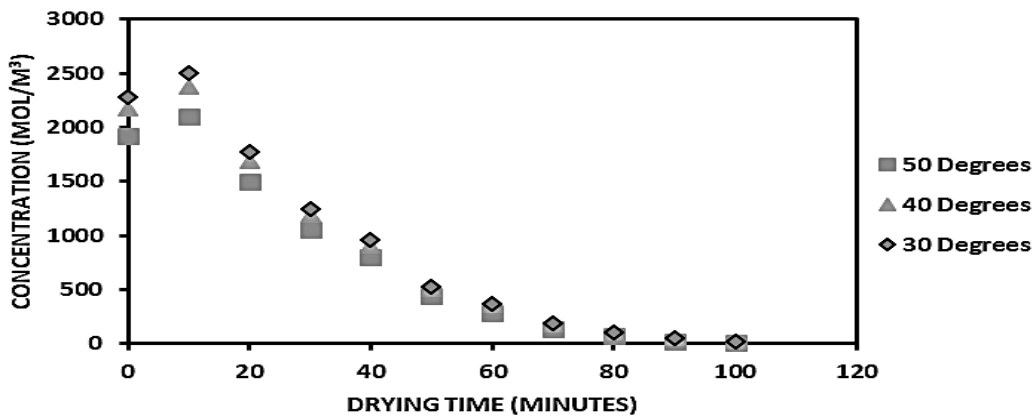
Figure 5.12. Moisture concentration reduction with time in the food slab

Figure 5.11 and *Figure 5.12* show the temperature profile, and moisture concentration profile respectively in the food material slab over the drying time. The temperature in the food slab drops marginally then begins to increase; and concentration moisture trend with time also adopts a decay curve. The drying process is a direct function of the air properties, an increment in the inlet drying

air temperature moves the system from equilibrium state and it would influence the initial drying mechanism. In the initial drying times, there is a process of attainment of the equilibrium; the water begins to evaporate in proportion to the capacity of the air to absorb the evaporated moisture and the temperature drops below the initial dry bulb temperature. In the initial points of drying, concentration is seen to marginally increase on the surface of the food material, before a constantly decreasing rate begins because as drying proceeds, the accumulation of moisture on the food surface subsides and the rate of evaporation equals or exceeds the rate of moisture transfer from the food material. The increase in wet bulb temperature may potentially cause initial humidification of the exposed surfaces, especially at higher values of air relative humidity. This phenomenon is caused by the condensation of water from the drying air on the cold food surfaces and continues until the surface temperature is lower than the wet bulb temperature. Once the wet bulb temperature is attained, evaporation of free water dominates over vapor condensation and the food begins to dry. Moreover, at a given relative humidity, an increase in the dry bulb temperature increases the moisture content of the air which causes a significant reduction in the driving force to mass transfer from food to air; however, this is accompanied by an improvement in heat transfer from air to food. The findings from the theoretical model concur with the expected trends from literature (Robert *et al.,* 1984).

The significance of the temperature profile is that it indicates the time when the temperature in food slab begins to increase. That would be essential to avoid significant loss of micro nutrients in the food material and also to prevent undesireable physical changes like crusting that affect the dried food texture.

The concentration of moisture in food reveals that the inlet air impact side surface looses moisture faster. This aspect is realized because the surface receives heat first and therefore its temperature rises quickly above the wet-bulb temperature. The aspect is a function of the airflow conditions and the heat transfer provides latent heat of vaporization for water evaporation and the sensible heat required to increase the temperature of the dry matter by conduction. On the opposite side, the flow conditions do not provide for efficient air contact with surface thus the moisture loss is slower. This reveals that the stationery bed drying does not give uniform drying of the food material especially for materials of significantly big dimensions. In that case, forced convection of

the air is necessary but with a mechanism to ensure uniform distribution of air the drying domain. Also, a rotating bed could enhance the uniform drying of the food material. Complete drying is important to avoid conditions that would favour microbial growth in the food.

5.3.1 Shrinkage modelling:

The hydrous compressability factor determined empirically was found to be in 3.66E-08 kg/m^3 (for 30^{0}C) and 5.46E-08 kg/m^3 (for 40 and 50^{0}C). The factor was applied in modelling shrinkage. *Figure 5.14* shows the trend of weight loss vs shrinkage coefficient as the hydrous compressability factor. Similar plots were obtained for 40°C and 50^{0}C.

In **Figure 5.13**, moisture loss is shown to proceed radially from the plant material. The diffusivity obtained in the experiment shows that the diffusion rates are significantly low and the drying air velocity is low, therefore the rate of moisture loss is a factor of material characteristics at the dryer operating conditions. The distribution of stress in the plant material tends to be uniform but is more concentrated at the centre of the material domain. This aspect directly correlates to the concentration profile that shows moisture movement in the material.
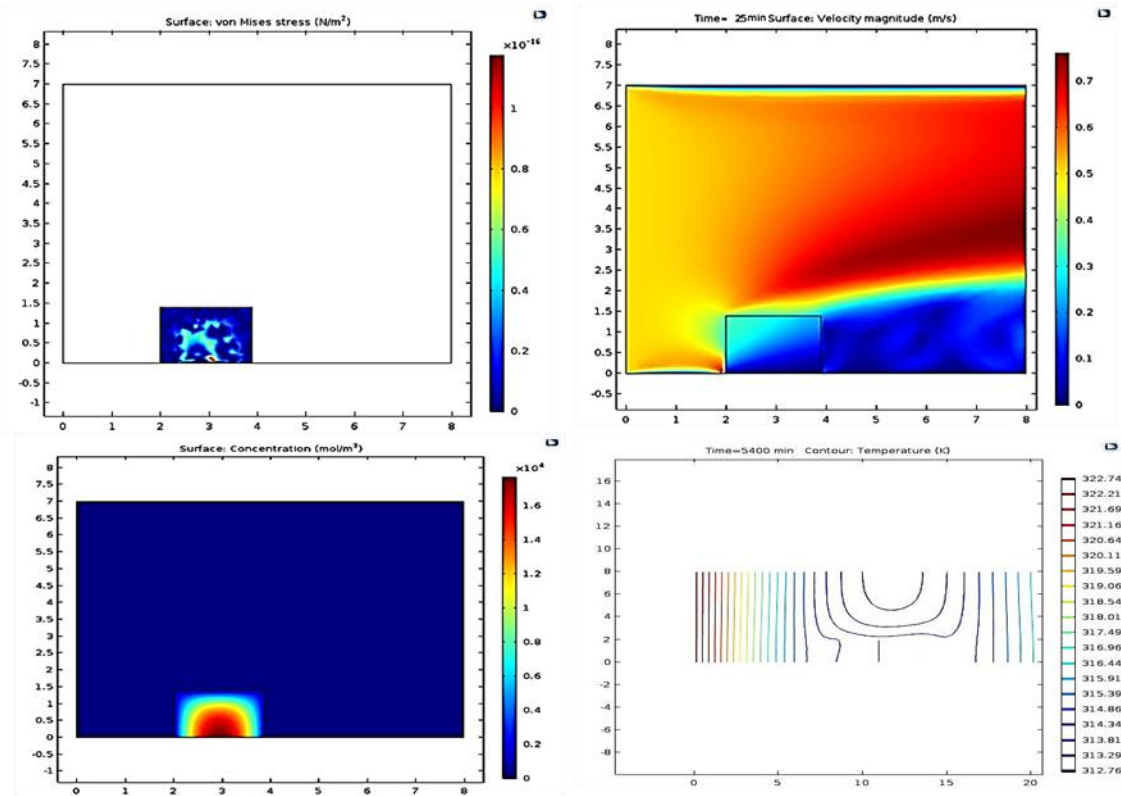
Figure 5.13. Spatial and temporal evolution of concentration, stress, and velocity profile
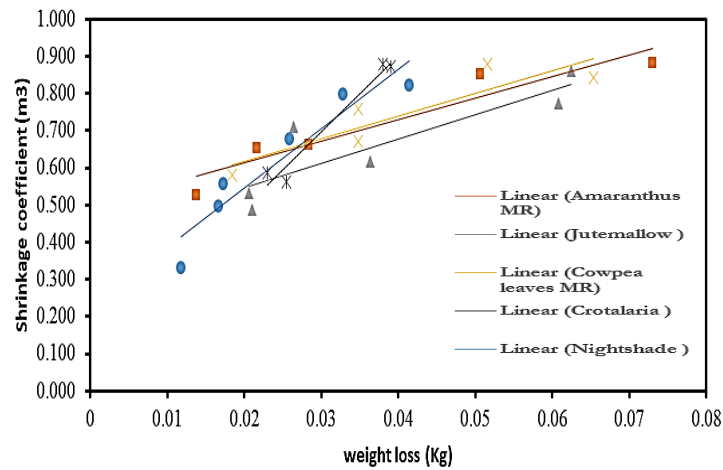
Figure 5.14: Hydrous compressibility plot at 30 degrees
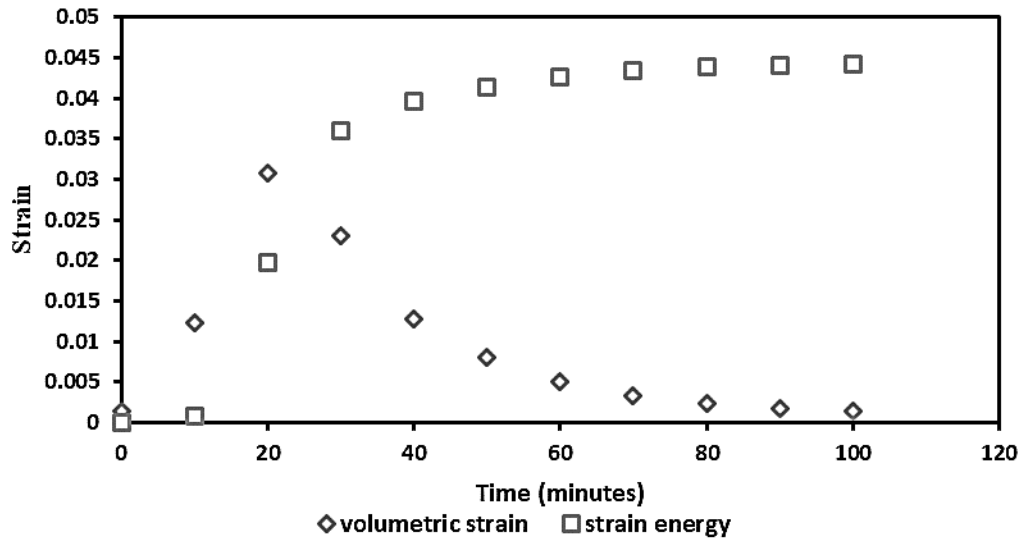
Figure 5.15. Comparison of strain energy and volumetric deformation.

Figure 5.15 shows the trends of volumetric strain and the strain energy over the simulated drying time. The strain energy increases with time evolution. In drying porous plant material, the free (unbound) water is easily lost in the process, however, the bound water which is present in the cells requires more energy for it to be removed from the material. therefore, and as drying proceeds it is expected that more energy will be required, as it is in the case in the results obtained. The is an increase in the strain energy with time is clarified by the reasons just mentioned.

Figure 5.16 shows the trend in volumetric ratio evolution with time. The volumetric ratio compares well with the shrinkage ratio results obtained from the experimental analysis. It should be noted that the material property parameters used for the theoretical simulation were an average of the determined values for the vegetables under this study.
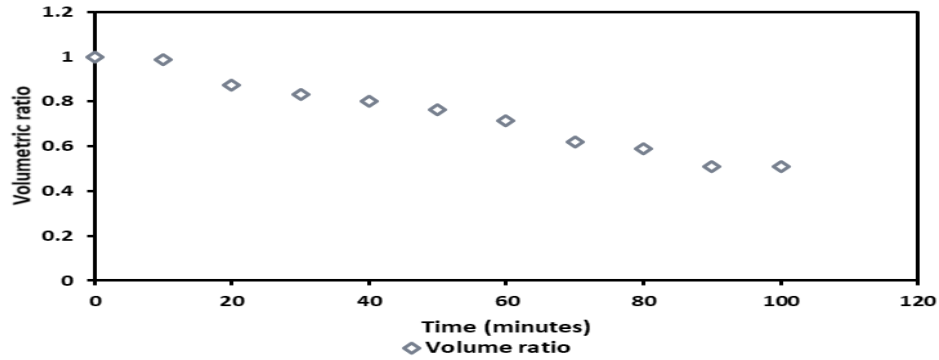
Figure 5.16. Volume ratio trend from simulation results

5.3.2 Model Validation:

Several numerical simulations were conducted in addition to those described therein, specifically to verify this proposed model through comparison with experimental results. A comparison was carried out between moisture concentration evolution and moisture ratio which both occur under the falling rate period. The time coefficient in decay Models in **Figure 5.12** were compared to those in **Figure 5.1** for general drying pattern as shown in **Table v**.

Table v: Comparison of the time coefficients

Temperature (ºC)	Time coefficient (simulation)	Time coefficient (experimental)
50	0.027	0.024, 0.021, 0.024, 0.027, 0.035
40	0.021	0.014, 0.015, 0.015, 0.014, 0.024
30	0.020	0.014, 0.014, 0.014, 0.018, 0.018

The evolution of food temperature was not compared because the experimentation process lacked sufficient equipment to accurately monitor the spatial and temporal distribution temperature of food. An increase in air-drying temperature was seen to affect the drying rate in both cases. In summary, the proposed model gives a good representation of the behavior of the real system, since it is capable of reproducing experimental data not only at the very beginning of the drying process but also over the entire time duration.

5.4 Suitable storage conditions.

Knowledge of post-harvest vegetable handling and storage is important to prevent deterioration or contamination of the product. The dried vegetables were exposed to controlled conditions of humidity to determine their storage requirements. Moreover, the susceptibility of the vegetables to contamination was investigated by incubating fresh and dried vegetables in controlled conditions after inoculation with aspergillus fungi spores.

5.4.1 Sorption isotherms:

The sorption experiments were done at 30, 40 and 50°C with the relative humidity maintained using saturated salt solutions. The salts were left for twenty days to equilibrate before being used. The measured equilibrium relative humidity in humidity jars is in ***Table w***.

Table w: Measured relative humidities from equilibrated saturated salt solutions

Temperature (ºC)	% Equilibrium Relative Humidity				
	Lithium chloride	Magnesium chloride	Sodium bromide	Sodium chloride	Potassium chloride
30	17.01	32.74	55.91	76.03	83.76
40	15.71	32.07	54.11	75.11	82.04
50	14.56	31.31	50.43	75.13	82.09

The sorption isotherms obtained are shown in **Figure** 5.17. Equilibrium moisture content **(EMC) trend** with increasing relative humidity
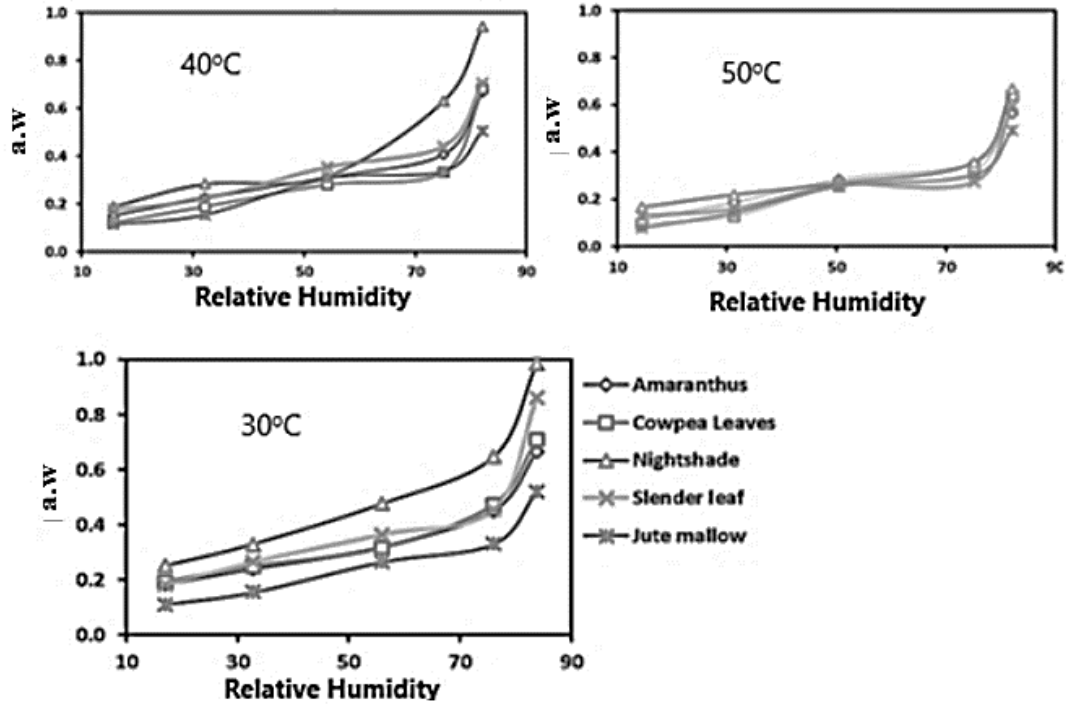
Figure 5.17. Equilibrium moisture content (EMC) trend with increasing relative humidity

From **Figure 5.17**, it is shown that the data points adopt a trend that tends to describe the typical S-shape curve of a type II isotherm typical of porous biological materials and other agricultural products (Bell and Labuza, 2000, Igathinathane *et al.,* 2005, Arabhosseini *et al.,* 2010). The effect of temperature on each isotherm can be observed as affecting each of the isotherm cycles; increased temperatures yield a decrease in equilibrium moisture content (for the vegetables) at equal values of relative humidity (Iglesias and Chirife, 1976a).

The data was modeled against existing sorption models shown in **Table l**. The models were selected based on the most common isotherms that are used to model food material. In the modeling, the data collected from all three replicates was pooled into a single set used to fit the model parameters using nonlinear regression. To judge the fit of each model coefficient of determination (R^2), and root mean squared error (MSE) between the experimental data sets and the predicted data were calculated (Equations 2.53, 2.54 and 2.55). The residuals for each modeled isotherm were plotted to determine if a pattern existed. The models that provided the lowest value for MSE and uniform distribution of residuals were the best fit for a given sorption isotherm.

Table 1 and **Table 2** (in the **Appendix 1**) shows the model parameters and statistical analysis of temperature-dependent and independent models of sorption isotherms. For the temperature-dependent models, the Modified-Hasley model had the highest R^2 values and lowest MSE values across all the vegetables compared to the Modified-Oswin model. However, both of them had patterned distributions of the residuals when comparing the predicted series to the combined experimental dataset. For the temperature-independent models, BET, GAB and Peleg show high suitability in terms of R^2 values and MSE values which cannot be easily distinguished. However, the Peleg model had a well uniform distribution of residuals. Comparison between the temperature-dependent and independent models shows that though the former could be used to describe the adsorption characteristics of the vegetables, the prediction that they would provide would not be entirely precise. Therefore, temperature-independent models would be more suitable, while the Peleg model is selected as the most suitable. Similar trends have been observed by other researchers: (Kouhila *et al.,* 2001) in a study of moisture sorption isotherms of *Mentha viridis*, sage (*Salvia officinalis*) and verbena (*Lippia citriodora*), GAB, modified Halsey and Peleg models were fitted to the experimental data, (Román and Hensel, 2010), in a study of desorption isotherms of celery leaves, Peleg model the most appropriate model of six models considered.

5.4.2 Monolayer Moisture Content and Safe Storage Moisture Content:

In the three temperature-independent sorption isotherms, the parameter "A" corresponds to the monolayer moisture content. Distinct ranges of the monolayer moisture content (Mo) across temperature are observed, and each exhibits a negative relationship between Mo and increasing temperatures, with a near-linear relationship between 30 and 50ºC *Figure 5.18*.

At the water activity range of 0.2 to 0.3, the monolayer moisture content presents the ideal moisture content at which the dried food products will have the maximum shelf-life. At this moisture content, chemical reactions that occur in aqueous environments will proceed, lipid oxidation will occur above this moisture content. Food physical properties like crispiness could be lost at a water activity range of 0.35 to 0.5. The critical moisture content in terms of microbial growth for food products has been suggested to be 0.6 aw (Labuza and Altunakar, 2007).

Using the individual temperature-independent sorption isotherms models for each sorption isotherm, the E.M.C at which the growth of microorganisms becomes inhibited was calculated at 0.6 aw. The E.M.C values of the leafy vegetables ranged from 28% to 8% on d.b. across the temperatures. The estimation using Peleg model which was selected as most appropriate for prediction of sorption characteristics of the vegetables, the E.M.C values and the interaction between vegetable variety and temperature was significant at α=0.05 (with P values< 0.5), indicating that relatively small changes in storage temperature are required to influence the adsorption-based monolayer moisture content.
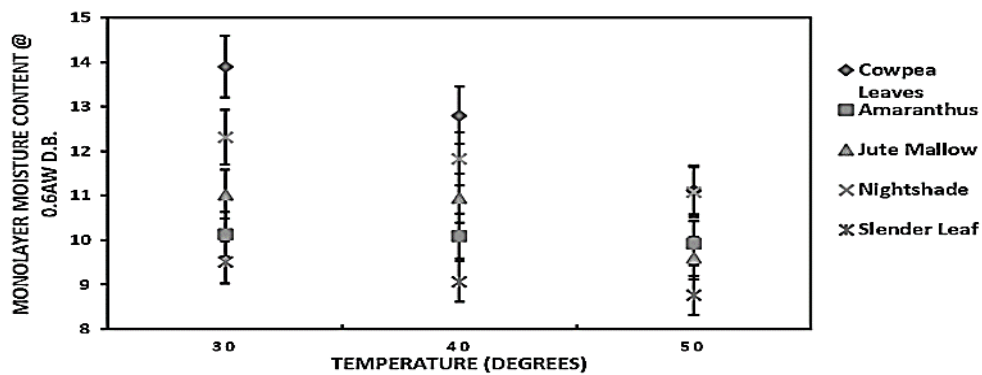
Figure 5.18. Mean safe storage moisture content for vegetables by temperature computed from the Peleg equation (Error bars represent percentage error)

5.4.3 Aflatoxin Contamination at varied relative humidity levels:

The drying pattern of the vegetables is captured in *Figure 5.19*. The curves show that the moisture in the vegetable substrate is generally bound water because there is no constant rate drying noted in the profile. Therefore, the moisture present in the leaves is generally not expected to contribute to chemical reactions. The equilibrium moisture content is shown to be attained at different times for the vegetable, which is affected by the moisture content and the structure of the material. The moisture content of the vegetables is also shown in *Table x*.
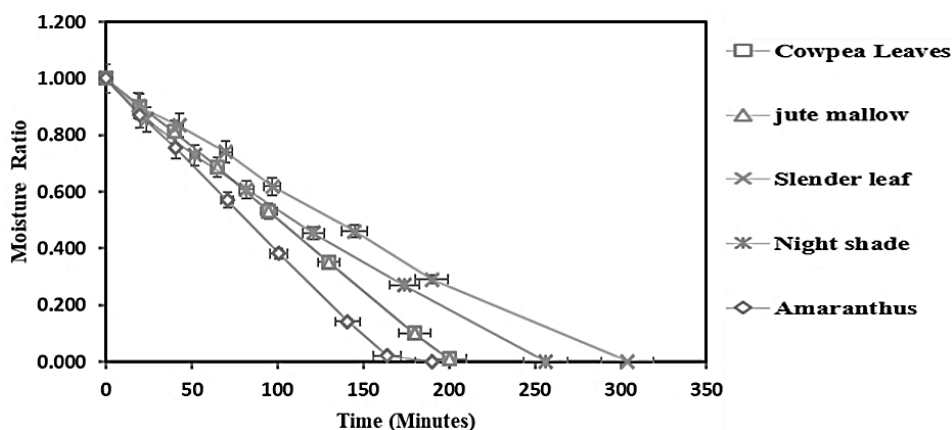
Figure 5.19. Drying curves for the vegetables at 40°C degrees

Table x. Moisture content for fresh vegetables

Vegetable	Moisture content (w.b)
Cowpea leaves	84.2%
Slender leaf	84.9%
Jute mallow	74.5%
Amaranthus	76.4%
Slender leaf	85.2%

The retention times for the chromatogram peaks for Aflatoxin standards B1, B2, G1, and G2strains were different; detected in the order of decreasing molar mass **[M+H]**+ (AFB1=313.2, AFB2=315.2, AFG1=329.2, AFG2=331.2). The mycotoxins in the vegetable sample analysis were identified from matching to the standards' retention time and respective molar mass. None of the mycotoxins were detected in the experimental control samples. It is worth noting that the temperature of incubation was above the optimum for aflatoxin progression, we can, therefore, suppose that the aflatoxin levels would exceed the amounts that were detected if the conditions were ideal. The concentrations of the aflatoxins determined from the integration of the chromatogram peaks are represented in the graphs in *Figure 5.20*, **Figure 5.21**, and *Figure 5.22*. The legend in the figures is abbreviated to show the vegetable variety (Jute mallow (JM), Nightshade (NS), Cowpea leaves (CP), Amaranthus (AM), Slender leaf (SL)), the relative humidity of incubation (32, 74, 82, 96) and whether the vegetable was pre-dried or fresh (D, F).
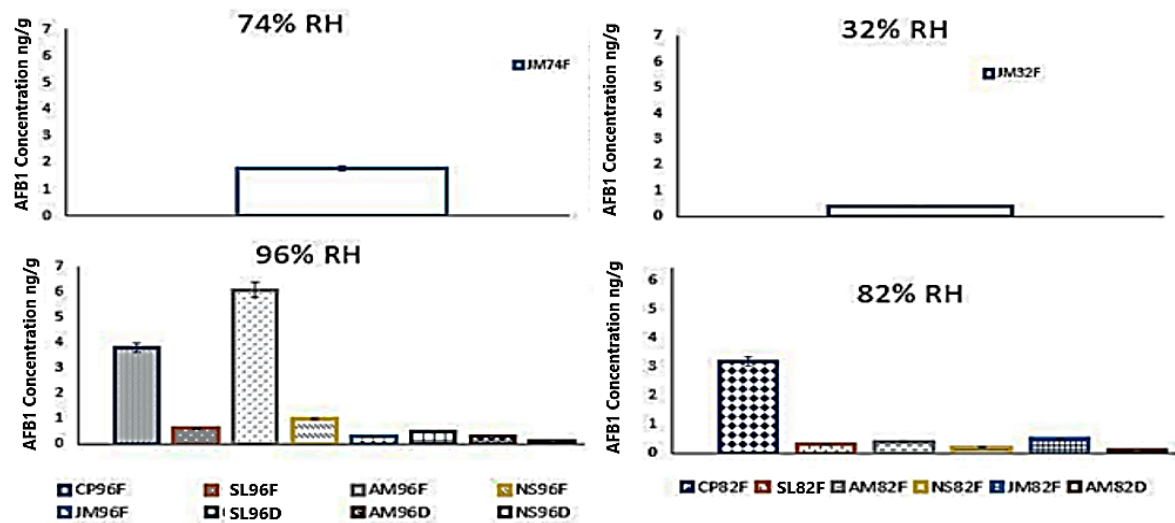
Figure 5.20. Aflatoxin B1 quantification
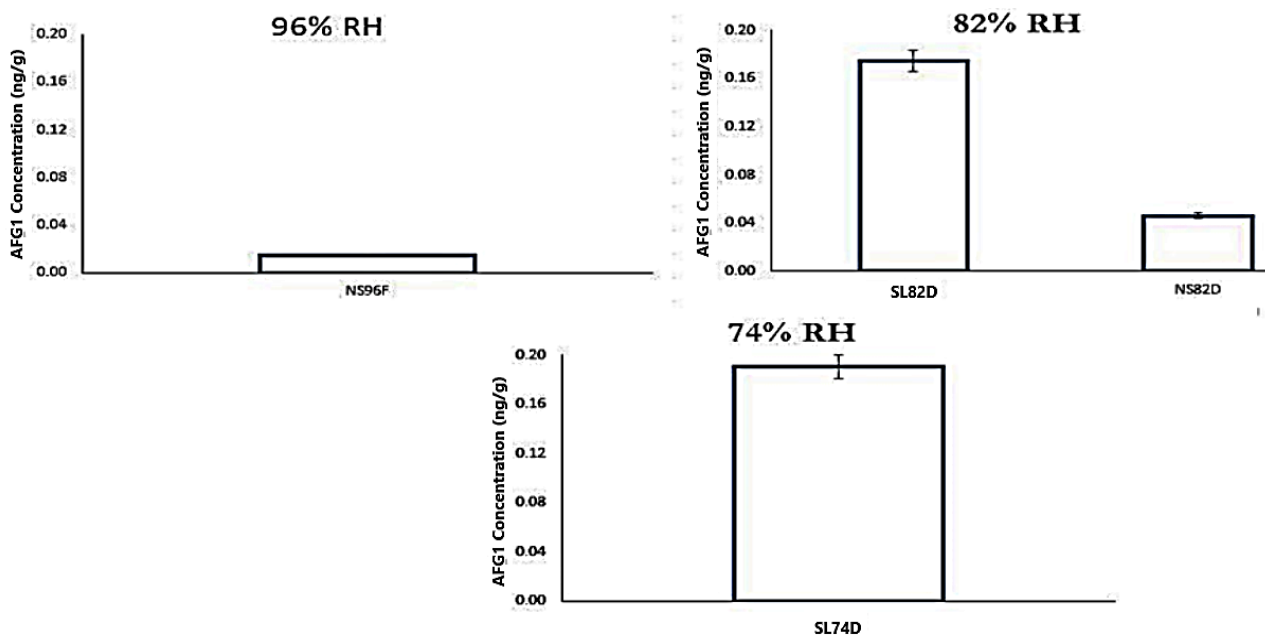
Figure 5.21. Aflatoxin G1 quantification
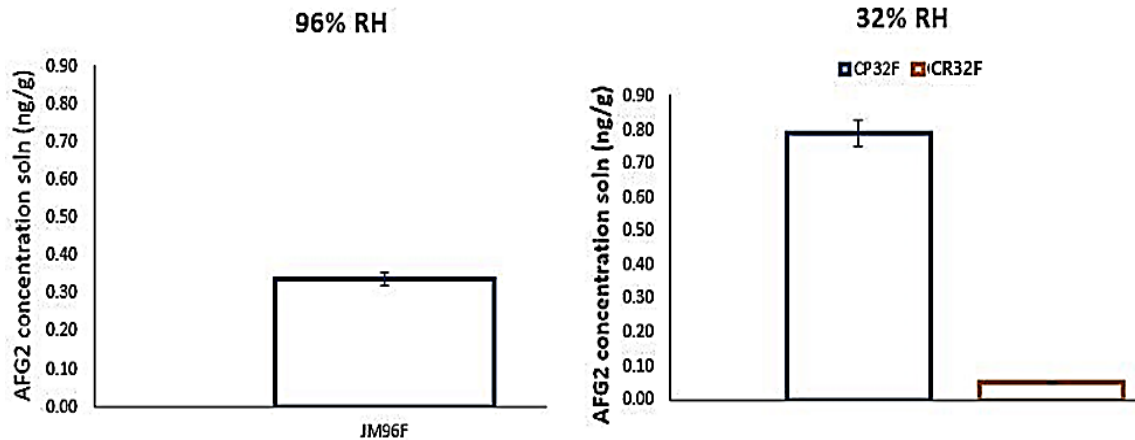
Figure 5.22. Aflatoxin G2 quantification

The error bar represents the standard error of the reported value. In general, aflatoxin B1 was the most prevalent of the toxins detected; it contaminated all the vegetable varieties in different extents. It is therefore established that the leafy vegetable material is a substrate that can support fungi progression under suitable environmental conditions and can, therefore, be contaminated by aflatoxins. The total aflatoxin contamination in the vegetables is shown in *Figure 5.23*. There is a general aflatoxin variation and the trend observed based on the vegetable variety and the equilibrium moisture content of the vegetables at the relative humidity values applied for the experiment.

From the results, it is clear that aflatoxin contamination is not a very serious problem in ALVs, except when stored at relative humidity levels above 80%. The maximum total aflatoxin allowed in the European Union is 2 ng/g and the maximum allowed in the Kenyan standard is 10ng/g. From **Figure 5.23**, all the values fall below the Kenyan standard while only two vegetables namely Cowpea leaves and Amaranthus exceed the European Union standard in the fresh state. All the dried samples fall below the European Union standard. The probable reason for the slightly higher values in Cowpea leaves and Amaranthus may be explained by the seeds in these vegetables that form early in the growth and have carbohydrate content, which seems to be a good substrate for aspergillus growth.
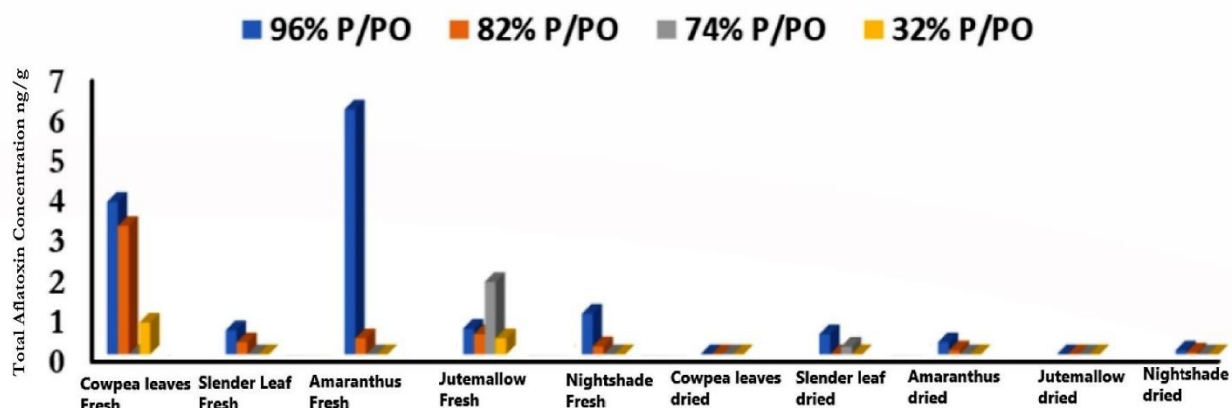
Figure 5.23. Total Aflatoxin concentrations in vegetable samples

5.4.3.1 Effect of moisture on aflatoxin contamination:

The general trend in the contamination level of the aflatoxin in ***Figure 5.20*** to ***Figure 5.22*** therein, was in the order of AFB1, AFG1, and AFG2 in decreasing order. The mean AFB1 contamination in all the vegetables was 1.2 ng/g with a standard deviation of 1.7 ng/g for the fresh incubated vegetables while the dried incubated vegetables had a mean of 0.1 ng/g and a standard deviation of 0.16 ng/g. The standard deviation is higher than the mean values indicating the high variability of the contamination levels at the different relative humidity conditions. The AFB1 contamination was detected in vegetables incubated under 96, 82, 74, and 32% relative humidity with a decreasing trend in quantity detected from 96% relative humidity incubation to 32%, however, no contamination was detected under 74 and 32% incubation for the dried incubated vegetables. Under the conditions of incubation dried vegetables are expected to absorb moisture and this has been shown in this study on the vegetables. Determined moisture sorption isotherms for the vegetables showed that their moisture sorption tends to describe a typical S-shape curve of a type II isotherm typical of porous biological materials (Bell and Labuza, 2000, Igathinathane *et al.,* 2005, Arabhosseini *et al.,* 2010). High relative humidity (>20%) present excess water in the leaves which mainly comprises the non-bound water while low relative humidity (<20%) presents for adsorption in the monolayer of the leaf. Non-bound water forms weak bonds with the solid and thus is available for deteriorative reactions unlike the strongly bound water in the monolayer which is not available for chemical and deteriorative reactions. It can be postulated that the moisture

adsorbed by the dry leaves is mostly comprised in the monolayer and thus unavailable for the biological process.

Noted was that the fresh incubated vegetables had higher aflatoxin levels than the dried incubated vegetables attributed to the presence of ideal moisture conditions that necessitated faster germination of the Aspergillus spores. From literature, it is expected that fresh leaves will suffer higher contamination than the dried vegetables. ***Table x*** shows the moisture content of the fresh vegetables, which is adequate for the progression of the aspergillus fungus. It has been shown that environmental conditions are a significant factor in the production of aflatoxin from *Aspergillus* in food crops by affecting the interactions between different mycotoxigenic species and the toxins produced by them (Paterson and Lima, 2010). The interaction between environmental temperature and humidity influences the expression levels of regulatory genes (*aflR* and *aflS*) and aflatoxin production in *A. flavus* and *A. parasiticus* (Schmidt-Heydt *et al.,* 2010).

Aflatoxin G1 and G2 are regarded as less toxic; in this study, they were detected in the vegetables. The mean quantity and standard deviation of AFG1 detected in the samples were 0.13 ng/g and 0.08 ng/g respectively, for the dried incubated vegetables. The toxin was detected in both dried and fresh incubated vegetables of two varieties: the slender leaf and the nightshade. AFG2 levels were at a mean of 0.09 ng/g and a standard deviation of 0.52 ng/g. The contamination only occurred in fresh incubated vegetables.

The trends shown in ***Figure 5.24*** can be simulated using a linear model with a 41 to 71% consistency with experimental data. Considering the high relative humidity in sub-Saharan Africa (70 – 80%) for most of the year we suggest drying and storage under dry conditions ensure storage of the ALVs below the microbial safe moisture content.
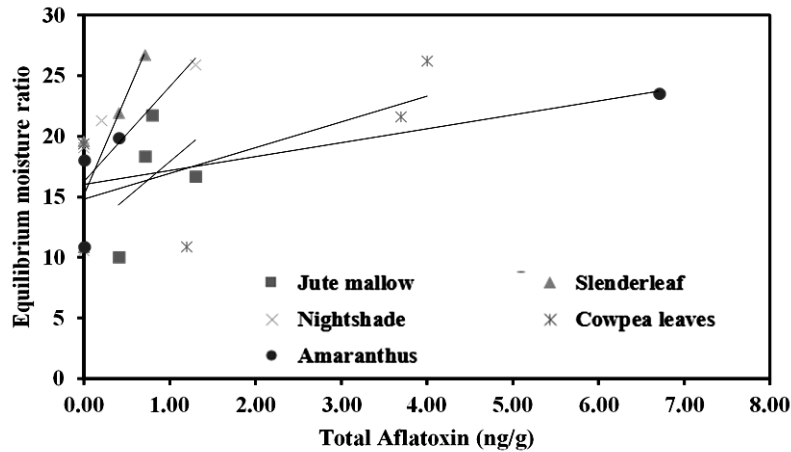
Figure 5.24. Total aflatoxin trends with EMC

Table y. Aflatoxin Trends with EMC models.

Vegetable	Model
Cowpea leaves	$y = 2.1301x + 14.807$ $R^2 = 0.4159$
Amaranthus	$y = 1.1507x + 16.035$ $R^2 = 0.5037$
Jute mallow	$y == 5.9274x + 11.978$ $R^2 = 0.5753$
Slender leaf	$y = 16.492x + 15.239$ $R^2 = 0.7112$
Nightshade	$y = 7.8293x + 16.286$ $R^2 = 0.5769$

5.4.3.2 The vegetable variety factor on aflatoxin contamination:

The level of contamination varied between the different vegetable varieties. Different vegetable substrate varies in the composition of nutrients and trace elements. Nutrients and trace elements are a factor of the genetics of the plant and the agronomic practices employed in production. The vegetables in this study were grown under controlled and similar conditions therefore the variance in the composition can only be attributed to their genetic factors. Studies have shown that the absence or presence of particular elements could have a stimulating effect on production particular mycotoxins: in a study to investigate the effects of nutrients in substrates of different grains on

Aflatoxin B1 production by *Aspergillus flavus* through the addition of lipids, sucrose, stachyose, glutamic acid, and zinc it was found that arginine and stachyose significantly stimulated AFB1 production and *A. flavus* growth, respectively (Liu *et al.,* 2016). In this study, however, the determination of the chemical composition of the vegetables was not under its scope. From the reports by other authors who have studied the African leafy vegetables, their consumption pattern and purpose can allude to uniqueness in their chemical composition e.g. specific vegetables have unique medicinal properties (Smith and Eyzaguirre, 2007). Therefore, the unique chemical composition either stimulated or suppressed the production of particular mycotoxins.

Generally, in sub-Saharan Africa, the problem of post-harvest loss due to mycotoxin contamination is most common in cereals but interest had not been shown to other foods like the indigenous vegetables which are an important component in the diets of the population. In this study, it has been shown that the vegetables are a substrate on which aspergillus can grow under suitable conditions of moisture and temperature to produce mycotoxins. AFB1 is the most prevalent strains of the mycotoxin which are the most carcinogenic. The mycotoxin levels exceeded the stipulated allowance levels in food for both human and animal consumption.

Inappropriate post-harvest handling of the vegetables could lead to their contamination with aspergillus spores. This contamination could be mainly from the soil from which the aspergillus spores are present.

It has been shown that dried vegetables are less susceptible to aflatoxin contamination because they don't provide appropriate incubation conditions for this fungus. Therefore, drying of the vegetables especially those that are not required for immediate consumption would not only increase the shelf life of the product but reduce the chances of the mycotoxin contamination.

5.5 Energy consumption analysis:

The sorption and desorption experiments were conducted (see the suitable storage conditions section) and the data modeled against temperature and temperature-independent models. Temperature independent models showed a good agreement with the data with the Peleg model selected as the most appropriate. In the estimation of energy required to remove moisture from the leaf, the Peleg model was applied in the determination of equilibrium relative humidity at different

moisture contents from 10 to 90 w.b. The water activity a_w was determined from equilibrium relative humidity.
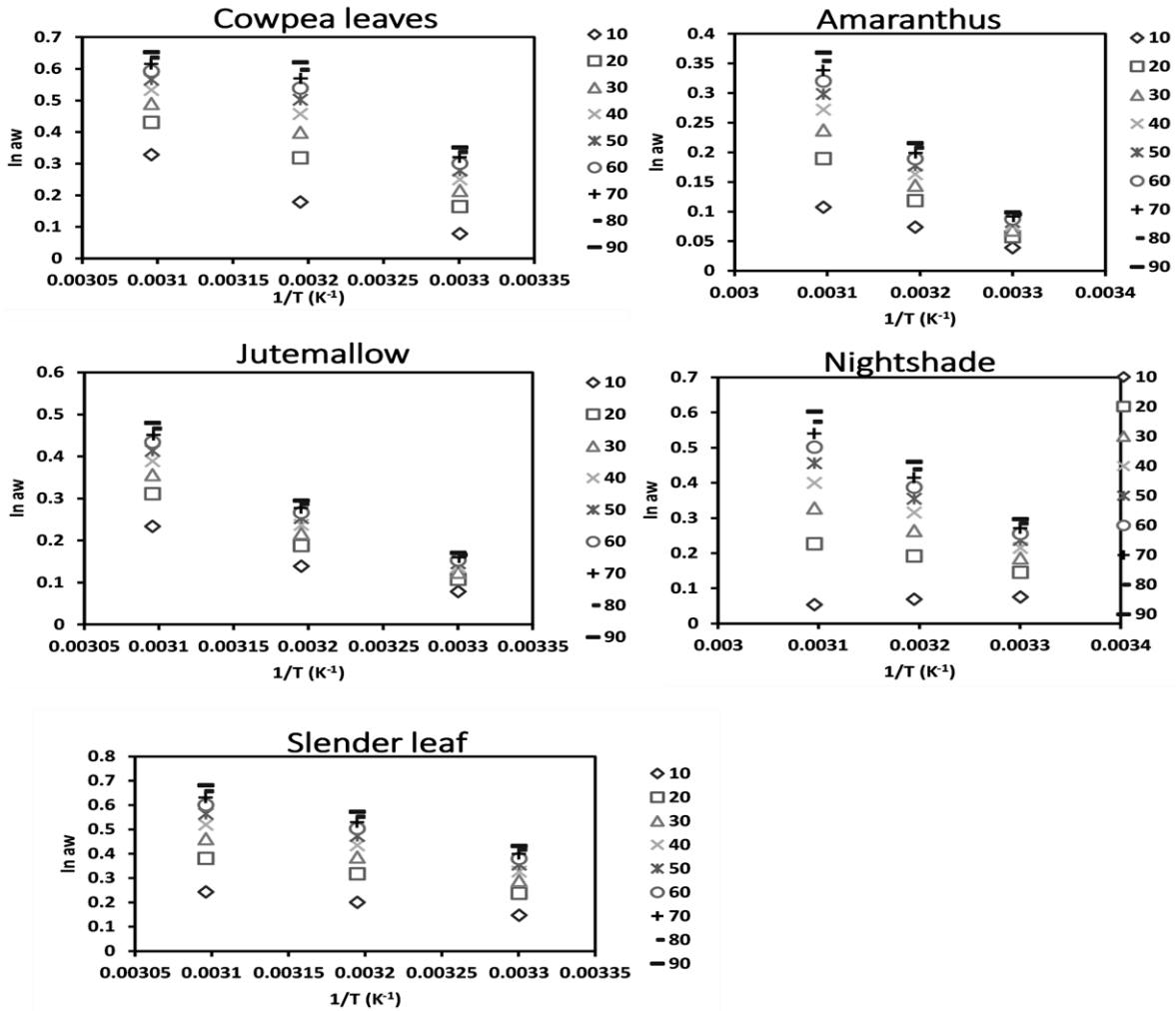
Figure 5.25. A plot of In a_w vs 1/T to determine the net heat of desorption.

Figure 5.25 shows the plot of $-In\ (a_w)$ vs 1/T which can be described using a linear model with a negative gradient. The gradient of the model represents the net isosteric heat of desorption. The heat energy was plotted against the initial moisture content of food material and the correlation obtained is plotted in *Figure 5.26*.
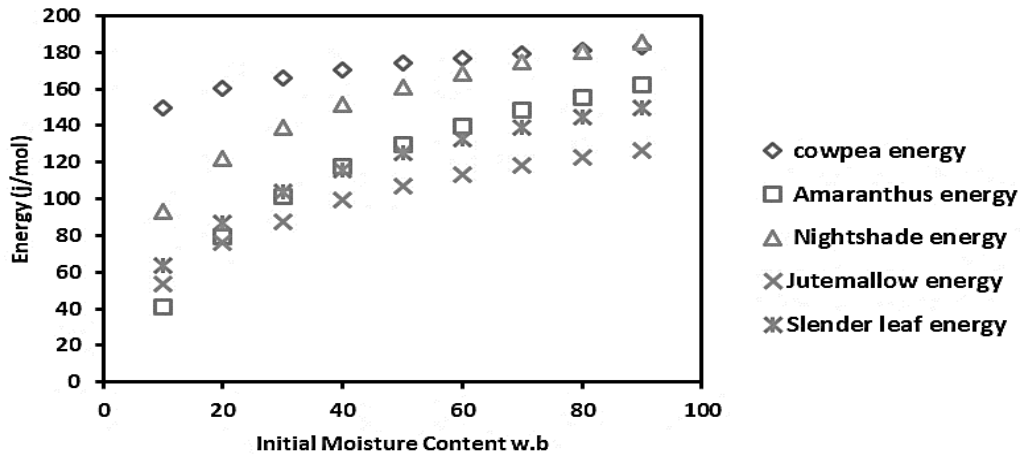
Figure 5.26. Estimated energy requirement trends at different moisture contents for the five varieties of vegetables

Table z: Models showing energy and moisture content correlation

Cowpea Leaves Model	Amaranthus Model	Nightshade Model	Jute Mallow Model	Slender Leaf Model
$h_d =$ $14.894In(MC) +$ 115.64	$h_d =$ $54.985In(MC) -$ 85.435	$h_d =$ $42.078In(MC) -$ 3.903	$h_d =$ $80.763In(MC) -$ 183.32	$h_d =$ $41.975In(MC) -$ 39.141
$R^2 = 1$	$R^2 = 1$	$R^2 = 1$	$R^2 = 0.9898$	$R^2 = 1$

The trends obtained in *Figure 5.26* can be best described by logarithmic models; there is an almost linear increase in the energy with moisture content but there is a drift from the vertical to horizontal. The energy requirement is characteristic of each vegetable material properties. Cowpea and nightshade vegetables tended to have high energy requirements than the others. The energy required to dehydrate the vegetables can be estimated with knowledge of the moisture content (MC). For the leafy vegetables, Peleg model equation can be substituted into the model equation to obtain equation 5.3, with which known values of equilibrium relative humidity can be used to estimate the energy required to dehydrate the vegetables. Equation 5.4 can be used to estimate the energy over a range of moisture contents.

$$h_d = y \, In \, (aRH^c + bRH^d) + k \qquad\qquad 5\text{-}3$$

$$dh_d = \int_{MC1}^{MC2} (y \; In \; MC + k) \; dMC \qquad\qquad 5\text{-}4$$

The calculated and estimated energy values are presented in *Table aa*:

Table aa: Estimated, Theoretical Energy and The Theoretical Energy Models

Vegetable	Calculated energy values (KJ/mol)	Theoretical energy estimation (KJ/mol) $dh_d = \int_{MC1}^{MC2} (y \; In \; MC + k) \; dMC$		
		Moisture content range (w.b)	Model equation	Energy (KJ/mol)
Cowpea leaves	9.426	85 to 7.5	$y = 6.894\ln(MC) + 85.64$ $R^2 = 1$	8.602
Nightshade	9.721	81.2 to 12	$y = 39.078\ln(MC) - 3.903$ $R^2 = 1$	9.812
Amaranthus	9.143	82.5 to 7.9	$y = 54.985\ln(MC) - 85.435$ $R^2 = 1$	8.645
Slender leaf	6.590	78.1 to 8.2	$y = 35.975\ln(MC) - 39.141$ $R^2 = 1$	6.373
Jute mallow	5.328	72.4 to 10.1	$y = 30.448\ln(MC) - 24.171$ $R^2 = 0.9991$	5.326

From *Table aa*, the values are relatively comparable with the estimated energies being lower than the calculated ones. It can be postulated that the variance accounts for the heat losses and with that, the drying efficiency can be determined.

The model developed (equation 5.4) can, therefore, be used to estimate the energy requirements in dehydrating the vegetables.

5.6. Drying air characteristics optimization:

From the findings of this study, it was revealed that vegetable quality parameters suffer degradation due to high temperatures and long drying times. Therefore, a study into the optimization of the dryer airflow characteristics to achieve low humidity and temperature of the air was conducted. Low humidity and temperature air characteristics would yield accelerated

drying with an improvement of preservation of the dried vegetable quality (nutrients and colour). Super absorbent polymer brand name Luquafleece® supplied by BASF in Germany (food grade) was tested for reduction of moisture load in the air and its desorption characteristics to test its reusability.

In the experimental set, there was a pressure drop experienced across the SAP fabric, the pressure drop increases as the moisture content of the fabric increased. Therefore, the backflow of air in the inlet airstream could be experienced, the air velocity was maintained at 0.5 ms^{-1} at the outlet of the fabric.

The experimental results for the effect of relative humidity on SAP desorption are represented in **Figure 5.27**.
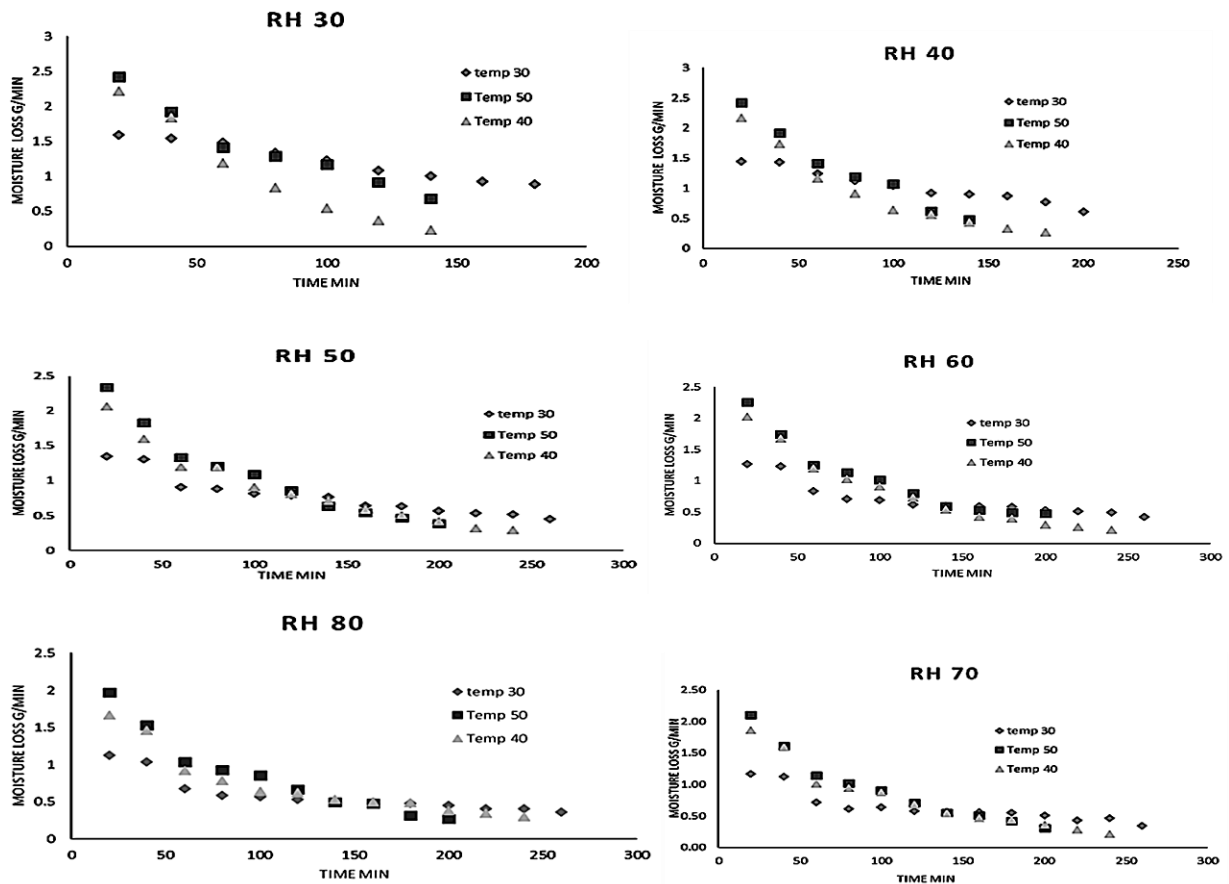
Figure 5.27. Rate of desorption at different RH and temperatures.

From **Figure 5.27** it is revealed that the SAP fabric can be regenerated when exposed to the air stream that is below saturation point at a particular temperature. Inlet air streams with increasing temperatures result in increasing desorption rates. The desorption rate decay to an equilibrium where the rate of exchange of moisture between the SAP and the air stream achieves symmetry. This aspect varies with both temperature and humidity.

Figure 5.28 below encapsulates the desorption rate in grams per minute of the SAP fabric for temperatures 50 to 30°C and relative humidity 30 to 80%.
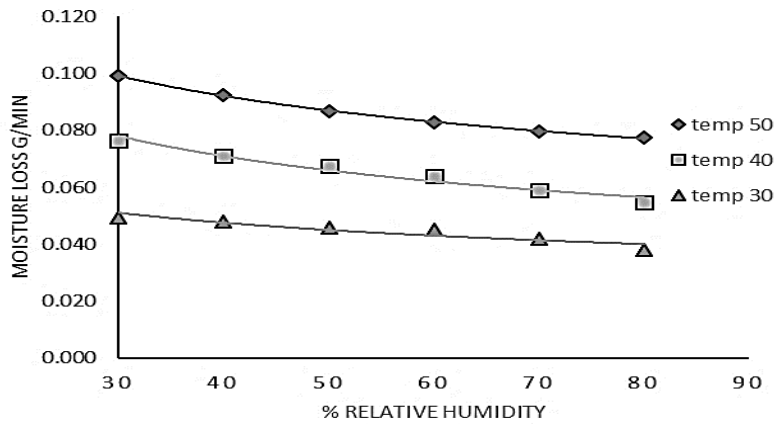
Figure 5.28. Desorption rates the SAP fabric for temperatures 50 to 30°C and relative humidity 30 to 80%.

Table bb: Summary desorption rate in grams per minute of the SAP fabric for temperatures 50 to 30°C and relative humidity 30 to 80% models.

Parameter	Model	R^2
30°C	$Y=0.1189X^{-0.249}$	0.868
40°C	$Y=0.2397X^{-0.33}$	0.962
50°C	$Y=0.2376X^{-0.257}$	0.998

In *Figure 5.28* and **Table bb**, it is revealed that temperature has a direct correlation with desorption rate at constant relative humidity also the coefficients of the models increase with temperature point to that finding.

The adsorption experiment was carried out at 30, 40 and 50°C and relative humidity values of 60 and 80%. The results obtained are represented in Figures 5.39 to 5.42.
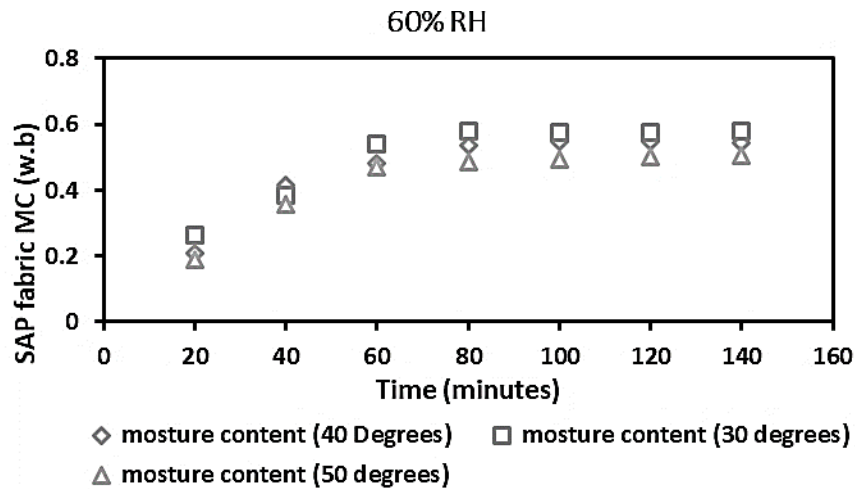
Figure 5.29. SAP fabric moisture content trend @ 60% RH
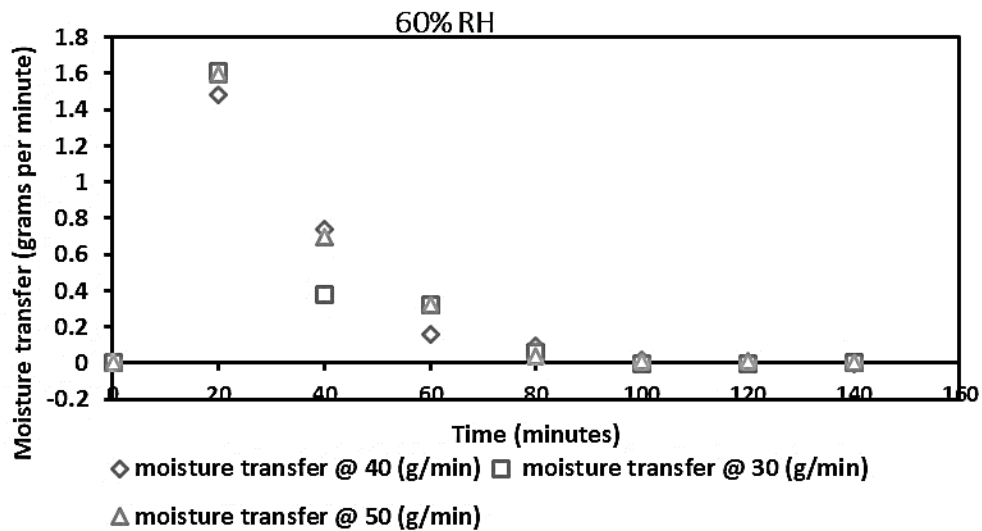
Figure 5.30. Moisture transfer rate with time evolution
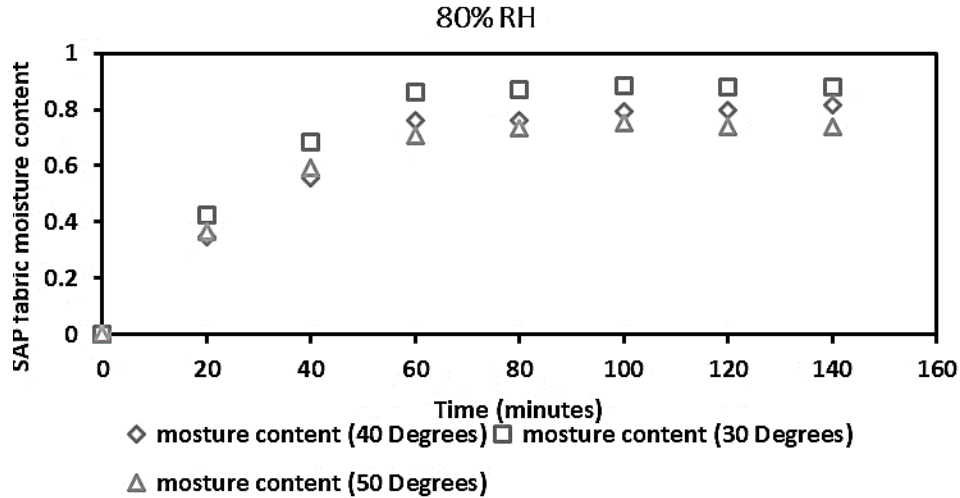
Figure 5.31. SAP fabric moisture content trend @ 60% RH
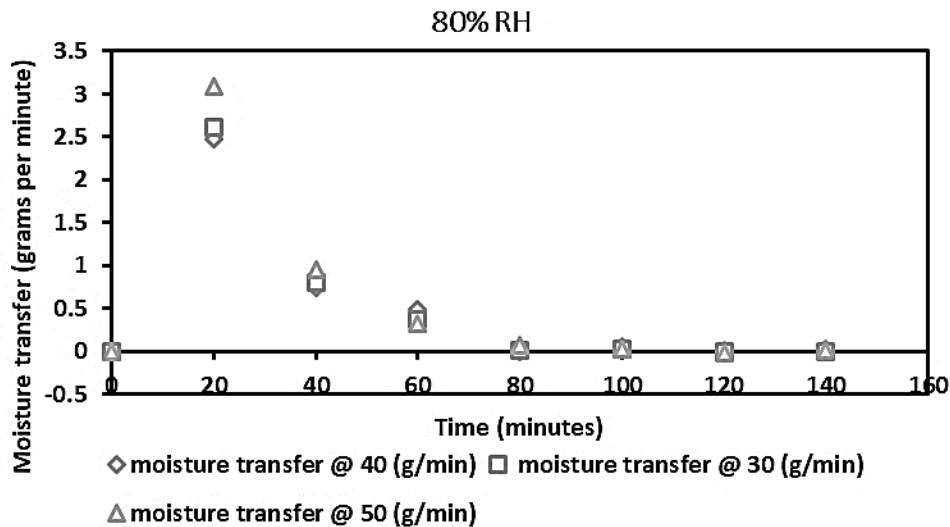
Figure 5.32. Moisture transfer rate with time evolution

The adsorption rate shows a strong dependence on relative humidity compared to temperature. SAP is known to absorb moisture up to 500 times its original weight therefore driving forces for adsorption would differ from other materials. For other materials temperature influence on absorption is highly pronounced. A precise assessment could be obtained from modelling the adsorption and desorption of the SAP with the existing sorption isotherm models, though that is not under the scope of the study.

From *Figure 5.29* to *Figure 5.32* it is revealed that the SAP would reduce the moisture load in the inlet drying stream way below the saturation point. That would accelerate drying by increasing the capacity of the to uptake evaporating moisture. The wet-bulb temperature would also be higher due to the lower relative humidity in the inlet air stream, therefore heat transfer which influences the moisture transport would be higher due to the heat transfer gradient between air and food material.

5.7 Summary of findings:

The summary of the findings in this study are presented in *Table cc* below:

Table cc. Summary of findings in this study

Number	Item description	Summary of findings
1	Drying patterns	• Drying of the vegetables mainly occurred in the falling rate period • Drying pattern adopted an exponential model
2	Drying models	• Page model best described the drying pattern of the vegetables with a 97% correlation with empirical values • The model is not precise at moisture contents of below 0.5 w.b. • A modified page model is proposed to account for changes in the rate of moisture transfer below 0.5 w.b.
3	Nutrient content analysis	• Vitamin C was the most labile nutrient, followed by vitamin E and β-carotene • 50 – 75% of the Vitamin A (β-carotene), C and E levels were retained by drying and storage for two months
4	Colour	• Colour development with drying is observed to be a function of temperature • Colour change with drying is due to non-enzymatic reactions
5	Shrinkage	• the analysis could be only realized at 30°C otherwise the leaf became brittle at moisture ratio of below 0.5 • shrinkage was only due to moisture loss • relationship between shrinkage coefficient and moisture ratio fitted into a linear model • the theoretical model developed based on physics of the material gave a precise prediction of shrinkage mechanism in the leaf
6	Transport phenomena	• non-uniform drying of the vegetables is reported

		• multiphase model developed gives an elaborate prediction of the temperature evolution, mass transfer and drying rate of food product • effective moisture diffusivity of the vegetables is in the range of other agricultural products • activation energies for moisture transport were distinct for each vegetable variety
7	Sorption isotherms	• sorption isotherms for the vegetables adopted a trend that tends to describe the typical S-shape curve of a type II isotherm • temperature inversely correlated with equilibrium relative humidity of the vegetables • for sorption modelling with temperature-dependent models, the Modified-Hasley model was most suitable • For the temperature-independent models, Peleg model showed the highest suitability • temperature-independent models best described the sorption mechanism of the vegetables • the E.M.C at which the growth of microorganisms becomes inhibited was calculated at 0.6 aw. The E.M.C values of the leafy vegetables ranged from 28% to 8% on d.b. across the temperatures • interaction between vegetable variety and the temperature was significant at $\alpha=0.05$, indicating that relatively small changes in storage temperature are required to influence the adsorption-based monolayer moisture content
8	Aflatoxins contamination	• trend in the contamination level was in the order of AFB1, AFG1, and AFG2 in decreasing order. • aflatoxin B1 was the most prevalent of the toxins detected; it contaminated all the vegetable varieties • The mean AFB1 contamination was 1.2 ng/g with a standard deviation of 1.7 ng/g for the fresh incubated vegetables while the dried incubated vegetables had a mean of 0.1 ng/g and a standard deviation of 0.16 ng/g. • AFB1 contamination was in decreasing trend in vegetables incubated under 96, 82, 74 and 32% relative humidity • fresh incubated vegetables had higher aflatoxin levels than the dried incubated vegetables
9	Energy consumption analysis	• The energy requirement was characteristic of each vegetable material properties • Theoretical energy model developed from Peleg model and Clausius–Clapeyron equation showed good agreement with calculated in results obtained

10	Drying air characteristics optimization	• The super absorbent polymer can be used to reduce the moisture load in drying air to achieve low-temperature drying • The adsorption rate shows a strong dependence on relative humidity compared to the temperature of the airflow • The super absorbent polymer can be reused several times

5.8 Contribution to knowledge and gaps filled

The contribution to knowledge in this study is summarized in *Table dd* below:

Table dd. Contribution to knowledge and gaps filled

Number	Item description	Contribution to knowledge and gaps filled
1	Drying models	• Development of a modified Page Model for drying of the leafy vegetables
5	Shrinkage	• Development of a theoretical model based on physics of the material which gave a precise prediction of shrinkage mechanism in the leaf
6	Transport phenomena	• Development of a multiphase model gives an elaborate prediction of the temperature evolution, mass transfer and drying rate of food product • Generating physical processes data that is necessary for the design of drying systems for vegetables
7	Sorption isotherms	• Determination of suitable storage conditions for the vegetables
8	Aflatoxins contamination	• Generated knowledge that can develop guidelines on handling and storage of vegetables to prevent mycotoxin contaminations.
9	Energy consumption analysis	• Development of a theoretical energy model that can be used to determine the energy requirements in the drying of the vegetables from the knowledge of moisture content.

CHAPTER SIX : Conclusions and recommendations.

6.1 Conclusion

The study gave an insight into various pertinent parameters in the drying and storage of ALVs; the investigated parameters were presented and modelled to generate patterns that aided in the understanding of the underlying mechanisms. These are summarised in the following statements.

The drying pattern of the vegetables exhibited the falling rate period of drying. There was a strong negative correlation between time and moisture ratio for all the vegetables ($\approx$-0.9), however, the correlation between temperature and moisture ratio is weak (between 0.05 and -0.08) implying that the magnitude of moisture movement is strongly dependent on drying time rather than temperature. Page model best described drying pattern of the vegetables, though it was noted that the model was the best fit at moisture ratio values of above 0.5 and therefore a modified model that accounts for the change in the rate of moisture was proposed. The drying pattern also revealed that moisture transport was predominantly by diffusion.

The empirical analysis of shrinkage was dependent on moisture loss. The empirical linear models developed showed that the vegetables had distinct shrinkage rates which were attributed to the difference in structure and hence the rate of moisture loss. Diffusivity rates did not develop a pattern with shrinkage and therefore the vegetables' structures were found to be the limiting factor. The theoretical shrinkage model developed revealed detailed shrinkage mechanisms that occur during drying and fitted well with empirical findings; the shrinkage factor (empirical) and volume ratio (theoretical) which are comparatively the same.

The multiphase model developed in the analysis of the transport phenomena showed detailed processes that occur during drying, for example, the distribution of moisture, the temperature in food material, and the drying air characteristics. The model that was developed assuming laminar airflow, which is practical for drying of leafy vegetables in a fixed bed dryer with inlet tunnel of appropriate length. The findings in the model correlated with experimental results. This model can be used to study vegetable drying characteristics and also other agricultural products with high accuracy of the findings. The model can aid in the design and configuration of drying chambers for agricultural products with precision.

The sorption curves provided valuable information about the hygroscopic equilibrium of food. They presented information on the stability domain of the food material after drying. From the observations, the product is to be stored under low humidity because it shows an increasing food water interaction with increasing humidity under ambient temperature conditions. Drying and storage at optimal conditions would also preserve nutrients.

For energy consumption, it has been shown that the energy requirements for drying a product can be estimated through the Clausius–Clapeyron approach. The model was developed together with the Peleg model. With the knowledge of the moisture content of the vegetables, the energy requirements in drying could be estimated using the model. The estimated energy requirements showed a good agreement with the calculated energy consumption. This equation can be applied to low sugar foods and to those that do not show significant hysteresis in adsorption-desorption.

Drying air characteristics can be improved to optimize energy use for drying by using the superabsorbent polymer (SAP). The polymer could be applied reduce on moisture load of the inlet air stream. It was observed that the SAP can be reused by desorbing it, and thus a mechanism that would enable simultaneous adsorption and desorption would enable continuous use of the fabric.

Aflatoxin B1 was the most prevalent strains of the mycotoxin detected in the vegetables. The total mycotoxin levels in fresh vegetables under high humidity conditions exceeded the stipulated allowed levels in food for human consumption. Mycotoxin contamination in dried vegetables was below the maximum limit for human consumption. The vegetable would require good post-harvest handling practices to prevent contamination that would result in the production of mycotoxins. Drying of the vegetables especially those that are not required for immediate consumption would not only increase the shelf life of the product but reduce the possibilities of mycotoxin contamination.

The findings of this study show that leafy vegetables can be preserved through drying and storage at optimal conditions.

6.2 Recommendations:

The findings of this study draw the recommendations:

- Adoption of the concept of drying of horticultural produce at farm level to reduce on the post-harvest loss along the suppy chain.
- Sensitization on the african leafy vegetables consumption since they are rich in micro-nutrients

6.3 Areas for further studies:

- Analytical analysis of the colour change
- Further analysis to determine the evolution of temperature and moisture in food material while drying
- A microscale/ multiscale study on shrinkage mass transfer and shrinkage

References:

ABASI, S., MOUSAVI, S., MOHEBI, M. & KIANI, S. 2009. Effect of time and temperature on moisture content, shrinkage, and rehydration of dried onion. *Iranian Journal of Chemical Engineering,* 6**,** 57-60.

ABERA, M. K., FANTA, S. W., VERBOVEN, P., HO, Q. T., CARMELIET, J. & NICOLAI, B. M. 2013. Virtual fruit tissue generation based on cell growth modelling. *Food Bioprocess Technology,* 6**,** 859-869.

ABUKUTSA-ONYANGO, M. O. Market survey on African indigenous vegetables in western Kenya. 2002.

AGUILERA, J. M. & LILLFORD, P. J. 2008. Structure–property relationships in foods. *Food Materials Science.* Springer.

AHMED, M. K. & MOHAMMED, E. I. Indigenous vegetables of Sudan: production, utilization and conservation. 1995 1995. 29-31.

AKDAŞ, S., BAŞLAR, M. & PRESERVATION 2015. Dehydration and degradation kinetics of bioactive compounds for mandarin slices under vacuum and oven drying conditions. *Journal of Food Processing and Preservation,* 39**,** 1098-1107.

AKIYAMA, T. & HAYAKAWA, K. 2000. Heat and Moisture Transfer and Hygrophysical Changes in Elastoplastic Hollow Cylinder-food During Drying. *Journal of food Science,* 65**,** 315-323.

AKPINAR, E., MIDILLI, A. & BICER, Y. 2003. Single layer drying behaviour of potato slices in a convective cyclone dryer and mathematical modeling. *Energy Conversion and Management,* 44**,** 1689-1705.

AKPINAR, E. K. 2006. Determination of suitable thin layer drying curve model for some vegetables and fruits. *Journal of food engineering,* 73**,** 75-84.

AL-MUHTASEB, A. H., MCMINN, W. A. M. & MAGEE, T. R. A. 2002. Moisture Sorption Isotherm Characteristics of Food Products: A Review. *Food and Bioproducts Processing,* 80**,** 118-128.

AL-MUHTASEB, A. H., MCMINN, W. A. M. & MAGEE, T. R. A. 2004. Water sorption isotherms of starch powders: Part 1: mathematical description of experimental data. *Journal of Food Engineering,* 61**,** 297-307.

ALIBAS, I. 2006. Characteristics of Chard Leaves during Microwave, Convective, and Combined Microwave-Convective Drying. *Drying Technology,* 24**,** 1425-1435.

AN, K., ZHAO, D., WANG, Z., JIJUN, W., YUJUAN, X. & GENGSHENG, X. 2015. Comparison of different drying methods on Chinese ginger (Zingiberofficinale Roscoe): Changes in volatiles, chemical profile, antioxidant properties, and microstructure. *Food Chemistry,* 197.

ARABHOSSEINI, A., HUISMAN, W. & MÜLLER, J. 2010. Modeling of the equilibrium moisture content (EMC) of Miscanthus (Miscanthus× giganteus). *biomass and bioenergy,* 34**,** 411-416.

AREGAWI, W. A., ABERA, M. K., FANTA, S. W., VERBOVEN, P. & NICOLAI, B. 2014. Prediction of water loss and viscoelastic deformation of apple tissue using a multiscale model. *Journal of physics: condensed matter,* 26**,** 464111.

AZZOUZ, S., GUIZANI, A., JOMAA, W. & BELGHITH, A. 2002. Moisture diffusivity and drying kinetic equation of convective drying of grapes. *Journal of Food Engineering,* 55**,** 323-330.

BANTLE, M. & EIKEVIK, T. M. 2011. Parametric study of high-intensity ultrasound in the atmospheric freeze drying of peas. *Drying Technology,* 29**,** 1230-1239.

BAUCOUR, P. & DAUDIN, J. 2000a. Development of a new method for fast measurement of water sorption isotherms in the high humidity range validation on gelatine gel. *Journal of Food Engineering,* 44**,** 97-107.

BAUCOUR, P. & DAUDIN, J. D. 2000b. Development of a new method for fast measurement of water sorption isotherms in the high humidity range validation on gelatine gel. *Journal of Food Engineering,* 44**,** 97-107.

BAZYMA, L. & KUTOVOY, V. 2005. Vacuum drying and hybrid technologies. *Stewart Postharvest Review*.

BELL, L. & LABUZA, T. 2000. Moisture sorption: practical aspects of isotherm measurement and use. American association of cereal chemists. *Inc., St. Paul***,** 33-36.

BIRD, R. S. 1960. WE; Lightfoot, EN. *Transport Phenomena*.

BRONLUND, J. & PATERSON, T. 2004. Moisture sorption isotherms for crystalline, amorphous and predominantly crystalline lactose powders. *International Dairy Journal,* 14**,** 247-254.

BROWN, Z., FRYER, P., NORTON, I., BAKALIS, S. & BRIDSON, R. 2008. Drying of foods using supercritical carbon dioxide—Investigations with carrot. *Innovative food science emerging technologies,* 9**,** 280-289.

BRUNAUER, S., EMMETT, P. H. & TELLER, E. 1938. Adsorption of Gases in Multimolecular Layers. *Journal of the American Chemical Society,* 60**,** 309-319.

BUCHAILLOT, A., CAFFIN, N. & BHANDARI, B. 2009. Drying of Lemon Myrtle (Backhousia citriodora) Leaves: Retention of Volatiles and Color. *Drying Technology,* 27**,** 445-450.

CANET, W. 1988. Determination of the moisture content of some fruits and vegetables by microwave heating. *Journal of Microwave Power and Electromagnetic Energy,* 23**,** 231-235.

CASTRO, A. M., MAYORGA, E. Y. & MORENO, F. L. 2018. Mathematical modelling of convective drying of fruits: A review. *Journal of Food Engineering,* 223**,** 152-167.

CAURIE, M. 2011. Bound water: its definition, estimation and characteristics. *International Journal of Food Science Technology,* 46**,** 930-934.

CHAKRAVERTY, A., MUJUMDAR, A. S. & RAMASWAMY, H. S. 2003. *Handbook of postharvest technology: cereals, fruits, vegetables, tea, and spices*, CRC Press.

CHANDRAMOHAN, V. 2015. Numerical Prediction and Analysis of Surface Transfer Coefficients on Moist Object During Heat and Mass Transfer Application. *Heat Transfer Engineering,* 37**,** 00-00.

CHANDRAMOHAN, V. 2016. Experimental Analysis and Simultaneous Heat and Moisture Transfer with Coupled CFD Model for Convective Drying of Moist Object. *International Journal for Computational Methods in Engineering Science and Mechanics,* 17**,** 1-46.

CHANDRAMOHAN, V. & TALUKDAR, P. 2010. Three dimensional numerical modeling of simultaneous heat and moisture transfer in a moist object subjected to convective drying. *International Journal of Heat and Mass Transfer - INT J HEAT MASS TRANSFER,* 53**,** 4638-4650.

CHANGRUE, V., SUNJKA, P. S., GARIEPY, Y., RAGHAVAN, G. V. & WANG, N. Real-time control of microwave drying process. Proc 14th Int Drying Symp Sao Paulo, Brazil, 2004. 22-25.

CHEMKHI, S., ZAGROUBA, F. & BELLAGI, A. 2004. Mathematical model for drying of highly shrinkable media. *Drying Technology,* 22**,** 1023-1039.

CHEN, C., CHI, Y.-J. & XU, W. 2012. Comparisons on the functional properties and antioxidant activity of spray-dried and freeze-dried egg white protein hydrolysate. *Food Bioprocess Technology,* 5**,** 2342-2352.

CHIRIFE, J. & IGLESIAS, H. A. 1978. Equations for fitting water sorption isotherms of foods: Part 1—a review. *International Journal of Food Science Technology,* 13**,** 159-174.

CHOU, S., CHUA, K. & TECHNOLOGY 2001. New hybrid drying technologies for heat sensitive foodstuffs. *Trends in Food Science,* 12**,** 359-369.

CHU, C. & LEE, D. 2001. Experimental analysis of centrifugal dewatering process of polyelectrolyte flocculated waste activated sludge. *Water Research,* 35**,** 2377-2384.

CHUNG, D. S. & PFOST, H. B. 1967. Adsorption and desorption of water vapor by cereal grains and their products Part II: Development of the general isotherm equation. *Transactions of the ASAE,* 10**,** 552-0555.

COHEN, H. 2011. *Numerical approximation methods*, Springer.

CURCIO, S. 2010. A Multiphase Model to Analyze Transport Phenomena in Food Drying Processes. *Drying Technology,* 28**,** 773-785.

CURCIO, S. & AVERSA, M. 2014. Influence of shrinkage on convective drying of fresh vegetables: A theoretical model. *Journal of food engineering,* 123**,** 36-49.

CURCIO, S., AVERSA, M., CALABRÒ, V. & IORIO, G. 2008. Simulation of food drying: FEM analysis and experimental validation. *Journal of Food Engineering,* 87**,** 541-553.

CURCIO, S., AVERSA, M., CALABRÒ, V. & IORIO, G. 2015. Modeling of microbial spoilage and color degradation occurring in convective drying of vegetables: a route to process optimization. *Journal of Food Process Engineering,* 38**,** 76-92.

CURCIO, S., AVERSA, M., CHAKRABORTY, S., CALABRÒ, V. & IORIO, G. 2016. Formulation of a 3D conjugated multiphase transport model to predict drying process behavior of irregular-shaped vegetables. *Journal of food engineering,* 176**,** 36-55.

DARICI, S. & ŞEN, S. 2015. Experimental investigation of convective drying kinetics of kiwi under different conditions. *Heat and Mass Transfer,* 51.

DATTA, A. 2007. Porous media approaches to studying simultaneous heat and mass transfer in food processes. I: Problem formulations. *Journal of food engineering,* 80**,** 80-95.

DE MICHELIS, A., MARQUEZ, C. A., MABELLINI, A., OHACO, E. & GINER, S. A. 2013. Effect of structural modifications on the drying kinetics of foods: changes in volume, surface area and product shape.

DEFRAEYE, T. 2014. Advanced computational modelling for drying processes – A review. *Applied Energy,* 131**,** 323-344.

DEFRAEYE, T., BLOCKEN, B. & CARMELIET, J. 2012. CFD simulation of heat transfer at surfaces of bluff bodies in turbulent boundary layers: Evaluation of a forced-convective temperature wall function for mixed convection. *Journal of Wind Engineering and Industrial Aerodynamics,* 104-106**,** 439-446.

DEFRAEYE, T., LEHMANN, V., GROSS, D., HOLAT, C., HERREMANS, E., VERBOVEN, P., VERLINDEN, B. E. & NICOLAI, B. M. 2013. Application of MRI for tissue characterisation of 'Braeburn'apple. *Postharvest biology technology,* 75**,** 96-105.

DEFRAEYE, T., NICOLAÏ, B., MANNES, D., AREGAWI, W., VERBOVEN, P. & DEROME, D. 2016. Probing inside fruit slices during convective drying by quantitative neutron imaging. *Journal of food engineering,* 178**,** 198-202.

DEFRAEYE, T. & RADU, A. 2017. Convective drying of fruit: A deeper look at the air-material interface by conjugate modeling. *International Journal of Heat and Mass Transfer,* 108**,** 1610-1622.

DELGADO, A. E. & SUN, D.-W. 2002a. Desorption isotherms and glass transition temperature for chicken meat. *Journal of food engineering,* 55**,** 1-8.

DELGADO, A. E. & SUN, D.-W. 2002b. Desorption isotherms for cooked and cured beef and pork. *Journal of food engineering,* 51**,** 163-170.

DESMORIEUX, H., MADIOULI, J., HERRAUD, C. & MOUAZIZ, H. 2010. Effects of size and form of Arthrospira Spirulina biomass on the shrinkage and porosity during drying. *Journal of food engineering,* 100**,** 585-595.

DHALL, A. & DATTA, A. K. 2011. Transport in deformable food materials: a poromechanics approach. *Chemical Engineering Science,* 66**,** 6482-6497.

DHALL, A., HALDER, A. & DATTA, A. 2012a. Multiphase and multicomponent transport with phase change during meat cooking. *Journal of Food Engineering,* 113**,** 299-309.

DHALL, A., SQUIER, G., GEREMEW, M., WOOD, W. A., GEORGE, J. & DATTA, A. K. 2012b. Modeling of Multiphase Transport during Drying of Honeycomb Ceramic Substrates. *Drying Technology,* 30**,** 607-618.

DOYMAZ, I. 2004. Convective air drying characteristics of thin layer carrots. *Journal of food engineering,* 61**,** 359-364.

DOYMAZ, İ. & İSMAIL, O. 2012. Experimental characterization and modelling of drying of pear slices. *Food Science Biotechnology,* 21**,** 1377-1381.

ERBAY, Z. & ICIER, F. 2010. A Review of Thin Layer Drying of Foods: Theory, Modeling, and Experimental Results. *Critical Reviews in Food Science and Nutrition,* 50**,** 441-464.

ERTEKIN, C. & FIRAT, M. Z. 2017. A comprehensive review of thin-layer drying models used in agricultural products. *Critical Reviews in Food Science and Nutrition,* 57**,** 701-717.

ERTEKIN, C. & YALDIZ, O. 2004. Drying of eggplant and selection of a suitable thin layer drying model. *Journal of food engineering,* 63**,** 349-359.

ESFAHANI, J. A., MAJDI, H. & BARATI, E. 2014. Analytical two-dimensional analysis of the transport phenomena occurring during convective drying: Apple slices. *Journal of Food Engineering,* 123**,** 87-93.

FAKRUDDIN, M., CHOWDHURY, A., HOSSAIN, M. N. & AHMED, M. M. 2015. Characterization of aflatoxin producing Aspergillus flavus from food and feed samples. *SpringerPlus,* 4**,** 159.

FANTA, S. W., ABERA, M. K., AREGAWI, W. A., HO, Q. T., VERBOVEN, P., CARMELIET, J. & NICOLAI, B. M. 2014. Microscale modeling of coupled water transport and mechanical deformation of fruit tissue during dehydration. *Journal of food engineering,* 124**,** 86-96.

FAO 2011. Global Food Waste Extent, Food Losses, Causes and Prevention. *FAO: Rome, Italy*.

FLETCHER, D., GUO, B., HARVIE, D., LANGRISH, T., NIJDAM, J. & WILLIAMS, J. 2006. What is important in the simulation of spray dryer performance and how do current CFD models perform? *Applied Mathematical Modelling,* 30**,** 1281-1292.

FLUENT, A. 2013. ANSYS fluent theory guide 15.0. *ANSYS, Canonsburg, PA*.

GABAS, A. L., BERNARDI, M., TELIS-ROMERO, J. & TELIS, V. R. Application of heat pump in drying of apple cylinders. Proc 14th Int Drying Symp, 2004. 1922-1929.

GARAU, M., SIMAL, S., FEMENIA, A. & ROSSELLÓ, C. 2006. Drying of orange skin: drying kinetics modelling and functional properties. *Journal of Food Engineering,* 75**,** 288-295.

GARCÍA-PÉREZ, J. V., OZUNA, C., ORTUÑO, C., CÁRCEL, J. A. & MULET, A. 2011. Modeling ultrasonically assisted convective drying of eggplant. *Drying Technology,* 29**,** 1499-1509.

GOCKOWSKI, J., MBAZO'O, J., MBAH, G. & MOULENDE, T. F. 2003. African traditional leafy vegetables and the urban and peri-urban poor. *Food policy,* 28**,** 221-235.

GOCKOWSKI, J. & NDOUMBE, M. 2004. The adoption of intensive monocrop horticulture in southern Cameroon. *Agricultural economics,* 30**,** 195-202.

GOLESTANI, R., RAISI, A. & AROUJALIAN, A. 2013. Mathematical Modeling on Air Drying of Apples Considering Shrinkage and Variable Diffusion Coefficient. *Drying Technology,* 31**,** 40-51.

GOULA, A. M., ADAMOPOULOS, K. G., CHATZITAKIS, P. C. & NIKAS, V. A. 2006. Prediction of lycopene degradation during a drying process of tomato pulp. *Journal of Food Engineering,* 74**,** 37-46.

GUAN, Z., WANG, X., LI, M. & JIANG, X. 2013. Mathematical modeling on hot air drying of thin layer fresh tilapia fillets. *Polish journal of food nutrition sciences,* 63**,** 25-33.

GULATI, T. & DATTA, A. K. 2015. Mechanistic understanding of case-hardening and texture development during drying of food materials. *Journal of Food Engineering,* 166**,** 119-138.

GULATI, T., ZHU, H., DATTA, A. K. & HUANG, K. 2015. Microwave drying of spheres: Coupled electromagnetics-multiphase transport modeling with experimentation. Part II: Model validation and simulation results. *Food Bioproducts Processing,* 96**,** 326-337.

GUPTA, K. & ALAM, M. 2014. Modeling of thin layer drying kinetics of grape juice concentrate and quality assessment of developed grape leather. *Agricultural Engineering International: CIGR Journal,* 16**,** 196-207.

GÜZEY, D., ÖZDEMIR, M., SEYHAN, F. G., DOĞAN, H. & DEVRES, Y. O. 2001. Adsorption isotherms of raw and roasted hazelnuts. *Drying technology,* 19**,** 691-699.

HALDER, A. & DATTA, A. 2012a. Surface heat and mass transfer coefficients for multiphase porous media transport models with rapid evaporation. *Food and Bioproducts Processing,* 90**,** 475–490.

HALDER, A. & DATTA, A. K. 2012b. Surface heat and mass transfer coefficients for multiphase porous media transport models with rapid evaporation. *Food Bioproducts Processing,* 90**,** 475-490.

HALDER, A., DHALL, A. & DATTA, A. 2011. Modeling Transport in Porous Media With Phase Change: Applications to Food Processing. *Journal of Heat Transfer,* 133**,** 031010.

HALSEY, G. 1948. Physical adsorption on non-uniform surfaces. *The Journal of chemical physics,* 16**,** 931-937.

HARIPRASAD, P., DURIVADIVEL, P., SNIGDHA, M. & VENKATESWARAN, G. 2013. Natural occurrence of aflatoxin in green leafy vegetables. *Food chemistry,* 138**,** 1908-1913.

HASSINI, L., AZZOUZ, S., PECZALSKI, R. & BELGHITH, A. 2007. Estimation of potato moisture diffusivity from convective drying kinetics with correction for shrinkage. *Journal of Food Engineering,* 79**,** 47-56.

HAWLADER, M., PERERA, C. O. & TIAN, M. 2006. Properties of modified atmosphere heat pump dried foods. *Journal of Food Engineering,* 74**,** 392-401.

HEINRICH, S., KRÜGER, G., MÖRL, L. J. C. E. & INTENSIFICATION, P. P. 1999. Modelling of the batch treatment of wet granular solids with superheated steam in fluidized beds. 38, 131-142.

HENDERSON, S. 1952. A basic concept of equilibrium moisture. *Agricultural engineering,* 33, 29-32.

HO, Q. T., VERBOVEN, P., VERLINDEN, B. E., LAMMERTYN, J., VANDEWALLE, S. & NICOLAÏ, B. M. 2008. A continuum model for metabolic gas exchange in pear fruit. *PLoS computational biology,* 4, e1000023.

HO, Q. T., VERBOVEN, P., VERLINDEN, B. E. & NICOLAÏ, B. M. 2010. A model for gas transport in pear fruit at multiple scales. *Journal of experimental botany,* 61, 2071-2081.

HODGES, R., BERNARD, M. & REMBOLD, F. 2014. *APHLIS - Postharvest cereal losses in Sub-Saharan Africa, their estimation, assessment and reduction*.

HOLOWATY, S. A., RAMALLO, L. A. & SCHMALKO, M. E. 2012. Intermittent drying simulation in a deep bed dryer of yerba maté. *Journal of Food Engineering,* 111, 110-114.

HORUZ, E. & MASKAN, M. 2015. Hot air and microwave drying of pomegranate (Punica granatum L.) arils. *Journal of Food Science Technology,* 52, 285-293.

IGATHINATHANE, C., WOMAC, A., SOKHANSANJ, S. & PORDESIMO, L. 2005. Sorption equilibrium moisture characteristics of selected corn stover components. *Transactions of the ASAE,* 48, 1449-1460.

IGLESIAS, H. & CHIRIFE, J. 1976a. Prediction of the effect of temperature on water sorption isotherms of food material. *International Journal of Food Science Technology,* 11, 109-116.

IGLESIAS, H. A. & CHIRIFE, J. 1976b. Prediction of the effect of temperature on water sorption isotherms of food material. *International Journal of Food Science & Technology,* 11, 109-116.

INTERNATIONAL AGENCY FOR RESEARCH ON, C. 2002. *IARC handbooks of cancer prevention*, The Agency.

ITAYA, Y., KOBAYASHI, T. & HAYAKAWA, K.-I. 1995. Three-dimensional heat and moisture transfer with viscoelastic strain-stress formation in composite food during drying. *International Journal of Heat Mass Transfer,* 38, 1173-1185.

JAMALEDDINE, T. J. & RAY, M. B. 2010. Application of computational fluid dynamics for simulation of drying processes: A review. *Drying Technology,* 28, 120-154.

JANGAM, S. V. 2011. An Overview of Recent Developments and Some R&D Challenges Related to Drying of Foods. *Drying Technology,* 29, 1343-1357.

JIANG, H., ZHANG, M., MUJUMDAR, A. S. & LIM, R. X. 2014. Comparison of drying characteristic and uniformity of banana cubes dried by pulse-spouted microwave vacuum drying, freeze drying and microwave freeze drying. *Journal of the Science of Food Agriculture,* 94, 1827-1834.

JIANG, N., LIU, C., LI, D., ZHANG, Z., LIU, C., WANG, D., NIU, L., ZHANG, M. & TECHNOLOGY 2017. Evaluation of freeze drying combined with microwave vacuum drying for functional okra

snacks: Antioxidant properties, sensory quality, and energy consumption. *LWT-Food Science,* 82**,** 216-226.

JOARDDER, M. U., KARIM, A., KUMAR, C. & BROWN, R. J. 2015. *Porosity: establishing the relationship between drying parameters and dried food quality*, Springer.

JOARDDER, M. U., KUMAR, C. & KARIM, M. 2017a. Multiphase transfer model for intermittent microwave-convective drying of food: Considering shrinkage and pore evolution. *International Journal of Multiphase Flow,* 95**,** 101-119.

JOARDDER, M. U., KUMAR, C. & KARIM, M. J. I. J. O. M. F. 2017b. Multiphase transfer model for intermittent microwave-convective drying of food: Considering shrinkage and pore evolution. 95**,** 101-119.

JOARDDER, M. U. H. & MASUD, M. H. 2019. Causes of Food Waste. *Food Preservation in Developing Countries: Challenges and Solutions.* Springer.

JOINT, F. A. O. W. H. O. E. C. O. F. A. M., JOINT, F. A. O. W. H. O. E. C. O. F. A. & WORLD HEALTH, O. 2004. *Evaluation of Certain Food Additives and Contaminants: Sixty-first Report of the Joint FAO/WHO Expert Committee on Food Additives*, World Health Organization.

KARUNASENA, H., SENADEERA, W., BROWN, R. J. & GU, Y. 2014. A particle based model to simulate microscale morphological changes of plant tissues during drying. *Soft matter,* 10**,** 5249-5268.

KATEKAWA, M. & SILVA, M. 2007. On the Influence of Glass Transition on Shrinkage in Convective Drying of Fruits: A Case Study of Banana Drying. *Drying Technology,* 25**,** 1659-1666.

KAYA, A., AYDıN, O. & DINCER, I. 2008. Experimental and numerical investigation of heat and mass transfer during drying of Hayward kiwi fruits (Actinidia Deliciosa Planch). *Journal of Food Engineering,* 88**,** 323-330.

KHALLOUFI, S., GIASSON, J. & RATTI, C. 2000. Water activity of freeze dried mushrooms and berries. *Canadian Agricultural Engineering,* 42**,** 51-56.

KHAN, M. I. H., NAGY, S. A. & KARIM, M. 2018. Transport of cellular water during drying: An understanding of cell rupturing mechanism in apple tissue. *Food research international,* 105**,** 772-781.

KHAN, M. I. H., WELLARD, R. M., NAGY, S. A., JOARDDER, M. U. H. & KARIM, M. A. 2017. Experimental investigation of bound and free water transport process during drying of hygroscopic food material. *International Journal of Thermal Sciences,* 117**,** 266-273.

KHAZAEI, J., CHEGINI, G.-R. & BAKHSHIANI, M. 2008. A novel alternative method for modeling the effects of air temperature and slice thickness on quality and drying kinetics of tomato slices: superposition technique. *Drying Technology,* 26**,** 759-775.

KHIN, M. M., ZHOU, W. & PERERA, C. 2005. Development in the combined treatment of coating and osmotic dehydration of food-a review. *International Journal of Food Engineering,* 1.

KITTIWORRAWATT, S. & DEVAHASTIN, S. 2009. Improvement of a mathematical model for low-pressure superheated steam drying of a biomaterial. *Chemical Engineering Science,* 64**,** 2644-2650.

KLICH, M. A. 2002. *Identification of common Aspergillus species*, Centraalbureau voor schimmelcultures Utrecht.

KOUHILA, M., BELGHIT, A., DAGUENET, M. & BOUTALEB, B. 2001. Experimental determination of the sorption isotherms of mint (Mentha viridis), sage (Salvia officinalis) and verbena (Lippia citriodora). *Journal of food engineering,* 47**,** 281-287.

KOWALSKI, S. & SZADZIŃSKA, J. 2014. Kinetics and Quality Aspects of Beetroots Dried in Non-Stationary Conditions. *Drying Technology,* 32.

KRISHNA MURTHY, T. P. & MANOHAR, B. 2012. Microwave drying of mango ginger (Curcuma amada Roxb): prediction of drying kinetics by mathematical modelling and artificial neural network. 47**,** 1229-1236.

KUDRA, T. & MUJUMDAR, A. 2009. Special drying technologies. *Advanced Drying Technologies***,** 427-455.

KUMAR, C., JOARDDER, M. U. H., FARRELL, T. W., MILLAR, G. J. & KARIM, M. A. 2016. Mathematical model for intermittent microwave convective drying of food materials. *Drying Technology,* 34**,** 962-973.

KUMAR, C., KARIM, M. A. & JOARDDER, M. U. H. 2014. Intermittent drying of food products: A critical review. *Journal of Food Engineering,* 121**,** 48-57.

KUMAR, N., SARKAR, B. C. & SHARMA, H. K. 2012. Mathematical modelling of thin layer hot air drying of carrot pomace. *Journal of food science and technology,* 49**,** 33-41.

KURIAKOSE, R. & ANANDHARAMAKRISHNAN, C. 2010. Computational fluid dynamics (CFD) applications in spray drying of food products. *Trends in Food Science Technology,* 21**,** 383-398.

KUROZAWA, L., HUBINGER, M. & PARK, K. 2012. Glass transition phenomenon on shrinkage of papaya during convective drying. *Journal of Food Engineering,* 108**,** 43–50.

LABUZA, T. P. & ALTUNAKAR, B. 2007. Water activity prediction and moisture sorption isotherms. *Water activity in foods: Fundamentals applications,* 1**,** 109-154.

LAMNATOU, C., PAPANICOLAOU, E., BELESSIOTIS, V. & KYRIAKIS, N. 2010. Finite-volume modelling of heat and mass transfer during convective drying of porous bodies – Non-conjugate and conjugate formulations involving the aerodynamic effects. *Renewable Energy,* 35**,** 1391-1402.

LEERATANARAK, N., DEVAHASTIN, S. & CHIEWCHAN, N. 2006. Drying kinetics and quality of potato chips undergoing different drying techniques. *Journal of food engineering,* 77**,** 635-643.

LEMUS-MONDACA, R., VEGA-GALVEZ, A., ZAMBRA, C. E. & MORAGA, N. 2017. Modeling 3D conjugate heat and mass transfer for turbulent air drying of Chilean papaya in a direct contact dryer. *Heat and Mass Transfer,* 53.

LEMUS-MONDACA, R. A., ZAMBRA, C. E., VEGA-GÁLVEZ, A. & MORAGA, N. O. 2013. Coupled 3D heat and mass transfer model for numerical analysis of drying process in papaya slices. *Journal of Food Engineering,* 116**,** 109-117.

LESPINARD, A., GOÑI, S., SALGADO, P. & MASCHERONI, R. 2009. Experimental determination and modelling of size variation, heat transfer and quality indexes during mushroom blanching. *Journal of Food Engineering,* 92**,** 8-17.

LIEDEKERKE, P., GHYSELS, P., TIJSKENS, E., SAMAEY, G., ROOSE, D. & RAMON, H. 2011. Mechanisms of soft cellular tissue bruising. A particle based simulation approach. *Soft Matter,* 7**,** 3580-3591.

LINDAHL, J. F. & GRACE, D. 2013. Aflatoxins, major contributions to harvest loss-what do we know and not know? *Agri4D conference.* Sweden.

LIU, J., SUN, L., ZHANG, J., GUO, J., CHEN, L., QI, D. & ZHANG, N. 2016. Aflatoxin B1, zearalenone and deoxynivalenol in feed ingredients and complete feed from central China. *Food Additives & Contaminants: Part B,* 9**,** 91-97.

LLAVE, Y., TAKEMORI, K., FUKUOKA, M., TAKEMORI, T., TOMITA, H. & SAKAI, N. 2016. Mathematical modeling of shrinkage deformation in eggplant undergoing simultaneous heat and mass transfer during convection-oven roasting. *Journal of Food Engineering,* 178**,** 124-136.

MABROUK, S., BENALI, E. & OUESLATI, H. 2012. Experimental study and numerical modelling of drying characteristics of apple slices. *Food and Bioproducts Processing,* 90**,** 719–728.

MALEKJANI, N. & JAFARI, S. M. 2018. Simulation of food drying processes by Computational Fluid Dynamics (CFD); recent advances and approaches. *Trends in Food Science Technology,* 78**,** 206-223.

MÁRQUEZ, C. A. & DE MICHELIS, A. 2011. Comparison of drying kinetics for small fruits with and without particle shrinkage considerations. *Food Bioprocess Technology,* 4**,** 1212-1218.

MASKAN, A., KAYA, S. & MASKAN, M. 2002. Hot air and sun drying of grape leather (pestil). *Journal of food engineering,* 54**,** 81-88.

MAZIYA-DIXON, B., AKINYELE, I. O., OGUNTONA, E. B., NOKOE, S., SANUSI, R. A. & HARRIS, E. 2004. Nigeria food consumption and nutrition survey 2001-2003. *International Institute of Tropical Agriculture (IITA), Ibadan, Nigeria.*

MAZZOCCHI, M., BRASILI, C. & SANDRI, E. 2008. Trends in dietary patterns and compliance with World Health Organization recommendations: a cross-country analysis. *Public Health Nutrition,* 11**,** 535-540.

MBUGE, D. O., NEGRINI, R., NYAKUNDI, L. O., KUATE, S. P., BANDYOPADHYAY, R., MUIRU, W. M., TORTO, B. & MEZZENGA, R. 2016. Application of superabsorbent polymers (SAP) as desiccants to dry maize and reduce aflatoxin contamination. *Journal of food science and technology,* 53**,** 3157-3165.

MCMINN, W. & MAGEE, T. 2003. Thermodynamic properties of moisture sorption of potato. *Journal of food engineering,* 60**,** 157-165.

MEISAMI-ASL, E., RAFIEE, S., KEYHANI, A. & TABATABAEEFAR, A. 2009. Mathematical Modeling of Kinetics of Thin-layer Drying of Apple (var. Golab). *Agricultural Engineering International : The CIGR e-journal,* 0.

MEISAMI-ASL, E., RAFIEE, S., KEYHANI, A. & TABATABAEEFAR, A. 2010. Determination of suitable thin layer drying curve model for apple slices (variety-Golab). *Plant OMICS,* 3**,** 103-108.

MENKOV, N. D. & DURAKOVA, A. G. 2005. Equilibrium moisture content of semi-defatted pumpkin seed flour. *International Journal of Food Engineering,* 1.

MERCIER, S., MARCOS, B., MORESOLI, C., MONDOR, M. & VILLENEUVE, S. 2014. Modeling of internal moisture transport during durum wheat pasta drying. *Journal of Food Engineering,* 124**,** 19–27.

MIDILLI, A., KUCUK, H. & MANAGEMENT 2003. Mathematical modeling of thin layer drying of pistachio by using solar energy. *Energy conversion,* 44**,** 1111-1122.

MIDILLI, A., KUCUK, H. & YAPAR, Z. 2002. A NEW MODEL FOR SINGLE-LAYER DRYING. *Drying Technology,* 20**,** 1503-1513.

MILIĆEVIĆ, D. R., ŠKRINJAR, M. & BALTIĆ, T. 2010. Real and perceived risks for mycotoxin contamination in foods and feeds: challenges for food safety control. *Toxins,* 2**,** 572-592.

MOON, J. H., PAN, C. H. & YOON, W. B. 2015. Drying characteristics and thermal degradation kinetics of hardness, anthocyanin content and colour in purple-and red-fleshed potato (S olanum tuberosum L.) during hot air drying. *International Journal of Food Science Technology,* 50**,** 1255-1267.

MORAES, M. A., ROSA, G. S. & PINTO, L. A. A. 2008. Moisture sorption isotherms and thermodynamic properties of apple Fuji and garlic. *International journal of food science & technology,* 43**,** 1824-1831.

MORAGA, N., JAURIAT, L. & LEMUS-MONDACA, R. 2012. Heat and mass transfer in conjugate food freezing/air natural convection. *International Journal of Refrigeration,* 35**,** 880–889.

MORAGA, N., TORRES, A., GUARDA, A. & GALOTTO, M. 2011. Non-newtonian canned liquid food, unsteady fluid mechanics and heat transfer prediction for pasteurization and sterilization. *Journal of Food Process Engineering,* 34.

MOTEVALI, A., MINAEI, S. & KHOSHTAGAZA, M. H. 2011. Evaluation of energy consumption in different drying methods. *Energy conversion management,* 52**,** 1192-1199.

MOTHIBE, K. J., ZHANG, M., NSOR-ATINDANA, J. & WANG, Y.-C. J. D. T. 2011. Use of ultrasound pretreatment in drying of fruits: drying rates, quality attributes, and shelf life extension. 29**,** 1611-1621.

MUCHOKI, N. 2007. *Nutritional, sensory and keeping properties of fermented solar-dried cowpea leaf vegetables.* Msc. Thesis. , University of Nairobi.

MUJUMDAR, A. S. & DEVAHASTIN, S. 2000. Fundamental principles of drying. *Exergex, Brossard, Canada,* 1**,** 1-22.

MUTHOMI, J. W., MUREITHI, B. K., CHEMINING'WA, G. N., GATHUMBI, J. K. & MUTIT, E. W. 2012. Aspergillus species and Aflatoxin b1 in soil, maize grain and flour samples from semi-arid and humid regions of Kenya. *International Journal of AgriScience,* 2**,** 22-34.

MUTHONI, J., NYAMONGO, D. & SILINGI, M. 2010. Participatory characterization and evaluation of some African leafy vegetables in Lari, Kiambu West District, Central Kenya. *Journal of Horticulture Forestry,* 2**,** 012-016.

MUTULI, G. P. & MBUGE, D. 2015. Drying characteristics and energy requirement of drying cowpea leaves and jute mallow vegetables. *Agricultural Engineering International: CIGR Journal,* 17**,** 265-272.

MUTULI, G. P. & MBUGE, D. 2018. Effect of Drying on the Nutritional and Organoleptic Characteristics of African Leafy Vegetables, Jute Mallow (*Corchorus olitorius L.*) and Cowpea (*Vigna unguiculata*). *Journal of Biosystems Engineering,* 43**,** 211–218.

NIAMNUY, C., DEVAHASTIN, S., SOPONRONNARIT, S. & RAGHAVAN, G. V. 2008a. Modeling coupled transport phenomena and mechanical deformation of shrimp during drying in a jet spouted bed dryer. *Chemical Engineering Science,* 63**,** 5503-5512.

NIAMNUY, C., DEVAHASTIN, S., SOPONRONNARIT, S. & VIJAYA RAGHAVAN, G. S. 2008b. Modeling coupled transport phenomena and mechanical deformation of shrimp during drying in a jet spouted bed dryer. *Chemical Engineering Science,* 63**,** 5503-5512.

NORTON, T. & SUN, D.-W. 2006. Computational fluid dynamics (CFD)–an effective and efficient design and analysis tool for the food industry: a review. *Trends in Food Science Technology,* 17**,** 600-620.

OCHOA, M. R., KESSELER, A. G., PIRONE, B. N., MÁRQUEZ, C. A. & DE MICHELIS, A. 2002. Shrinkage During Convective Drying of Whole Rose Hip (Rosa Rubiginosa L.) Fruits. *LWT - Food Science and Technology,* 35**,** 400-406.

ODHIAMBO, B. O., MURAGE, H. & WAGARA, I. N. 2013. Isolation and characterisation of aflatoxigenic Aspergillus species from maize and soil samples from selected counties of Kenya. *African Journal of Microbiology Research,* 7**,** 4379-4388.

ODHIAMBO, Z. & OLUOCH, M. 2008. African leafy vegetables come out of the shade. *New Agriculturalist-online*.

OGUNTONA, T. 1998. Green leafy vegetables. *Nutritional quality of plant foods,* 1998**,** 120-133.

OKENO, J. A. & CHEBET, D. K. 2003. PW Mathenge Status of indigenous vegetables in Kenya. *Acta Hort,* 621**,** 95-100.

ORECH, F. O., AKENGA, T., OCHORA, J., FRIIS, H. & AAGAARD-HANSEN, J. 2005. Potential toxicity of some traditional leafy vegetables consumed in Nyang'oma Division, Western Kenya. *African Journal of Food, Agriculture, Nutrition and Development,* 5.

PANYAWONG, S. & DEVAHASTIN, S. 2007a. Determination of deformation of a food product undergoing different drying methods and conditions via evolution of a shape factor. *Journal of Food Engineering,* 78**,** 151-161.

PANYAWONG, S. & DEVAHASTIN, S. J. J. O. F. E. 2007b. Determination of deformation of a food product undergoing different drying methods and conditions via evolution of a shape factor. 78**,** 151-161.

PARK, K. J., VOHNIKOVA, Z. & BROD, F. P. R. 2002. Evaluation of drying parameters and desorption isotherms of garden mint leaves (Mentha crispa L.). *Journal of Food Engineering,* 51**,** 193-199.

PATERSON, R. R. M. & LIMA, N. 2010. How will climate change affect mycotoxins in food? *Food Research International,* 43**,** 1902-1914.

PELEG, M. 1988. An empirical model for the description of moisture sorption curves. *Journal of Food science,* 53**,** 1216-1217.

PELEG, M. 1993. ASSESSMENT of A SEMI-EMPIRICAL FOUR PARAMETER GENERAL MODEL FOR SIGMOID MOISTURE SORPTION ISOTHERMS 1. *Journal of Food Process Engineering,* 16**,** 21-37.

PERERA, C. O. 2005. Selected quality attributes of dried foods. *Drying Technology,* 23**,** 717-730.

PEREZ, N. E. & SCHMALKO, M. E. 2009. Convective Drying of Pumpkin: Influence of Pretreatment and Drying Temperature. 32**,** 88-103.

PERRÉ, P. 2006. Multiscale aspects of heat and mass transfer during drying. *Drying of Porous Materials.* Springer.

PONSART, G., VASSEUR, J., FRIAS, J., DUQUENOY, A. & MÉOT, J.-M. 2003. Modelling of stress due to shrinkage during drying of spaghetti. *Journal of Food Engineering,* 57**,** 277-285.

PRACHAYAWARAKORN, S., TIA, W., PLYTO, N. & SOPONRONNARIT, S. 2008. Drying kinetics and quality attributes of low-fat banana slices dried at high temperature. *Journal of Food Engineering,* 85**,** 509-517.

RAGHAVAN, G. V., RENNIE, T. J., SUNJKA, P., ORSAT, V., PHAPHUANGWITTAYAKUL, W. & TERDTOON, P. 2005. Overview of new techniques for drying biological materials with emphasis on energy aspects. *Brazilian Journal of Chemical Engineering,* 22**,** 195-201.

RAHMAN, M. M., JOARDDER, M. U. & KARIM, A. 2018. Non-destructive investigation of cellular level moisture distribution and morphological changes during drying of a plant-based food material. *Biosystems Engineering,* 169**,** 126-138.

RAHMAN, M. S. & LABUZA, T. P. 2007. Water activity and food preservation. *Handbook of food preservation.* CRC Press.

RAKESH, V. & DATTA, A. K. 2011. Microwave puffing: Determination of optimal conditions using a coupled multiphase porous media–Large deformation model. *Journal of Food Engineering,* 107**,** 152-163.

RAMACHANDRAN, R. P., AKBARZADEH, M., PALIWAL, J. & CENKOWSKI, S. 2018. Computational fluid dynamics in drying process modelling—a technical review. *Food bioprocess technology,* 11**,** 271-292.

RAPUSAS, R. S. & DRISCOLL, R. H. 1995. The Thin-layer drying characterstics of white onion slices. *Drying Technology,* 13**,** 1905-1931.

REGALADO, C., GARCÍA-ALMENDÁREZ, B. E. & DUARTE-VÁZQUEZ, M. A. 2004. Biotechnological applications of peroxidases. *Phytochemistry Reviews,* 3**,** 243-256.

ROBERT, H. P., DON, W. G. & JAMES, O. M. 1984. Perry's chemical engineers' handbook. *Nova Iorque.*

RODRÍGUEZ, J., MULET, A. & BON, J. 2014. Influence of high-intensity ultrasound on drying kinetics in fixed beds of high porosity. *Journal of Food Engineering,* 127**,** 93-102.

ROMÁN, F. & HENSEL, O. 2010. Sorption isotherms of celery leaves (Apium graveolens var. secalinum). *Agricultural Engineering International: CIGR Journal,* 12**,** 137-141.

RUEL, M. T., MINOT, N. & SMITH, L. 2005. *Patterns and determinants of fruit and vegetable consumption in sub-Saharan Africa: a multicountry comparison*, WHO Geneva.

RUIZ-LÓPEZ, I. & GARCÍA-ALVARADO, M. 2007. Analytical solution for food-drying kinetics considering shrinkage and variable diffusivity. *Journal of Food Engineering,* 79**,** 208-216.

SABAREZ, H. T. 2012. Computational modelling of the transport phenomena occurring during convective drying of prunes. *Journal of food engineering,* v. 111**,** pp. 279-288-2012 v.111 no.2.

SAKAI, N., YANG, H. & WATANABE, M. 2002. Theoretical analysis of the shrinkage deformation in viscoelastic food during drying. *Japan Journal of Food Engineering*.

SAN MARTIN, M., MATE, J., FERNANDEZ, T. & VIRSEDA, P. 2001. Modelling adsorption equilibrium moisture characteristics of rough rice. *Drying technology,* 19**,** 681-690.

SANDOVAL, A. & BARREIRO, J. 2002. Water sorption isotherms of non-fermented cocoa beans (Theobroma cacao). *Journal of food engineering,* 51**,** 119-123.

SCHMIDT-HEYDT, M., RÜFER, C. E., ABDEL-HADI, A., MAGAN, N. & GEISEN, R. 2010. The production of aflatoxin B 1 or G 1 by Aspergillus parasiticus at various combinations of temperature and water activity is related to the ratio of aflS to aflR expression. *Mycotoxin Research,* 26**,** 241-246.

SCHUBERT, H. & REGIER, M. 2005. *The microwave processing of foods*, Woodhead Cambridge.

SENA, L. P., VANDERJAGT, D. J., RIVERA, C., TSIN, A. T. C., MUHAMADU, I., MAHAMADOU, O., MILLSON, M., PASTUSZYN, A. & GLEW, R. H. 1998. Analysis of nutritional components of eight famine foods of the Republic of Niger. *Plant Foods for Human Nutrition,* 52**,** 17-30.

SENADEERA, W., BHANDARI, B., YOUNG, G. & WIJESINGHE, B. 2000. Physical properties and fluidization behaviour of fresh green bean particulates during fluidized bed drying. *Food Bioproducts Processing,* 78**,** 43-47.

SHISHEHGARHA, F., MAKHLOUF, J. & RATTI, C. 2002. Freeze-drying characteristics of strawberries. *Drying technology,* 20**,** 131-145.

SHIUNDU, K. M. & ONIANG'O, R. K. 2007. Marketing African leafy vegetables: Challenges and opportunities in the Kenyan context. *African Journal of Food, Agriculture, Nutrition Development,* 7**,** 1-17.

SMITH, J. M., VAN NESS, H. C. & ABBOTT, M. M. 2001. Introduction to Chemical. *Engineering Thermodynamics***,** 474-478.

SONG, X.-J., ZHANG, M. & MUJUMDAR, A. S. 2007. Effect of vacuum-microwave predrying on quality of vacuum-fried potato chips. *Drying Technology,* 25**,** 2021-2026.

STENCL, J. 2004. Modelling the water sorption isotherms of yoghurt powder spray. *Mathematics and computers in simulation,* 65**,** 157-164.

STRUMILLO, C. 2009. A Review of:"Advanced Drying Technologies, 2nd ed., by T. Kudra and A.S. Mujumdar.". *Drying Technology,* 27**,** 1164-1165.

SUN, W., ZHU, S., RAMASWAMY, H., YU, Y. & LI, J. 2018. Thermal Conductivity of Selected Foods at High-Pressure Processing Conditions. *Transactions of the ASABE,* 61**,** 317-325.

SUVARNAKUTA, P., DEVAHASTIN, S., MUJUMDAR, A. S. & INTENSIFICATION, P. P. 2007. A mathematical model for low-pressure superheated steam drying of a biomaterial. *Chemical Engineering,* 46**,** 675-683.

SUVARNAKUTA, P., DEVAHASTIN, S., SOPONRONNARIT, S. & MUJUMDAR, A. 2005. Drying kinetics and inversion temperature in a low-pressure superheated steam-drying system. *Industrial Engineering Chemistry Research,* 44**,** 1934-1941.

TAECHAPAIROJ, C., PRACHAYAWARAKORN, S. & SOPONRONNARIT, S. 2006. Modelling of parboiled rice in superheated-steam fluidized bed. *Journal of Food Engineering,* 76**,** 411-419.

THOMKAPANICH, O., SUVARNAKUTA, P. & DEVAHASTIN, S. 2007. Study of intermittent low-pressure superheated steam and vacuum drying of a heat-sensitive material. *Drying Technology,* 25**,** 205-223.

THOMPSON, T., PEART, R. & FOSTER, G. 1968. Mathematical Simulation of Corn Drying A New Model. *Transaction of the ASAE,* 11**,** 582-586.

TIAN, Y., ZHAO, Y., HUANG, J., ZENG, H. & ZHENG, B. 2016. Effects of different drying methods on the product quality and volatile compounds of whole shiitake mushrooms. *Food Chemistry,* 197**,** 714-722.

TIMMERMANN, E., CHIRIFE, J. & IGLESIAS, H. 2001. Water sorption isotherms of foods and foodstuffs: BET or GAB parameters? *Journal of food engineering,* 48**,** 19-31.

TIMMERMANN, E. O. 1989. A BET-like three sorption stage isotherm. *Journal of the Chemical Society, Faraday Transactions 1: Physical Chemistry in Condensed Phases,* 85**,** 1631-1645.

TOPUZ, A., DINCER, C., ÖZDEMIR, K. S., FENG, H. & KUSHAD, M. 2011. Influence of different drying methods on carotenoids and capsaicinoids of paprika (Cv., Jalapeno). *Food Chemistry,* 129**,** 860-865.

TROLLER, J. A. 1977. Statistical analysis of Aw measurements obtained with the sina scope. *Journal of Food Science,* 42**,** 86-90.

TSAMI, E., MARINOS-KOURIS, D. & MAROULIS, Z. 1990a. Water sorption isotherms of raisins, currants, figs, prunes and apricots. *Journal of food science,* 55**,** 1594-1597.

TSAMI, E., MAROULIS, Z., MARINOS-KOURIS, D. & SARAVACOS, G. 1990b. Heat of sorption of water in dried fruits. *International Journal of Food Science Technology,* 25**,** 350-359.

TZEMPELIKOS, D. A., VOUROS, A. P., BARDAKAS, A. V., FILIOS, A. E. & MARGARIS, D. P. 2014. Case studies on the effect of the air drying conditions on the convective drying of quinces. *Case Studies in Thermal Engineering,* 3**,** 79-85.

TZEMPELIKOS, D. A., VOUROS, A. P., BARDAKAS, A. V., FILIOS, A. E. & MARGARIS, D. P. 2015. Experimental study on convective drying of quince slices and evaluation of thin-layer drying models. *Engineering in Agriculture, Environment and Food,* 8**,** 169-177.

U.H.JOARDDER, M., KUMAR, C., KARIM, A. & BROWN, R. 2015. Effect of cell wall properties on porosity and shrinkage of dried apple. *International Journal of Food Properties*.

VALDRAMIDIS, V., TAOUKIS, P., STOFOROS, N. & VAN IMPE, J. 2012. Modeling the Kinetics of Microbial and Quality Attributes of Fluid Food During Novel Thermal and Non-Thermal Processes.

VAN DEN BERG, C. 1984. Description of water activity of foods for engineering purposes by means of the GAB model of sorption. *Engineering science in the food industry***,** 311-321.

VAN DEN BERG, C. & BRUIN, S. Water activity and its estimation in food systems. Proceedings Int. Symp. Properties of Water in Relation to Food Quality and Stability, Osaka, 1978, 1978.

VAN LIEDEKERKE, P., GHYSELS, P., TIJSKENS, E., SAMAEY, G., SMEEDTS, B., ROOSE, D. & RAMON, H. 2010. A particle-based model to simulate the micromechanics of single-plant parenchyma cells and aggregates. *Physical biology,* 7**,** 026006.

VASIĆ, M., RADOJEVIĆ, Z. & GRBAVČIĆ, Ž. 2012. Calculation of the effective diffusion coefficient during the drying of clay samples. *Journal of the Serbian Chemical Society,* 77**,** 523-533.

VERAVERBEKE, E. A., VERBOVEN, P., VAN OOSTVELDT, P. & NICOLAı, B. M. 2003. Prediction of moisture loss across the cuticle of apple (Malus sylvestris subsp. Mitis (Wallr.)) during storage: part 1. Model development and determination of diffusion coefficients. *Postharvest Biology Technology,* 30**,** 75-88.

VERBOVEN, P., NICOLAÏ, B. M., SCHEERLINCK, N. & DE BAERDEMAEKER, J. 1997. The local surface heat transfer coefficient in thermal food process calculations: a CFD approach. *Journal of Food Engineering,* 33**,** 15-35.

VERBOVEN, P., SCHEERLINCK, N., DE BAERDEMAEKER, J. & NICOLAï, B. M. 2001. Sensitivity of the food centre temperature with respect to the air velocity and the turbulence kinetic energy. *Journal of Food Engineering,* 48**,** 53-60.

VERSTEEG, H. K., & MALALASEKERA, W. . 2007. *An introduction to computational fluid dynamics: the finite volume method*, Harlow, England, Pearson Education Ltd.

VILLA-CORRALES, L., FLORES-PRIETO, J., XAMÁN-VILLASEÑOR, J. & GARCÍA-HERNÁNDEZ, E. 2010. Numerical and experimental analysis of heat and moisture transfer during drying of Ataulfo mango. *Journal of food engineering*

98**,** 198-206.

VIOLLAZ, P. E. & ROVEDO, C. O. 1999. Equilibrium sorption isotherms and thermodynamic properties of starch and gluten. *Journal of Food Engineering,* 40**,** 287-292.

VIOLLAZ, P. E. & ROVEDO, C. O. 2002. A drying model for three-dimensional shrinking bodies. *Journal of Food Engineering,* 52**,** 149-153.

WANG, J., FANG, X.-M., MUJUMDAR, A., QIAN, J.-Y., ZHANG, Q., YANG, X.-H., LIU, Y.-H., GAO, Z.-J. & XIAO, H.-W. 2017a. Effect of high-humidity hot air impingement blanching (HHAIB) on drying and quality of red pepper (Capsicum annuum L.). *Food chemistry,* 220**,** 145-152.

WANG, J. & XI, Y. 2005. Drying characteristics and drying quality of carrot using a two-stage microwave process. *Journal of food Engineering,* 68**,** 505-511.

WANG, J., YANG, X.-H., MUJUMDAR, A., WANG, D., ZHAO, J.-H., FANG, X.-M., ZHANG, Q., XIE, L., GAO, Z.-J. & XIAO, H.-W. 2017b. Effects of various blanching methods on weight loss, enzymes inactivation, phytochemical contents, antioxidant capacity, ultrastructure and drying kinetics of red bell pepper (Capsicum annuum L.). *LWT,* 77**,** 337-347.

WANG, W., CHEN, G. & MUJUMDAR, A. S. 2007. Physical Interpretation of Solids Drying: An Overview on Mathematical Modeling Research. *Drying Technology,* 25**,** 659-668.

WANG, W., THORAT, B., CHEN, G. & MAJUMDAR, A. Fluidized bed drying of heat sensitive porous material with microwave heating. Proc 13th Int Drying Symp, Beijing, China, 2002. 30.

WELTY, J. R., WICKS, C. E., WILSON, R. E. & RORRER, G. 2001. Fundamentals of Mass Transfer, Fundamentals of Momentum. *Heat, and Mass Transfer,* 4**,** 438-442.

WILHELM, R, L., A. SUTER, D. & GERALD H. BRUSEWITZ, A. 2004a. *Energy Use in Food Processing,* St. Joseph, MI, ASAE.

WILHELM, R, L., A. SUTER, D. & GERALD H. BRUSEWITZ, A. 2004b. *Physical Properties of Food Materials,* St. Joseph, MI, ASAE.

WORLD HEALTH, O. 2005. Fruit and vegetables for health: report of the Joint FAO.

XIA, B. & SUN, D.-W. 2002. Applications of computational fluid dynamics (CFD) in the food industry: a review. *Computers electronics in agriculture,* 34**,** 5-24.

XIAO, H.-W., BAI, J.-W., XIE, L., SUN, D.-W. & GAO, Z.-J. 2015. Thin-layer air impingement drying enhances drying rate of American ginseng (Panax quinquefolium L.) slices with quality attributes considered. *Food Bioproducts Processing,* 94**,** 581-591.

XIONG, D., WANG, D., LIU, X., PENG, S., HUANG, J. & LI, Y. 2016. Leaf density explains variation in leaf mass per area in rice between cultivars and nitrogen treatments. *Annals of Botany,* 117**,** 963-971.

YALDIZ, O., ERTEKIN, C. & UZUN, H. I. 2001. Mathematical modeling of thin layer solar drying of sultana grapes. *Energy,* 26**,** 457-465.

YANG, D., WANG, Z., HUANG, X., XIAO, Z. & LIU, X. 2011a. Numerical simulation on superheated steam fluidized bed drying: I. Model construction. *Drying Technology,* 29**,** 1325-1331.

YANG, D., WANG, Z., HUANG, X., XIAO, Z. & LIU, X. 2011b. Numerical simulation on superheated steam fluidized bed drying: I. Model construction. *Drying Technology,* 29**,** 1325-1331.

YANG, H., SAKAI, N. & WATANABE, M. 2001. DRYING MODEL WITH NON-ISOTROPIC SHRINKAGE DEFORMATION UNDERGOING SIMULTANEOUS HEAT AND MASS TRANSFER. *Drying Technology,* 19**,** 1441-1460.

YAO, L., FAN, L. & DUAN, Z. 2020. Effect of different pretreatments followed by hot-air and far-infrared drying on the bioactive compounds, physicochemical property and microstructure of mango slices. *Food Chemistry,* 305**,** 125477.

ZHAO, F. & CHEN, Z. 2011. Numerical study on moisture transfer in ultrasound-assisted convective drying process of sludge. *Drying Technology,* 29**,** 1404-1415.

Appendix 1.

Table 1. Temperature-Dependent Model Parameters

Model And Parameters		Cowpea Leaves	Amaranthus	Jute Mallow	Nightshade	Slender Leaf
		30-50ºc	30-50ºc	30-50ºc	30-50ºc	30-50ºc
Modified Halsey	A	3.13	5.35	5.51	4.10	3.06
	B	-0.005	-0.001	-0.004	-0.002	-0.002
	C	1.80	1.22	1.97	1.20	1.01
	R^2	0.90	0.91	0.91	0.90	0.90
	MSE	0.53	0.46	0.46	0.50	0.56
	Residual Plot	Pattern	Pattern	Pattern	Pattern	Pattern
Modified Oswin	A	8.22	14.06	14.48	9.10	8.89
	B	-0.03	-0.01	-0.02	-0.01	-0.01
	C	1.36	0.92	1.48	0.77	0.85
	R^2	0.87	0.88	0.87	0.85	0.86
	MSE	0.71	0.70	0.84	0.80	0.76
	Residual Plot	Pattern	Pattern	Pattern	Pattern	Pattern

Table 2. Temperature Independent Model Parameters

Model And Parameters		Cowpea Leaves			Amaranthus			Jute Mallow			Nightshade			Slender Leaf		
		30ºc	40ºc	50ºc	30ºc	40ºc	50ºc	30ºc	40ºc	50ºc	30ºc	40ºc	50ºc	30ºc	40ºc	50ºc
GAB	A	.55	.52	.51	.58	.51	.46	.51	.51	.48	.42	.41	.44	.55	.48	.48
	B	.200	.150	.120	.125	.210	.130	.150	.210	.216	.210	.140	.108	.210	.210	.245
	C	2.48	3.39	3.50	5.97	2.35	4.54	5.94	2.46	1.73	5.11	5.88	6.39	4.34	4.56	2.64
	R^2	.997	.989	.997	.998	.988	.992	.999	.999	.997	.998	.998	.999	.999	1.00	1.00

BET					Peleg								
Residual Plot	MSE	R²	B	A	Residual Plot	MSE	R²	D	C	B	A	Residual Plot	MSE
Pattern	.026	.987	31.40	.06	uniform	.197	.998	.271	10.66	15.96	.004	Pattern	.018
Pattern	.035	.978	44.70	.05	uniform	.194	.998	.142	5.64	13.77	.004	Pattern	.020
Pattern	.037	.973	35.61	.04	uniform	.231	.999	1.084	8.00	19.36	.002	Pattern	.289
Pattern	.034	.976	41.45	.06	uniform	.197	.998	.356	12.51	12.15	.009	Pattern	.339
Pattern	.039	.984	43.55	.05	uniform	.214	.998	.360	23.66	12.14	.004	Pattern	.214
Pattern	.041	.983	45.66	.05	uniform	.216	.996	.419	62.48	12.30	.001	Pattern	.216
Pattern	.044	.982	46.53	.07	uniform	.162	.995	.596	57.53	14.96	.002	Pattern	.179
Pattern	.032	.981	47.59	.07	uniform	.222	.994	.505	9.36	14.17	.001	Pattern	.145
Pattern	.055	.981	48.66	.06	uniform	.182	.993	.505	7.01	12.42	.001	Pattern	.214
Pattern	.051	.985	48.97	.06	uniform	.172	.991	.451	17.28	15.51	.005	Pattern	.076
Pattern	.054	.986	51.78	.05	uniform	.172	.990	.005	7.25	11.86	.002	Pattern	.179
Pattern	.056	.982	45.47	.04	uniform	.182	.989	1.016	8.20	18.62	.003	Pattern	.138
Pattern	.066	.965	48.97	.05	uniform	.167	.988	.380	28.83	11.55	.005	Pattern	.131
Pattern	.075	.961	45.51	.05	uniform	.178	.987	.327	8.30	12.72	.001	Pattern	.124
Pattern	.083	.958	46.24	.04	uniform	.184	.985	.852	8.20	13.53	.001	Pattern	.117

Appendix 2: RESULTS:

- Vitamin and aflatoxin results are available on this link: https://drive.google.com/open?id=1RnPfqm_oPCCJBeDoKEuMH4DQy01T_-9-

Appendix 2.1: Activation energy:

Vegetable	Temperature	Calculated Deff	slope	R2 value	Intercept	Ln Deff	absolute temperature	slope	intercept	Activation Energy
Amaranthus	50	1.021E-06	-0.0252	0.8993	0.2659	-13.795	0.0031	-0.0007	-0.006	5.69394E-06
	40	8.266E-07	-0.0204	0.8241	0.4589	-14.006	0.0032			
	30	8.711E-07	-0.0215	0.9028	0.2528	-13.953	0.0033			
Night shade	50	8.671E-07	-0.0214	0.9667	0.2339	-13.958	0.0031	-0.0002	-0.0002	1.62684E-06
	40	5.024E-07	-0.0124	0.9006	2512	-14.504	0.0032			
	30	3.687E-07	-0.0091	0.969	0.1446	-14.813	0.0033			
Slender leaf	50	3.363E-07	-0.0083	0.9741	0.0716	-14.905	0.0031	-0.0006	-0.086	4.88052E-06
	40	2.634E-07	-0.0065	0.9695	0.0802	-15.150	0.0032			
	30	2.553E-07	-0.0063	0.9709	0.066	-15.181	0.0033			
JuteMallow	50	4.579E-07	-0.0113	0.9635	0.0862	-14.597	0.0031	-0.0011	-0.129	8.94762E-06
	40	4.376E-07	-0.0108	0.9045	0.1815	-14.642	0.0032			
	30	3.849E-07	-0.0095	0.9203	0.2127	-14.770	0.0033			
Cowpea leaves	50	3.930E-07	-0.0097	0.9499	0.068	-14.749	0.0031	-0.0007	-0.0071	5.69394E-06
	40	3.201E-07	-0.0079	0.9721	0.0669	-14.955	0.0032			
	30	2.998E-07	-0.0074	0.9521	0.1322	-15.020	0.0033			

Cowpea Leaves 30 deg		
Time/Min	Moisture Ratio	Loge 30 deg Cowpea Leaves
0	1.000	0.000
25	0.902	-0.103
50	0.802	-0.221
75	0.709	-0.344
101	0.608	-0.498
125	0.510	-0.673
150	0.412	-0.887
175	0.311	-1.168
200	0.213	-1.546
250	0.023	-3.772
300	0.001	-6.908
Cowpea Leaves 40 deg		
Time/Min	Moisture Ratio	Loge 40 deg Cowpea Leaves
0	1.000	0.000
20	0.901	-0.104
40	0.812	-0.208
65	0.687	-0.375
95	0.531	-0.633
130	0.352	-1.044
180	0.101	-2.293
200	0.010	-4.605
Cowpea Leaves 50 deg		
Time/Min	Moisture Ratio	Loge 50 deg Cowpea Leaves
0	1.000	0.000
15	0.919	-0.084
32	0.834	-0.182
66	0.547	-0.603
90	0.528	-0.639
120	0.294	-1.224
150	0.219	-1.519
195	0.077	-2.564
231	0.001	-6.908

jute mallow 30 deg		
Time/Min	Moisture Ratio	Loge 30 deg jutemallow
0	1.000	0.000
25	0.891	-0.115
50	0.785	-0.242
75	0.694	-0.365
101	0.562	-0.576
125	0.453	-0.792
150	0.346	-1.061
175	0.237	-1.440
200	0.128	-2.056
220	0.001	-6.908
jute mallow 40 deg		
Time/Min	Moisture Ratio	Loge 40 deg jutemallow
0	1.000	0.000
20	0.901	-0.104
40	0.812	-0.208
65	0.687	-0.375
95	0.531	-0.633
130	0.352	-1.044
160	0.151	-1.890
200	0.010	-4.605
jute mallow 50 deg		
Time/Min	Moisture Ratio	Loge 50 deg jutemallow
0	1.000	0.000
14	0.907	-0.098
31	0.804	-0.218
66	0.587	-0.533
93	0.415	-0.879
120	0.244	-1.411
146	0.077	-2.564
160	0.001	-6.908

slenderleaf 30		
Time/min	Moisture ratio	Loge 40 deg slenderleaf
0	1.000	0.000
25	0.901	-0.104
50	0.799	-0.224
75	0.710	-0.342
101	0.604	-0.504
125	0.512	-0.669
150	0.411	-0.889
175	0.309	-1.174
200	0.209	-1.565
250	0.022	-3.817
300	0.001	-6.908
slenderleaf 40		
Time/min	Moisture ratio	Loge 30 deg slenderleaf
0	1.000	0.000
19	0.903	-0.102
43	0.835	-0.180
70	0.741	-0.300
97	0.619	-0.480
145	0.461	-0.774
190	0.291	-1.234
304	0.001	-6.908
slenderleaf 50		
Time/min	Moisture ratio	Loge 50 deg slenderleaf
0	1.000	0.000
16	0.921	-0.082
34	0.831	-0.185
66	0.671	-0.399
91	0.553	-0.592
120	0.402	-0.911
140	0.304	-1.191
195	0.038	-3.270
231	0.001	-6.908

| Night shade 30 deg | | |
Time/min	Moisture ratio	Loge 40 deg Nightshade
0	1.000	0.000
25	0.871	-0.138
50	0.739	-0.302
75	0.608	-0.498
101	0.450	-0.799
125	0.351	-1.047
150	0.225	-1.492
175	0.092	-2.386
200	0.010	-4.605

| Night shade 40 deg | | |
Time/min	Moisture ratio	Loge 30 deg Nightshade
0	1.000	0.000
24	0.856	-0.155
52	0.729	-0.316
82	0.608	-0.498
121	0.454	-0.790
174	0.271	-1.306
256	0.091	-2.397

| Night shade 50 deg | | |
Time/min	Moisture ratio	Loge 50 deg Nightshade
0	1.000	0.000
15	0.872	-0.137
30	0.743	-0.297
60	0.472	-0.751
95	0.202	-1.599
110	0.098	-2.323
138	0.058	-2.847
172	0.001	-6.908

| Amaranthus 30 deg | | |
Time/min	Moisture ratio	Loge 30 deg Amaranthus
0	1.000	0.000
25	0.870	-0.139
50	0.739	-0.302
75	0.605	-0.503
101	0.447	-0.805
125	0.347	-1.058
150	0.221	-1.510
175	0.091	-2.397
200	0.001	-6.908

| Amaranthus 40 deg | | |
Time/min	Moisture ratio	Loge 40 deg Amaranthus
0	1.000	0.000
20	0.871	-0.138
41	0.755	-0.281
71	0.571	-0.560
101	0.382	-0.962
141	0.142	-1.952
164	0.021	-3.863
190	0.001	-6.908

| Amaranthus 50 deg | | |
Time/min	Moisture ratio	Loge 50 deg Amaranthus
0	1.000	0.000
14	0.869	-0.140
32	0.711	-0.341
66	0.401	-0.914
91	0.150	-1.897
100	0.064	-2.749
120	0.001	-6.908

Appendix 2.2: Drying curves:

Cowpea Leaves 30 deg				
Time/Min	Moisture Ratio R1	Moisture Ratio R2	Moisture Ratio R3	Mean Moisture Ratio
0	1.000	1.000	1.000	1.000
25	0.908	0.895	0.904	0.902
50	0.808	0.796	0.804	0.802
75	0.714	0.703	0.710	0.709
101	0.612	0.603	0.609	0.608
125	0.514	0.506	0.511	0.510
150	0.415	0.409	0.413	0.412
175	0.313	0.309	0.312	0.311
200	0.214	0.211	0.213	0.213
250	0.023	0.023	0.023	0.023
300	0.001	0.001	0.001	0.001
Cowpea Leaves 40 deg				
Time/Min	Moisture Ratio R1	Moisture Ratio R2	Moisture Ratio R3	Mean Moisture Ratio
0	1.000	1.000	1.000	1.000
20	0.907	0.894	0.903	0.901
40	0.818	0.805	0.814	0.812
65	0.692	0.681	0.688	0.687
95	0.535	0.527	0.532	0.531
130	0.354	0.349	0.353	0.352
180	0.102	0.100	0.101	0.101
200	0.010	0.010	0.010	0.010
Cowpea Leaves 50 deg				
Time/Min	Moisture Ratio R1	Moisture Ratio R2	Moisture Ratio R3	Mean Moisture Ratio
0	1.000	1.000	1.000	1.000
15	0.925	0.912	0.921	0.919
32	0.840	0.827	0.836	0.834
66	0.551	0.543	0.548	0.547
90	0.532	0.524	0.529	0.528
120	0.296	0.292	0.295	0.294
150	0.221	0.217	0.219	0.219
195	0.078	0.076	0.077	0.077
231	0.001	0.001	0.001	0.001

jute mallow 30 deg				
Time/Min	Moisture Ratio R1	Moisture Ratio R2	Moisture Ratio R3	Mean Moisture Ratio
0	1.000	1.000	1.000	1.000
25	0.897	0.884	0.893	0.891
50	0.790	0.779	0.787	0.785
75	0.699	0.688	0.695	0.694
101	0.566	0.557	0.563	0.562
125	0.456	0.449	0.454	0.453
150	0.348	0.343	0.347	0.346
175	0.239	0.235	0.237	0.237
200	0.129	0.127	0.128	0.128
220	0.001	0.001	0.001	0.001
jute mallow 40 deg				
Time/Min	Moisture Ratio R1	Moisture Ratio R2	Moisture Ratio R3	Mean Moisture Ratio
0	1.000	1.000	1.000	1.000
20	0.907	0.894	0.903	0.901
40	0.818	0.805	0.814	0.812
65	0.692	0.681	0.688	0.687
95	0.535	0.527	0.532	0.531
130	0.354	0.349	0.353	0.352
180	0.102	0.100	0.101	0.101
200	0.010	0.010	0.010	0.010
jute mallow 50 deg				
Time/Min	Moisture Ratio R1	Moisture Ratio R2	Moisture Ratio R3	Mean Moisture Ratio
0	1.000	1.000	1.000	1.000
14	0.913	0.900	0.909	0.907
31	0.810	0.798	0.806	0.804
66	0.591	0.582	0.588	0.587
93	0.418	0.412	0.416	0.415
120	0.246	0.242	0.244	0.244
146	0.078	0.076	0.077	0.077
160	0.001	0.001	0.001	0.001

Slender leaf 30				
Time/min	Moisture Ratio R1	Moisture Ratio R2	Moisture Ratio R3	Mean Moisture Ratio
0	1.000	1.000	1.000	1.000
25	0.907	0.894	0.903	0.901
50	0.805	0.793	0.801	0.799
75	0.715	0.704	0.711	0.710
101	0.608	0.599	0.605	0.604
125	0.516	0.508	0.513	0.512
150	0.414	0.408	0.412	0.411
175	0.311	0.307	0.310	0.309
200	0.210	0.207	0.209	0.209
250	0.022	0.022	0.022	0.022
300	0.001	0.001	0.001	0.001
Slender leaf 40				
Time/min	Moisture Ratio R1	Moisture Ratio R2	Moisture Ratio R3	Mean Moisture Ratio
0	1.000	1.000	1.000	1.000
19	0.909	0.896	0.905	0.903
43	0.841	0.828	0.837	0.835
70	0.746	0.735	0.742	0.741
97	0.623	0.614	0.620	0.619
145	0.464	0.457	0.462	0.461
190	0.293	0.289	0.292	0.291
304	0.001	0.001	0.001	0.001
Slender leaf 50				
Time/min	Moisture Ratio R1	Moisture Ratio R2	Moisture Ratio R3	Mean Moisture Ratio
0	1.000	1.000	1.000	1.000
16	0.927	0.914	0.923	0.921
34	0.837	0.824	0.833	0.831
66	0.676	0.666	0.672	0.671
91	0.557	0.549	0.554	0.553
120	0.405	0.399	0.403	0.402
140	0.306	0.302	0.305	0.304
195	0.038	0.038	0.038	0.038
231	0.001	0.001	0.001	0.001

Night shade 30				
Time/min	Moisture Ratio R1	Moisture Ratio R2	Moisture Ratio R3	Mean Moisture Ratio
0	1.000	1.000	1.000	1.000
25	0.877	0.864	0.873	0.871
50	0.744	0.733	0.740	0.739
75	0.612	0.603	0.609	0.608
101	0.453	0.446	0.451	0.450
125	0.353	0.348	0.352	0.351
150	0.227	0.223	0.225	0.225
175	0.093	0.091	0.092	0.092
200	0.010	0.010	0.010	0.010
Night shade 40				
Time/min	Moisture Ratio R1	Moisture Ratio R2	Moisture Ratio R3	Mean Moisture Ratio
0	1.000	1.000	1.000	1.000
24	0.862	0.849	0.858	0.856
52	0.734	0.723	0.730	0.729
82	0.612	0.603	0.609	0.608
121	0.457	0.450	0.455	0.454
174	0.273	0.269	0.272	0.271
256	0.001	0.001	0.001	0.001
Night shade 50				
Time/min	Moisture Ratio R1	Moisture Ratio R2	Moisture Ratio R3	Mean Moisture Ratio
0	1.000	1.000	1.000	1.000
15	0.878	0.865	0.874	0.872
30	0.748	0.737	0.744	0.743
60	0.475	0.468	0.473	0.472
95	0.203	0.200	0.202	0.202
110	0.099	0.097	0.098	0.098
138	0.058	0.058	0.058	0.058
172	0.001	0.001	0.001	0.001

Night shade 30

Time/min	Moisture Ratio R1	Moisture Ratio R2	Moisture Ratio R3	Mean Moisture Ratio
0	1.000	1.000	1.000	1.000
25	0.876	0.863	0.872	0.870
50	0.744	0.733	0.740	0.739
75	0.609	0.600	0.606	0.605
101	0.450	0.443	0.448	0.447
125	0.349	0.344	0.348	0.347
150	0.223	0.219	0.221	0.221
175	0.092	0.090	0.091	0.091
200	0.001	0.001	0.001	0.001

Night shade 40

Time/min	Moisture Ratio R1	Moisture Ratio R2	Moisture Ratio R3	Mean Moisture Ratio
0	1.000	1.000	1.000	1.000
20	0.877	0.864	0.873	0.871
41	0.760	0.749	0.757	0.755
71	0.575	0.566	0.572	0.571
101	0.385	0.379	0.383	0.382
141	0.143	0.141	0.142	0.142
164	0.021	0.021	0.021	0.021
190	0.001	0.001	0.001	0.001

Night shade 50

Time/min	Moisture Ratio R1	Moisture Ratio R2	Moisture Ratio R3	Mean Moisture Ratio
0	1.000	1.000	1.000	1.000
14	0.875	0.862	0.871	0.871
32	0.000	0.000	0.000	0.000
66	0.404	0.398	0.402	0.571
91	0.151	0.149	0.150	0.382
100	0.064	0.063	0.064	0.142
120	0.001	0.001	0.001	0.021

Appendix 2.3: Effective moisture diffusivity:

Vegetable	Temperature	Calculated Deff	slope	R2 value	Intercept	Dynamic viscosity	volume	Mass	Density
Amaranthus	50	8.104E-09	-0.0002	0.8993	0.2659	1.524E-02	5.31638E-07	0.0707	132.9853268
	40	8.104E-09	-0.0002	0.8241	0.4589	1.524E-02	5.31638E-07	0.0707	132.9853268
	30	8.104E-09	-0.0002	0.9028	0.2528	1.524E-02	5.31638E-07	0.0707	132.9853268
Night shade	50	1.621E-08	-0.0004	0.9667	0.2339	2.817E-02	5.75415E-07	0.0695	120.7823918
	40	8.104E-09	-0.0002	0.9006	0.2512	1.408E-02	5.75415E-07	0.0695	120.7823918
	30	4.052E-09	-0.0001	0.969	0.0443	7.042E-03	5.75415E-07	0.0695	120.7823918
Slender leaf	50	8.104E-09	-0.0002	0.9741	0.3687	1.494E-02	5.42241E-07	0.0491	90.55012613
	40	8.104E-09	-0.0002	0.9695	0.4886	1.494E-02	5.42241E-07	0.0491	90.55012613
	30	4.052E-09	-0.0001	0.9709	0.066	7.472E-03	5.42241E-07	0.0491	90.55012613
JuteMallow	50	1.216E-08	-0.0003	0.9635	0.2328	2.568E-02	4.73355E-07	0.0461	97.38990821
	40	8.104E-09	-0.0002	0.9045	0.1815	1.712E-02	4.73355E-07	0.0461	97.38990821
	30	8.104E-09	-0.0002	0.9203	0.2127	1.712E-02	4.73355E-07	0.0461	97.38990821
Cowpea leaves	50	8.104E-09	-0.0002	0.9499	0.1903	1.544E-02	5.24755E-07	0.0743	141.5898848
	40	8.104E-09	-0.0002	0.9721	0.2359	1.544E-02	5.24755E-07	0.0743	141.5898848
	30	8.104E-09	-0.0002	0.9521	0.4812	1.544E-02	5.24755E-07	0.0743	141.5898848

eaf measurements					
Cowpea leaves	Jute mallow	Slender leaf	Nightshade	Amaranthus	
0.2034	0.2014	0.1942	0.2022	0.2026	
0.203	0.201	0.2008	0.202	0.2026	
0.2026	0.2006	0.1966	0.202	0.2022	
0.2022	0.2002	0.1982	0.2026	0.202	
0.2038	0.2018	0.1988	0.2028	0.202	
0.2034	0.2014	0.1994	0.2022	0.2014	
0.203	0.201	0.199	0.2018	0.202	
0.2026	0.2006	0.1986	0.202	0.2006	
0.2022	0.2002	0.1982	0.2008	0.202	
0.2038	0.2018	0.1988	0.2006	0.2002	
0.203	**0.201**	**0.19826**	**0.2019**	**0.20176**	0.201184
					0.100592
	Anova: Single Factor				
	SUMMARY				
	Groups	*Count*	*Sum*	*Average*	*Variance*
	Cowpea leaves	10	2.03	0.203	3.56E-07
	Jute mallow	10	2.01	0.201	3.56E-07
	Slender leaf	10	1.9826	0.19826	3.14E-06
	Nightshade	10	2.019	0.2019	4.91E-07
	Amaranthus	10	2.0176	0.20176	6.38E-07

Appendix 2.3: Energy requirement:

Amaranthus		RUN 1			RUN 2		
Drying Time/Minutes		Leaf Weight/g	Leaf dimensions	Leaf area	initial Leaf Weight/g	Leaf dimensions	Leaf area
	S1	0.073	1.90E-02	0.000247	0.072	1.40E-02	0.00028
	S2	0.076	1.30E-02		0.073	2.00E-02	
150 minutes	S3	0.063			0.075		
	S4	0.063			0.076		
	S5	0.064			0.072		
		0.068			**0.074**		
	average weight	0.0000707					
	Average area	0.000527					
	specific heat capacity	1.297					
	Density	1.006					
	Temperature (K)	303					
	Drying time	9000					
	air velocity	0.4					
	Energy (kJ/kg)	0.331431004					
	Energy (kJ/mol)	9.599799601					

Cowpea leaves		Leaf Weight/g	Leaf dimensions	Leaf area	Leaf Weight/g	Leaf dimensions	Leaf area
Time/Minutes		Leaf Weight/g	Leaf dimensions	Leaf area	Leaf Weight/g	Leaf dimensions	Leaf area
	S1	0.074	0.019	0.000247	0.052	0.015	0.00027
	S2	0.084	0.013		0.094	0.018	
120	S3	0.053			0.104		
	S4	0.063			0.083		
	S5	0.053			0.083		
		0.065			**0.083**		
	average weight	0.0000743					
	Average area	0.000517					
	specific heat cap	1.297					
	Density	1.006					
	Temperature (K)	303					
	Drying time	9000					
	air velocity	0.4					
	Energy (kJ/kg)	0.341698018					
	Energy (kJ/mol)	9.897180595					

Nightshade		RUN 1			RUN 2		
Time/Minutes		Leaf Weight/g	Leaf dimensions	Leaf area	Leaf Weight/g	Leaf dimensions	Leaf area
	S1	0.072	0.019	0.000247	0.095	0.019	0.000323
	S2	0.072	0.013		0.065	0.017	
180	S3	0.062			0.080		
	S4	0.072			0.088		
	S5	0.031			0.058		
		0.062			**0.077**		
	average weight	0.0000695					
	Average area	0.00057					
	specific heat capaci	1.297					
	Density	1.006					
	Temperature (K)	303					
	Drying time	9000					
	air velocity	0.4					
	Energy (kJ/kg)	0.352389341					
	Energy (kJ/mol)	10.20685155					

Slender leaf		RUN 1			RUN 2		
Time/Minutes		Leaf Weight/g	Leaf dimensions	Leaf area	Leaf Weight/g	Leaf dimensions	Leaf area
	S1	0.041	0.019	0.000247	0.039	0.020	0.0003
	S2	0.052	0.013		0.058	0.015	
90	S3	0.053			0.049		
	S4	0.051			0.039		
	S5	0.051			0.058		
		0.050			**0.049**		
	average weight	0.0000491					
	Average area	0.000547					
	specific heat capa	1.297					
	Density	1.006					
	Temperature (K)	303					
	Drying time	9000					
	air velocity	0.4					
	Energy (kJ/kg)	0.238908676					
	Energy (kJ/mol)	6.919918134					

Jutemallow			RUN 1			RUN 2	
Time/Minutes		Leaf Weight/g	Leaf dimensions	Leaf area	Leaf Weight/g	Leaf dimensions	Leaf area
	S1	0.037	1.90E-02	0.000247	0.053	0.014	0.000224
	S2	0.049	1.30E-02		0.051	0.016	
90	S3	0.041			0.052		
	S4	0.038			0.054		
	S5	0.037			0.049		
		0.040			**0.052**		
	average weight	**0.0000461**					
	Average area	**0.000471**					
	specific heat capac	**1.297**					
	Density	**1.006**					
	Temperature (K)	**303**					
	Drying time	**9000**					
	air velocity	**0.4**					
	Energy (kJ/kg)	0.193145652					
	Energy (kJ/mol)	5.594405866					

Appendix 2.4: Isosteric heat of sorption:

moisture content	cowpea energy	Amaranthus energy	Nightshade energy	Jutemallow energy	Slender leaf energy
10	149.934843	41.17184234	92.98394433	53.33898847	63.74935458
20	160.2616115	79.28499422	122.1509183	76.40333407	86.60347668
30	166.2978535	101.5797497	139.2146738	87.68286986	103.6229746
40	170.5883799	117.3981461	151.3240392	99.46767967	115.6979174
50	173.9076984	129.662413	160.7041873	106.8931179	125.0645423
60	176.624622	139.694131	168.375501	112.9600944	132.7112685
70	178.9235573	148.1645398	174.8666126	118.0890561	139.1900863
80	180.9028546	155.5162155	180.4848664	122.5320253	144.7960463
90	182.660864	161.9827395	185.4392565	126.4537385	149.7381427

Appendix 2.5: Mathematical modelling of drying curves:

30 degrees Cowpea leaves		n=1.443, k=6.772exp-4	k=4.585exp-3	0.9079, k=3.2967*10^	n=1.4431, k=6.3636*10^-3
Time/Min	Moisture Ratio	page model	lewis	Henderson & Pabis	Modified page
0	1.000	1.000	1.000	0.908	1.000
25	0.902	0.932	0.892	0.836	0.932
50	0.802	0.826	0.795	0.770	0.826
75	0.709	0.709	0.709	0.709	0.709
101	0.608	0.590	0.629	0.651	0.590
125	0.510	0.487	0.564	0.601	0.487
150	0.412	0.393	0.503	0.554	0.393
175	0.311	0.311	0.448	0.510	0.311
200	0.213	0.243	0.400	0.470	0.243
250	0.023	0.142	0.318	0.398	0.142
300	0.001	0.079	0.253	0.338	0.079
	SDE	0.041	0.052	0.038	0.041
	R2	0.987	0.979	0.989	0.987

40 degrees Cowpea leaves		n=1.3676, k=1.3419exp-	k=5.2064exp-3	1.3155, k=8.2417*10^	k=7.9391*10^-3, n=1.4431
Time/Min	Moisture Ratio	page model	lewis	Henderson & Pabis	Modified page
0	1.000	1.000	1.000	1.316	1.000
20	0.901	0.922	0.901	1.116	0.922
40	0.812	0.812	0.812	0.946	0.812
65	0.687	0.667	0.713	0.770	0.667
95	0.531	0.507	0.610	0.601	0.507
130	0.352	0.352	0.508	0.451	0.352
180	0.101	0.196	0.392	0.298	0.196
240	0.010	0.089	0.287	0.182	0.089
	SDE	0.037	0.047	0.078	0.037
	R2	0.991	0.986	0.962	0.991

50 degrees Cowpea leaves		n=1.2878, k=2.092exp-3	k=5.6726exp-3	0.9451 k= 3.9072*10^	k=7.4719*10^-3, n=1.1926
Time/Min	Moisture Ratio	page model	lewis	Henderson & Pabis	Modified page
0	1.000	1.000	1.000	0.945	1.000
15	0.919	0.934	0.918	0.891	0.929
32	0.834	0.834	0.834	0.834	0.834
66	0.547	0.631	0.688	0.730	0.650
85	0.528	0.528	0.617	0.678	0.559
120	0.294	0.369	0.506	0.591	0.416
145	0.219	0.281	0.439	0.536	0.333
185	0.001	0.176	0.350	0.459	0.230

30 degrees Jute mallow		n=1.3453, k=1.2541ex	k=4.8414exp-3	a=1.0552, k=6.7645*10^	k=5.2475*
Time/Min	Moisture Ratio	page model	lewis	Henderson & Pabis	Modifie
0	1.000	1.000	1.000	1.055	1.00
25	0.891	0.909	0.886	0.891	0.89
50	0.785	0.785	0.785	0.752	0.78
75	0.694	0.659	0.696	0.635	0.69
101	0.562	0.536	0.613	0.533	0.60
125	0.453	0.436	0.546	0.453	0.52
150	0.346	0.346	0.484	0.383	0.46
175	0.237	0.271	0.429	0.323	0.40
200	0.128	0.210	0.380	0.273	0.34
220	0.001	0.169	0.345	0.238	0.3
	SDE	0.053	0.062	0.081	0.05
	R2	0.977	0.970	0.948	0.9

40 degrees Jute mallow		n=1.3676, k=1.3419ex	k=5.7757exp-3	a=1.0374, k=7.0499*10^	k=0.01, n=
Time/Min	Moisture Ratio	page model	lewis	Henderson & Pabis	Modified page
0	1.000	1.000	1.000	1.037	1.000
20	0.901	0.922	0.891	0.901	0.901
40	0.812	0.812	0.794	0.782	0.759
65	0.687	0.667	0.687	0.656	0.579
95	0.531	0.507	0.578	0.531	0.394
130	0.352	0.352	0.472	0.415	0.236
180	0.101	0.196	0.354	0.292	0.102
200	0.010	0.152	0.315	0.253	0.071
	SDE	0.049	0.064	0.077	0.076
	R2	0.985	0.974	0.962	0.963

50 degrees Jute mallow		n= 1.3791, k=1.9144ex	k=8.7071exp-3	a=1.0805, k=0.0124	k=0.011, n=1.2438
Time/Min	Moisture Ratio	page model	lewis	Henderson & Pabis	Modified page
0	1.000	1.000	1.000	1.081	1.000
14	0.907	0.930	0.885	1.064	0.907
31	0.804	0.804	0.763	1.045	0.769
66	0.587	0.539	0.563	1.006	0.511
93	0.415	0.371	0.445	0.977	0.357
120	0.244	0.244	0.352	0.949	0.244
146	0.077	0.157	0.280	0.923	0.165
160	0.001	0.123	0.248	0.909	0.133
	SDE	0.057	0.071	0.009	0.067
	R2	0.9809093	0.97010473	0.999467589	0.973245494

30 degrees Slender leaf		n=1.4545, k=6.4169e	4.9919*10	.0541, k=6.2793*10	.502*10^-3, n=1.
Time/min	Moisture ratio	page model	lewis	Henderson & Pabis	Modified page
0	1.000	1.000	1.000	1.054	1.000
25	0.901	0.933	0.883	0.901	0.901
50	0.799	0.827	0.779	0.770	0.781
75	0.710	0.711	0.688	0.658	0.664
101	0.604	0.591	0.604	0.559	0.553
125	0.512	0.488	0.536	0.481	0.462
150	0.411	0.392	0.473	0.411	0.379
175	0.309	0.310	0.417	0.351	0.309
200	0.209	0.241	0.368	0.300	0.250
250	0.102	0.140	0.287	0.219	0.160
300	0.001	0.077	0.224	0.160	0.101
	SDE	0.030	0.046	0.063	0.043
	R2	0.993	0.982	0.968	0.985

40 degrees Slender leaf		n=1.2613, k=1.71	5.3294*10	a=1.0648, k=6.591	4121*10^-3, n=1.
Time/min	Moisture ratio	page model	lewis	Henderson & Pabis	Modified page
0	1.000	1.000	1.000	1.065	1.000
25	0.903	0.905	0.875	0.903	0.903
40	0.835	0.835	0.808	0.818	0.833
67	0.741	0.708	0.700	0.685	0.706
90	0.619	0.606	0.619	0.588	0.604
127	0.461	0.461	0.508	0.461	0.461
167	0.291	0.335	0.411	0.354	0.337
265	0.001	0.141	0.244	0.186	0.144
	SDE	0.040	0.056	0.072	0.041
	R2	0.988	0.976	0.961	0.988

50 degrees Slender leaf		n=1.2638, 2.1478	6.0452*10	a=1.0626, k=8.939	2306*10^-3, n=1.
Time/min	Moisture ratio	page model	lewis	Henderson & Pabis	Modified page
0	1.000	1.000	1.000	1.063	1.000
16	0.921	0.931	0.908	0.921	0.921
34	0.831	0.831	0.814	0.784	0.812
66	0.671	0.652	0.671	0.589	0.624
91	0.553	0.526	0.577	0.471	0.496
120	0.402	0.402	0.484	0.364	0.374
140	0.304	0.330	0.429	0.304	0.304
195	0.038	0.186	0.308	0.186	0.167
231	0.001	0.124	0.247	0.135	0.110
	SDE	0.049	0.056	0.087	0.058
	R2	0.985	0.979	0.951	0.978

40 degrees Nightshade		n=1.4523, k=1.031	k=6.6344*	k=1.1467,	k=9.009*10^-3,
Time/min	Moisture ratio	page model	lewis	derson & P	Modified page
0	1.000	1.000	1.000	1.147	1.000
25	0.871	0.895	0.847	0.871	0.871
50	0.739	0.739	0.718	0.662	0.707
75	0.608	0.580	0.608	0.503	0.552
101	0.450	0.432	0.512	0.378	0.414
125	0.351	0.318	0.436	0.290	0.310
150	0.225	0.225	0.370	0.220	0.225
175	0.092	0.155	0.313	0.167	0.160
200	0.010	0.104	0.265	0.127	0.112
	SDE	0.042	0.057	0.097	0.050
	R2	0.987	0.977	0.932	0.982

30 degrees Nightshade		n=1.1744, k=3.051	k=6.0681*	a=1.029, k	k=6.5328*10^-3,
Time/min	Moisture ratio	page model	lewis	derson & P	Modified page
0	1.000	1.000	1.000	1.029	1.000
24	0.856	0.880	0.864	0.856	0.856
52	0.729	0.729	0.729	0.691	0.713
82	0.608	0.583	0.608	0.549	0.586
121	0.454	0.426	0.480	0.407	0.454
174	0.271	0.271	0.348	0.271	0.321
256	0.001	0.128	0.212	0.145	0.187
	SDE	0.052	0.052	0.071	0.057
	R2	0.981	0.981	0.965	0.977

50 degrees Nightshade		n=1.5829, k=1.363	k=9.902*1	k=0.023, a	k=0.016, n=1.393
Time/min	Moisture ratio	page model	lewis	derson & P	Modified page
0	1.000	1.000	1.000	1.230	1.000
15	0.872	0.906	0.862	0.871	0.872
30	0.743	0.743	0.743	0.617	0.698
60	0.472	0.411	0.552	0.309	0.389
95	0.202	0.159	0.390	0.138	0.167
110	0.098	0.098	0.336	0.098	0.111
138	0.058	0.036	0.255	0.051	0.049
172	0.001	0.009	0.182	0.024	0.017
	SDE	0.030	0.043	0.110	0.037
	R2	0.995	0.990	0.935	0.993

30 degrees Amaranthus		n=1.6523, k=4.715exp-4	
Time/min	Moisture ratio	page model	Residuals
0	1.000	1.000	0.000
25	0.870	0.908	-0.038
50	0.739	0.739	0.000
75	0.605	0.554	0.051
101	0.447	0.380	0.067
125	0.347	0.253	0.094
150	0.221	0.156	0.065
175	0.091	0.091	0.000
200	0.001	0.050	-0.049
	SDE	0.052	
	R2	0.981	

40 degrees Amaranthus		n=1.891, k=2.5043exp-4	
Time/min	Moisture ratio	page model	Residuals
0	1.000	1.000	0.000
20	0.871	0.930	-0.059
41	0.755	0.755	0.000
71	0.571	0.452	0.119
101	0.382	0.213	0.169
141	0.142	0.055	0.087
164	0.021	0.021	0.000
190	0.001	0.006	-0.005
			0.000
	SDE	0.076	
	R2	0.968	

50 degrees Amaranthus		n=1.4976, k=2.6975exp-3	
Time/min	Moisture ratio	page model	
0	1.000	1.000	
14	0.869	0.869	
32	0.711	0.616	
66	0.401	0.239	
91	0.150	0.099	
100	0.064	0.069	
120	0.001	0.030	
	SDE	0.075	
	R2	0.972	

Temperature degrees	Relative humidity	Amaranthus Eq=m wt.(0.266)	Amaranthus wt change.	Amaranthus emc
30	17.01	0.285	0.019	12.000
	32.74	0.290	0.024	14.000
	55.91	0.298	0.032	17.000
	76.03	0.311	0.045	22.000
	83.76	0.333	0.067	30.000
		wt=0.371	Amaranthus wt change.	
40	15.71	0.386	0.015	9.100
	32.07	0.394	0.023	11.100
	54.11	0.402	0.031	13.400
	75.11	0.412	0.041	16.000
	82.04	0.438	0.067	23.000
		wt=0.369	Amaranthus wt change.	
50	14.56	0.380	0.011	8.000
	31.31	0.387	0.018	10.000
	50.43	0.402	0.028	12.645
	75.13	0.402	0.035	14.542
	82.09	0.435	0.056	20.290

Temperature degrees	Relative humidity	Cowpea Eq=m wt.(0.287)	Cowpea L wt change.	Cowpea emc
30	17.01	0.306	0.019	11.700
	32.74	0.312	0.025	13.700
	55.91	0.319	0.032	16.000
	76.03	0.334	0.047	21.500
	83.76	0.358	0.071	29.700
		wt=0.310	Cowpea L wt change.	
40	15.71	0.322	0.012	9.000
	32.07	0.329	0.019	11.100
	54.11	0.338	0.028	14.100
	75.11	0.343	0.033	15.800
	82.04	0.378	0.068	27.000
		wt=0.319	Cowpea L wt change.	
50	14.56	0.329	0.010	8.000
	31.31	0.332	0.013	9.000
	50.43	0.345	0.026	13.000
	75.13	0.351	0.032	15.000
	82.09	0.383	0.064	25.000

Temperature degrees	Relative humidity	Nightshade Eq=m wt.(0.412)	Nightshade wt change.	Nightshade emc
30	17.01	0.437	0.025	11.100
	32.74	0.445	0.033	13.000
	55.91	0.460	0.048	16.553
	76.03	0.477	0.065	20.700
	83.76	0.510	0.098	28.900
		wt=0.472	Nightshade wt change.	
40	15.71	0.491	0.019	9.000
	32.07	0.500	0.028	11.000
	54.11	0.504	0.032	11.700
	75.11	0.535	0.063	18.400
	82.04	0.566	0.094	25.000
		wt=0.445	Nightshade wt change.	
50	14.56	0.461	0.016	8.700
	31.31	0.467	0.022	9.900
	50.43	0.472	0.030	11.779
	75.13	0.481	0.036	13.000
	82.09	0.512	0.067	20.000

Temperature degrees	Relative humidity	Slender leaf Eq=m wt.(0.358)	Slender leaf wt change.	Slender leaf emc
30	17.01	0.376	0.018	10.100
	32.74	0.384	0.026	12.400
	55.91	0.394	0.036	15.193
	76.03	0.403	0.045	17.707
	83.76	0.444	0.086	29.100
		wt=0.219	Slender leaf wt change.	
40	15.71	0.230	0.018	9.096
	32.07	0.234	0.022	10.196
	54.11	0.247	0.035	15.196
	75.11	0.256	0.044	16.196
	82.04	0.283	0.071	26.196
		wt=0.274	Slender leaf wt change.	
50	14.56	0.287	0.013	9.800
	31.31	0.288	0.016	10.830
	50.43	0.297	0.026	14.495
	75.13	0.301	0.027	15.000
	82.09	0.332	0.060	26.730

Temperature degrees	Relative humidity	Jute mallow Eq=m wt.(0.219)	Jute mallow wt change.	Jutemallow emc
30	17.01	0.230	**0.011**	**10.100**
	32.74	0.235	**0.016**	**12.100**
	55.91	0.246	**0.027**	**17.132**
	76.03	0.252	**0.033**	**20.100**
	83.76	0.271	**0.052**	**28.800**
		wt=338	Jute mallow wt change.	
40	15.71	0.349	0.011	**8.400**
	32.07	0.354	0.016	**9.600**
	54.11	0.369	0.031	**14.100**
	75.11	0.372	0.034	**15.000**
	82.04	0.389	0.051	**20.000**
		wt=0.402	Jute mallow wt change.	
50	14.56	0.410	**0.008**	**6.900**
	31.31	0.418	**0.014**	**8.502**
	50.43	0.429	**0.025**	**11.302**
	75.13	0.434	**0.030**	**12.502**
	82.09	0.450	**0.049**	**17.249**

Appendix 3:List of terminologies:

Dry-bulb temperature−Actual temperature of the air.

Dry basis (d.b.)−One method of calculating the moisturecontent of grain ‑ ratio of weight of water to the dry weight of the grain

Equilibrium relative humidity (ERH)−For a sample of grain, at a fi xed moisture content, the ERH would be reached when moisture in the air is in equilibrium with the grain, i.e. there is no net movement of moisture from or to the grain.

Isotherm−The relationship between the m.c. of the grain (in equilibrium with the surrounding air) and the r.h. of the air at a constant temperature ‑ usually depicted by a graph.

Mathematical modelling: the use of mathematical equations to predict the behaviour of the operation

Moisture content (m.c.)−A measure of how much moisture an object actually holds. Usually expressed as a percentage (see **Dry basis** and **Wet basis**).

Moisture diffusion/diffusivity−A measure of how easily moisture can move through an object.

Relative humidity (r.h.): Measure of the quantity of moisture held by air, expressed as a percentage of what the air could hold at that temperature. Defi ned as the ratio of the partial pressure to the saturation pressure.

Thermal conductivity: A measure of the ability of an object to conduct heat.

Safe moisture content: That moisture content with a corresponding ERH of 70% or below, i.e. the lower limit for mould growth

Organoleptic properties−Those properties of a foodstuff or food ingredient which are perceived in the mouth during consumption. The properties include taste, mouth-feel, consistency, texture, chewability, stickiness, etc.

Water activity: The water activity (a_w) is the ratio of the water vapour pressure of the food to the water vapour pressure of pure water under the same conditions. It is expressed as a fraction.

Wet basis (w.b.): One method of calculating the moisture content of grain – ratio of weight of water to the total weight of the grain

Wet-bulb temperature−The temperature indicated on the wet bulb of a wet-and-dry thermometer (lower than the dry-bulb temperature since water evaporating from the wet bulb cools the thermometer slightly).